Gene expression analyses on skin lesions from patients with familial adenomatous polyposis

Inauguraldissertation

zur

Erlangung der Würde eines Doktors der Philosophie

vorgelegt der

Philosophisch-Naturwissenschaftlichen Fakultät

der Universität Basel

von

Danielle Alexandra Stegmann

aus Liestal (BL)

Basel, 2014

Genehmigt von der Philosophisch-Naturwissenschaftlichen Fakultät
auf Antrag von

Prof. Dr. med. Stephan Krähenbühl

Dr. rer. nat. Bettina Burger

Prof. Dr. Raija L.P. Lindberg Gasser

Basel, den 22.4.2014

Dekan
Prof. Dr. Jörg Schibler

TABLE OF CONTENTS

ABBREVIATIONS

AFAP	Attenuated familial adenomatous polyposis
ANOVA	Analysis of variance
APC	Adenomatous polyposis coli
BCC	Basal-cell carcinoma
CHRPE	Congenital hypertrophy of the retinal pigment epithelium
CK1	Casein kinase 1
CNRQ	Calibrated normalized relative quantity (normalized mRNA expression values after qBasePLUS-based normalization on selected house keeping genes)
CRC	Colorectal cancer
C_T	Cycle threshold
CTNNB1	β-catenin
CV	Coefficient of variation
DAVID	Database for Annotation, Visualization and Integrated Discovery
DEG	Differentially expressed gene
EB1 binding site	End-binding protein domain of APC
ECM	Extra cellular matrix
EKBB	Ethical Committee of Basel
ENTF	Extra-nuchal type fibroma
FAP	Familial adenomatous polyposis
FDR	False discovery rate
GAF	Gardner Fibroma
GO	Gene ontology
GSK3β	Glycogen synthase kinase 3β
HDLG	human disc large (tumor suppressor that binds to APC)
HGMD®	Human Gene Mutation Database
HKG	House keeping genes
HNPCC	Hereditary non-polyposis colorectal cancer
IHC	Immunohistochemistry
IPA®	Ingenuity pathway analysis
LEF	Lymphoid enhancing factor
LOH	Loss of heterozygosity
LSD	Fisher's Least Significant Difference

MAF	Minor allele frequency
MAP	*MUTHY*-associated polyposis
MCR	Mutation cluster region
MLPA	Multiplex ligation-dependent probe amplification
MMR	Mismatch repair
MSI	Microsatellite instability
NF	Nuchal fibroma
NNTF	Non-nuchal type fibroma
NTF	Nuchal-type fibroma
PCA	Principal components analysis
PCFH	Precalcaneal congenital fibrolipomatous hamartomas
PM	Perfect match
PO	Proto-oncogene
QA/QC	Quality Assessment/Quality Control
qPCR	Quantitative real time PCR
REML	Restricted maximum likelihood
RIN	RNA integrity number
RMA	Robust Multi-Array Averaging
RQ	Relative quantities
SCC	Squamous-cell carcinoma
SAMP repeats	Ser-Ala-Met-Pro repeats (axin/conductin binding site of APC)
TCF	T-cell factor
TS	Tumor suppressor gene
Wnt	Combination of Drosophila gene *Wingless (Wg)*, and the murine *Int1*

1 ABSTRACT

Familial adenomatous polyposis coli (FAP) is an autosomal dominant colorectal cancer predisposition syndrome caused by germline mutations in the *APC* gene. It is characterized by an increased risk for the development of both several internal cancers and benign skin tumors such as fibromas, lipomas, and epidermal cysts occurring with different frequencies early in life. The molecular mechanisms underlying these skin lesions are still poorly understood.

In this study we aimed to clarify the underlying molecular mechanisms in the development of FAP-associated skin lesions. Such mechanisms were hypothesized to either follow the *APC* second hit model or to include other genes, possibly such independent of Wnt signaling.

To this end we analyzed 9 fibromas, 3 lipomas, and 3 epidermal cysts from 14 FAP patients of 7 families with pathogenic *APC* germline mutations for somatic alterations by direct sequencing of the mutation cluster region (MCR), exon-overlapping cDNA analysis, and locus-specific marker analysis. Somatic changes were found in two skin lesions, one lipoma and one epidermal cyst. Both lesions displayed loss of heterozygosity (LOH) at *APC* marker locus D5S346. The epidermal cyst in addition carried a somatic mutation (c.4778delA) in the MCR of *APC.* These results suggest that somatic *APC* alterations may influence the development of FAP-associated lipomas and epidermal cysts.

For the investigation of *APC*-independent processes we analyzed in total 5 fibromas, 6 lipomas and 3 epidermal cysts compared to healthy skin of 13 FAP patients by whole genome expression analysis and confirmed targets of highest expression changes by qPCR. We show that genes mostly changed in fibromas and lipomas of FAP patients mainly function in cell proliferation processes. Therefore we suggest that FAP-associated cutaneous neoplasia might develop by the influence of activated proto-oncogenes and deactivated tumor suppressors similar to other tumors. We suppose that an invasive growth is prevented by increased expression of tumor suppressors in those benign neoplasms. In comparison to the general population expression results of FAP lipomas have also been compared to similar lesions of non-FAP individuals. Non-FAP lipomas tend to be mainly influenced by genes involved in lipid metabolism.

In conclusion, we assume that FAP-associated skin lesions are mostly not caused by *APC* second hits. In contrast, we rather suppose Wnt independent mechanisms. In addition, we suggest that lipomas develop differentially in FAP patients and in the general population.

2 AIM OF THE THESIS

The general aim of this study was to reveal new insights into the development of benign cutaneous neoplasms (fibromas, lipomas, and epidermal cysts) that are associated with FAP. Based on the second hit model we aimed to investigate FAP-associated skin lesions for *APC* second hit mutations as well as for major gene expression changes. Similar skin neoplasms could also occur in the general population. Therefore, we aimed to further investigate, whether such primary skin lesions are developed by similar mechanisms as FAP-associated ones. To this end we analyzed the FAP-associated skin lesions by two different approaches.

The first approach based on the second hit model, which is known for colorectal cancer development in *APC* mutation carriers. Such somatic mutations are thought to indicate a role of Wnt signaling deregulation due to *APC* inactivation. This hypothesis was followed by several techniques. First, we examined the *APC* MCR of skin lesion samples for possible somatic mutations by direct sequencing. In a second step, skin lesion samples were investigated for aberrant transcripts that would indicate possible splice site mutations. And third, we analyzed skin lesion samples at a microsatellite locus 3' of *APC* to reveal information of allelic loss of the wildtype *APC* allele.

The second approach aimed to clarify possible effects of additional gene regulations on the development of benign skin lesions in FAP patients. For this purpose we aimed to investigate differential gene expression between skin lesion and healthy skin samples of FAP patients by microarray-based whole genome expression analysis. Furthermore, we examined those gene expression profiles for gene ontology and pathways. To reveal information about potential similar or different mechanisms of the same skin lesion in FAP patients compared to non-FAP individuals, we applied similar techniques on skin lesion samples derived from both groups.

3 INTRODUCTION

3.1 Familial adenomatous polyposis (FAP)

3.1.1 FAP disease and prevalence

Familial adenomatous polyposis (FAP; OMIM #175100) is an autosomal dominantly inherited colorectal cancer syndrome caused by mutations in the *APC* gene (5q21-q22). The syndrome is characterized by the development of hundreds to thousands of adenomatous polyps in the colon that further could progress to colorectal cancer (CRC). Without surgical treatment CRC on average occurs by the age of 35-40 years[1]. To date, FAP is a well-known and well-documented disease. Written descriptions of "multiple colorectal polypoid lesions" reach back to 1721[2]. The first comprehensive clinical characterization was done by Bussey in 1975, based on records of FAP families treated in the first polyposis registry at St. Marks Hospital in London UK[3]. Up to now, several polyposis registries have been established in Europe as well as worldwide, with the most important ones in Northern Europe, in the UK, US, and Japan[1]. Polyposis registries from Northern Europe estimated an annual incidence rate between 0.9 to 1.9 per million live births and a prevalence rate of 2 to 3 per 100 000 individuals. Relating to other CRC malignancies, FAP accounts for less than 1% of all hereditary and sporadic CRC diseases[4]. Approximately 5% of all CRC diseases cover inherited cancer syndromes of known genetic background and with well-described clinical features. FAP presents as the second-most common, well-characterized inherited CRC syndrome after Lynch syndrome, (prior denoted as hereditary non-polyposis colorectal cancer (HNPCC))[5]. Overall, inherited CRC diseases are categorized by their main expression of adenomatous (benign epithelial tissue tumors of glandular origin with the potential for dysplastic growth) or hamartomatous polyps (overgrowth of cells native to the area at which they normally occur[6]). Lynch syndrome, FAP and *MUTHY*-associated polyposis (MAP) are among the adenomatous polyposis diseases, whereas Peutz-Jeghers syndrome (PJS) and the juvenile polyposis syndrome mainly express hamartomatous polyps[7].

3.1.2 FAP, AFAP and MAP

Regarding the severity of the colorectal polyposis, the disease is differentiated in a classical phenotype with more than 100 adenomas (classical FAP) and a lighter phenotype with less than 100 adenomas, latter referred to as attenuated familial adenomatous polyposis (AFAP; OMIM # 175100)[8]. Classical FAP may be also differentiated into the sparse or intermediate type with hundreds to thousands of adenomas and a profuse or severe type with more than 5000 adenomas[9,10]. AFAP presents with a delayed onset of

adenomatosis (20-25 years later) and CRC (15-20 years later) compared to classical FAP as well as an overall milder course of disease and less extracolonic features[8]. It is described to affect approximately 8% of investigated FAP families[11]. A third colorectal cancer syndrome that includes the development of *APC*-independent multiple adenomatous polyps is caused by biallelic mutations of the base excision repair gene *MUTYH* (1p34.1)[12] and therefore named *MUTYH*-associated polyposis (MAP; OMIM #604933). MAP was found to account for up to 7.5% of *APC*-mutation negative adenomatous polyposis[13]. MAP patients generally present a milder phenotype with 10-100 colorectal adenomas, starting at advanced age [14].

3.1.3 Extracolonic manifestations of FAP

In FAP patients, not only colorectal adenomas are observed but also various extracolonic manifestations, among others also such affecting the skin. More than 70% of FAP patients were found to present at least one extracolonic manifestation[15]. Most prominent extracolonic features are upper gastrointestinal tract polyps such as duodenal polyps[16] and fundic gland polyps[17], characteristic retinal fundus lesions (congenital hypertrophy of the retinal pigment epithelium (CHRPE)[18] as well as desmoid tumors[19]). Other more rare features are thyroid carcinomas[20] and hepatoblastoma[21].

Among the cutaneous manifestations are fibromas, lipomas, and epidermal cysts[19,22]. Such benign neoplasms of the skin are the hallmark of the present study and were previously investigated by our group[22]. In 1953 the triad of polyposis, osteomas, and skin lesions (fibromas, epidermal cysts, and desmoids) has initially been described as Gardner syndrome[19]. To date, upon having identified *APC* mutations as the underlying cause for both diseases, the term “Gardner syndrome” is still commonly used to define a clinical variant of FAP with prominent features at bones, teeth and skin[1].

In addition, two other FAP variants are known. Turcot syndrome[23] relates tumors of the central nervous system, mostly medulloblastoma, to colorectal polyposis (FAP or Lynch syndrome). Hereditary desmoid disease[24] associates *APC* germline mutations with the presence of multiple inherited desmoid tumors, whereas colorectal features only present scarcely or may lack completely.

3.2 Genetics of FAP

3.2.1 The *APC* gene

The adenomatous polyposis coli (*APC*; OMIM # 611731) gene is a tumor suppressor gene that was localized to the long arm of chromosome 5 (5q21-22) in 1987[25,26] and was further cloned and characterized in 1991[27-30]. *APC* contains an 8538bp open reading frame and consists of 15 coding exons encoding a 312 kDa protein of 2843 amino acids[31]. The APC protein is expressed in a variety of normal human tissues in addition to the colorectal epithelium. In the skin, APC was described to mainly express in the stratum granulosum and stratum spinosum as well as diffusely in sebaceous glands, apocrine glands, and eccrine glands[32]. *Apc* knockout mice showed aberrant development of hair follicles, appendages, and cells requiring epidermal-mesenchymal interactions for their development therefore revealing the evidence for a major importance of *APC* for accurate development of normal skin and thymus[33]. Furthermore, APC was described to express in epithelia of normal oral mucosa and to a higher extend in oral squamous cell cancer. There it was suggested to be involved in oral carcinogenesis and malignant transformation[34].

In normal tissue several mRNA isoforms are known to occur due to alternative splicing[35]. The *APC* gene encodes a multifunctional protein involved in cell adhesion and migration, stabilization of the microtubule cytoskeleton, cell cycle regulation, and apoptosis[36,37]. The protein function in a scaffold complex of the canonical Wnt signaling pathway displaying an integral part in the degradation of β-catenin is one of its best examined functions.

3.2.2 Wnt signaling and the *APC* gene

Three different intracellular signaling pathways are known to exist, that are all activated by Wnt signaling molecules. The name Wnt resulted from a combination of the Drosophila gene *Wingless (Wg*), and the murine *Int1,* as both genes were discovered independently in those species. In humans, totally 19 Wnts have been described[38]. Such signaling molecules activate at least three types of intracellular signaling pathways that all branch off at the level of Dishevelled: the canonical or Wnt/β-catenin pathway, the planar polarity pathway, and the Wnt/Ca^{2+} pathway. The canonical or Wnt/β-catenin pathway is centered on β-catenin-mediated Wnt target transcription, as it also occurs in FAP. The planar polarity pathway regulates cell polarity by regulation of the cytoskeletal organization. And the Wnt/Ca^{2+} pathway is known to mediate intracellular Ca^{2+} increase, possibly resulting in antagonism of the Wnt/β-catenin pathway, as shown in Xenopus[38,39]. Those non-canonical Wnt pathways were described to function independently of β-catenin[40].

Within the canonical Wnt signaling pathway APC functions as a scaffold protein in modulating the degradation of intracellular β-catenin[36]. Herein, APC constitutes the degradation complex together with axin/conductin, the serine/threonine kinases casein kinase 1 (CK1), and glycogen synthase kinase 3β (GSK3β). In unstimulated cells without bound Wnt on Frizzled receptor, CK1 phosphorylates β-catenin on a serine, priming it for further phosphorylation by GSK3β that also phosphorylates axin, activating it for efficient binding to APC and β-catenin in the destruction complex[39,41,42]. Bound β-catenin is phosphorylated and therefore marked for subsequent degradation by ubiquitylation in proteasomes. Upon binding of Wnt molecules to the Frizzled receptor and its co-receptor low-density lipoprotein-receptor-related protein LRP6 (or LRP5) Dishevelled (Dvl) is hyperphosphorylated and inactivates GSK3β activity. Furthermore, LRP6 directly interacts with axin and leads to its destabilization. Therefore, the formation of the destruction complex is impacted, and free β-catenin accumulates in the cytoplasm[31,36]. B-catenin is then able to translocate into the nucleus where it acts as a co-activator in the transcription of various target genes. In the absence of β-catenin, transcription is inhibited by transcriptional co-repressors such as Groucho[41]. In the presence of nuclear β-catenin, this co-repressor is displaced by the association of β-catenin with several members of the T-cell factor (TCF) and lymphoid enhancing factor (LEF) family that finally stimulates the transcription of Wnt target genes (Figure 1)[36]. Main Wnt targets include the cell cycle protein cyclin-D1, the proto-oncogene c-myc, the gap junction protein connexin, and the metalloproteinase matrilysin[36,43].

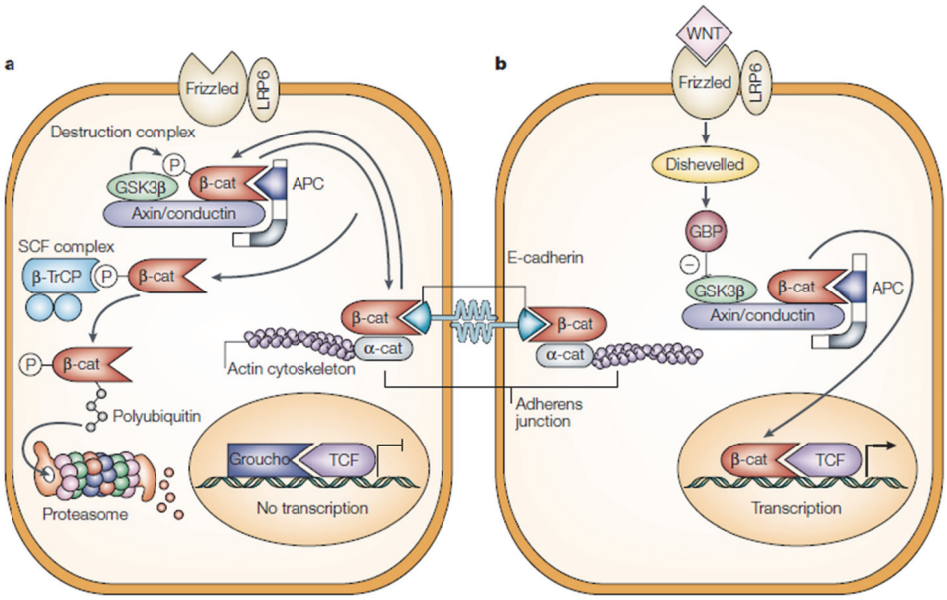

Figure 1. The Wnt signaling pathway and the *APC* gene. a. In the absence of Wnt signal the destruction complex consisting of APC, axin/conductin, GSK3β and β-catenin associate that leads to phosphorylation of β-catenin by CK1 (not shown) and GSK-β and its further degradation by ubiquitylation in the proteasome. **b.** By the presence of Wnt signaling, Wnt molecules bind to Frizzled receptor and LRP6 co-receptor. Furthermore, the association of the destruction complex is disabled by two mechanisms: On one hand, axin translocates to the membrane and directly interacts with LRP6 that leads to axin destabilization (not shown). On the other hand, Dvl is hyperphosphorylated and inhibits GSK3β activity. B-catenin therefore is able to accumulate in the cytoplasm and to translocate in the nucleus, where it activates the transcription of certain proto-oncogenes by interaction with TCF and other transcriptional activation genes. *Figure adopted from Fodde et al, 2001*.

3.2.3 Wnt signaling in cancer and in the skin

Wnt signaling pathway is known to be involved in several differentiation events during embryonic development and will lead to tumor formation if it is aberrantly activated[39]. Due to permanent Wnt stimulation, the phosphorylation and degradation of β-catenin is disabled, leading to an enhanced activation and transcription of Wnt target genes[36,43]. Wnt activation mostly occurs by either inactivating mutations of *APC* or by activating mutations of *CTNNB1* (*β-catenin*)[39].

Especially CRC (sporadic and hereditary) is known to be a direct consequence of mutations affecting Wnt target genes (in more than 90% of all CRC). Besides CRC, several other cancer types were reported to be caused by aberrant Wnt signaling, such as gastrointestinal tumors and adenomas, juvenile nasopharyngeal angiofibromas, hepatocellular carcinomas, tumors of reproductive organs as well as several childhood malignancies (hepatoblastoma, medullablastoma, pancreatoblastoma) or breast cancer[39].

In the skin, Wnt signaling plays an important role in skin organogenesis and morphogenesis. There it is especially involved in the development of the dermis, epidermis, and the formation of hair follicles, but also in stem cell maintenance and wound healing[40,44]. Relating to skin tumors, melanomas have been reported to contain both, *β-catenin* as well as *APC* mutations[39]. In addition, expression of Wnt5a was described to possibly lead to increased melanoma progression[45]. Furthermore, desmoids and Gardner fibromas were associated with Wnt signaling due to mutations in *β-catenin* and *APC*. Furthermore, immunohistochemistry (IHC) studies revealed overexpression of Wnt target proteins (β-catenin, cyclin-D1 and c-myc) indicating an aberrant Wnt activation[46-48]. For pilomatricomas (particular tumors of hair matrix cells*) β-catenin* activating mutations were described[49,50]. In experiments with transgenic mice activating *β-catenin* mutations were found to induce *de novo* hair morphogenesis and formation of hair follicle tumors.

3.2.4 Functional domains of APC

The multifunctional protein APC consists of different domains. Figure 2 illustrates the most important functional domains of APC. These domains facilitate the interaction of the APC protein with various protein partners, conducting several functions.

Most important domains will be summarized starting from their localization at the amino terminus of APC. The **oligomerization domain** at the beginning of the protein (aa 6-57) consists of a heptad repeat structure and allows APC to form homo-dimers. The following **armadillo region** (aa 463-767) contains seven highly conserved repeats involved in the stabilization and motility of the actin cytoskeleton. Further downstream are three repeats of **15-amino acids** (aa 1020-1170) and seven repeats of **20-amino acids** (aa 1265-2035) that both bind β-catenin (after phosphorylation by GSK3β). At least three 20-amino acid repeats are necessary for degradation of bound β-catenin. In the tumorigenic process, truncating mutations frequently delete all or most of the seven 20-amino acids repeats. Another motif located within the 20-amino acids repeats region are the three **SAMP** (Ser-Ala-Met-Pro) **repeats** that bind axin and its homolog conductin. Axin itself contains binding sites for β-catenin and GSK3β to enable the establishment of the multi-protein destruction complex for β-catenin phosphorylation. The succeeding **basic domain** (aa 2200-2400; named after its large proportion of basic arginine and lysine residues) as well as the end-binding protein domain (**EB1 binding site**; aa 2559-2771) bind microtubules whereas the latter also facilitates the interaction of APC with other cellular membrane structures. The C-terminus of APC, the **human disc large (HDLG) binding site** (aa 2771-2843), forms complexes with the tumor suppressor HDLG and thus leads to a suppression of cell cycle

progression by APC overexpression. This effect is supposed to be independent of β-catenin function[36].

Deletions of several motifs located downstream of the 15 amino-acid repeats (such as the 20 amino-acid repeats, SAMP repeats, or the HDLG) are suggested to contribute to tumorigenesis in FAP disease and sporadic cancer.

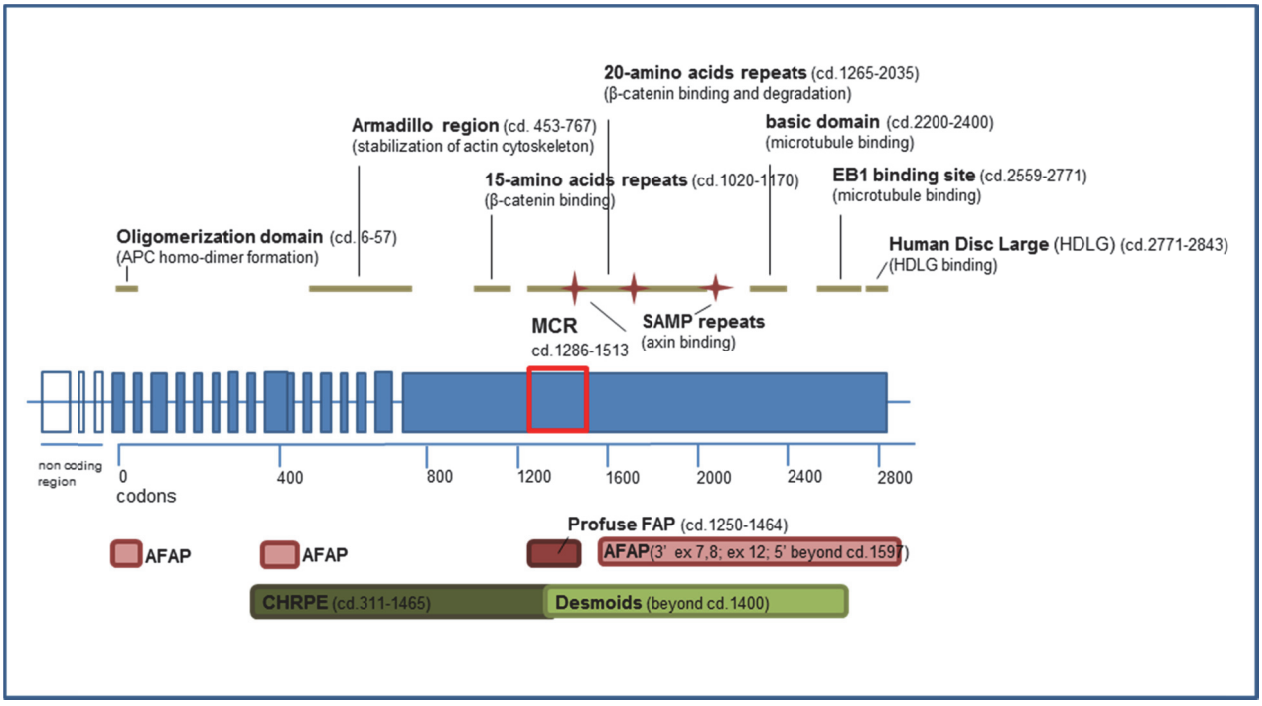

Figure 2. Functional domains of APC and genotype-phenotype correlations. Illustration shows the functional domains of *APC* (top), a schematic outline of *APC* with its 18 exons (middle) and selected genotype-phenotype correlations (bottom). The three axin-binding SAMP repeats are indicated by purple asterisks. The red frame indicates the region of the mutation cluster region (MCR). *Illustration adapted from Fearnhead et al., and Macrae et al.*

3.2.5 Genotype-phenotype correlations in FAP

The severity of colorectal polyposis and the development of extracolonic manifestations seem to correlate with the localization of the germline mutation in *APC*. Since 1991, several authors have stated genotype-phenotype correlations that have very comprehensively been summarized by Nieuwenhuis and Vasen in 2007[51].

Patients suffering from severe FAP with more than 5000 adenomas mostly carried germline mutations between codons 1250-1464. Within this region, codon 1309 indicates a mutational hotspot that especially accounts for severe polyposis with early onset (34 years) of colorectal cancer[9,15]. An intermediate phenotype is associated with mutations of all other regions, spanning exons 7-18, excluding the mutation cluster region. For the attenuated phenotype, germline mutations were described to localize mainly at three different parts of

the *APC* gene, at the 5'[52] and 3' end of the gene as well as within the alternatively spliced region of exon 12[53].

Relating to the extracolonic manifestations, CHRPE as the most common extracolonic feature is very well localized by several investigators to cover codons 311-1465[51]. However, our group recently suggested to extend the CHRPE-associated region to *APC* codons 148-2043[22]. Desmoid tumors tend to cluster at the 3' end of the gene (beyond 1400) with a higher incidence and severe manifestation if the germline mutation is located between codons 1445 and 1580 (Figure 2)[54-56]. Genotype-phenotype correlations for other extracolonic manifestations are not well established. Multiple extracolonic manifestations tend to cluster beyond codon 1400[51]. For particular cutaneous features such as fibromas, lipomas, and epidermal cysts, no consistent correlation with the *APC* genotype has been found. Such lesions rather evenly distribute throughout the *APC* gene[15,22,57].

3.3 First and second hits in *APC*

3.3.1 *APC* germline mutations

Germline *APC* mutations are seen in the majority of FAP patients. In classical FAP, *APC* germline mutations are usually identified in 90% of the cases by applying routine diagnostics as direct sequencing of the coding exons or deletion/duplication analysis with multiplex ligation-dependent probe amplification analysis (MLPA). In AFAP, germline mutations in *APC* or *MUTYH* could only be revealed in 20-50% of patients[58]. Totally up to about 25% of all *APC* mutations occur *de novo*[59-61]. In addition to routine diagnostics, cDNA analysis of the 15 coding exons was proposed to unravel otherwise undetected intronic mutations[58]. Furthermore, the today largely replaced protein-truncation test as a prescreening tool was proposed to readopt into the diagnostic repertoire. Its value could has especially been shown in the identification of mosaic mutations in apparently *APC* mutation negative FAP patients with *de novo* classical FAP[62].

To date, the Human Gene Mutation Database (HGMD®) describes totally 1158 different *APC* germline mutations (http://www.hgmd.cf.ac.uk/ac/gene.php?gene=APC). Most of these mutations are predicted to result in truncated proteins. The vast majority of these mutations present missense or nonsense mutations, frameshift mutations (small deletions and insertions) or large genomic deletions. Germline mutations are mainly scattered in the 5' half of the *APC* gene[41] with mutational hot spots at codons 1061 and 1309[36] accounting for one third of all germline mutations[63].

3.3.2 Somatic mutations and the mutation cluster region

In accordance with Knudson's two-hit model[64,65] colorectal adenomas in FAP patients carry additional somatic mutations in *APC*. These *APC* mutations occur very early during colorectal tumorigenesis (see below). Most (around 60%) of these second hit mutations occur in the so-called mutations cluster region (MCR) covering codons 1286-1513 (Figure 2) with two mutational hotspots at 1309 and 1450[63,66].

3.3.3 First hit-second hit association in colorectal tumorigenesis

It has further been refined, that the *APC* gene does not entirely follow the predicted Knudson's two hit model, as Knudson's hypothesis postulates two independent mutational events[41]. For *APC* the position and type of the somatic mutation was described to depend on the localization of the germline mutation[67]. Accordingly, mutations near codon 1300 are associated with allelic loss of the wildtype allele, whereas germline mutations at other regions of the *APC* gene mostly related to second hit mutations within the MCR leading to an *APC* truncation[67,68]. In most human colorectal adenomas, truncated APC proteins are identified, that retain only one or two 20-amino acids repeats, whereas three 20-amino acids repeats are needed for successful β-catenin degradation[36]. Therefore, somatic mutations are selected based on the growth advantage they provide to the tumor cell[67,68].
The dependence of first and second hits has reported to be more complex as indicated by recent work[68-70]. Results lead to the assumption that an ideal amount of residual *APC* signaling (β-catenin down-regulation/degradation) needs to exist for tumor formation and a "just-right" signaling model[69] was established that was further refined to a less stringent "loose fit" model[68]. Excessive nuclear accumulation of β-catenin has in contrast been shown to induce apoptosis[71]. For desmoid tumors, second hit mutations were determined to be nonrandom but not just right neither[72]. Furthermore, the optimal level of β-catenin binding and degrading 20-amino acids repeats were found to differ between colorectal tumors of profuse, classical FAP and AFAP, as well as between colorectal and extracolonic tumors. This would suggest different mechanisms of tumorigenesis in various tissues of FAP patients[10].

3.3.4 The adenoma-carcinoma cascade

Mutational inactivation or loss of *APC* were described to be the earliest event in the adenoma-carcinoma sequence. *APC* mutations are not only present in almost all FAP adenomas but also in about 85% of sporadic colorectal adenomas[39]. Inactivation of both alleles of *APC* in most intestinal tumors may be detected at an early stage of tumor

development (Figure 3). Furthermore, several additional mutations in other genes have been reported. The most reported are the oncogene (*KRAS*), and the tumorsuppressor genes *SMAD4* and *TP53*[39,41].

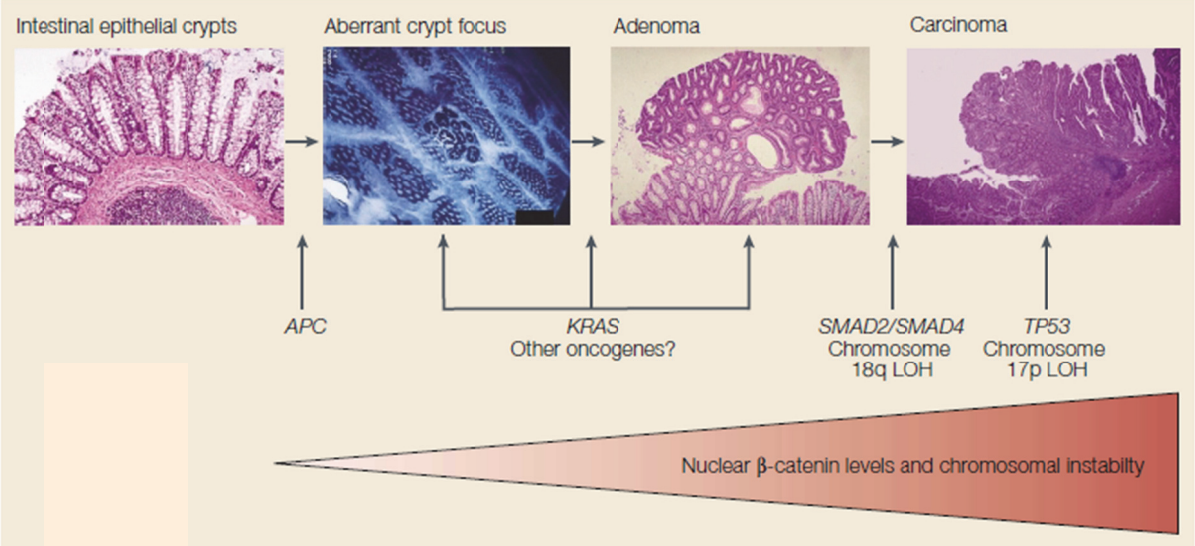

Figure 3. The histopathology of colorectal cancer starting with two hits in *APC*. The so-called adenoma-carcinoma sequence in colorectal cancer development is initiated by activation of Wnt signaling achieved by inactivation of the *APC* gene (by two mutations) or alternatively by a mutation in β-catenin. Subsequent mutations activating among others the oncogene *KRAS*, or inactivating other tumor suppressor genes as *SMAD2, SMAD4,* and *TP53,* lead to further malignant progression. The whole process is accompanied by increasing β-catenin concentrations leading to rising amounts of chromosomal instability. The upper part of the image illustrates the different structures within the large intestine during pathogenic progress. Aberrant crypt foci display the first manifestation of colorectal neoplasia that contains dysplastic cells that may further proliferate to become adenomatous polyps the progenitors of cancer[39,41]. *Image adopted from Fodde et al., 2001.*

3.4 FAP-associated skin lesions

3.4.1 Gardner syndrome

As already mentioned above (3.1.3), Gardner syndrome[19] is characterized by intestinal polyposis associated with specific extracolonic features, such as osteomas, dental anomalies, epidermal cysts, and desmoid tumors (Figure 4)[19,73-75]. This syndrome has initially been described as a subtype of FAP, but was later considered as a clinical variant after the identification of the *APC* gene in 1991. Today, FAP is mostly referred to as Gardner syndrome in the case extracolonic manifestations are especially prominent[1].

Since the first formal description of Gardner syndrome in 1953, numerous associated manifestations have been added affecting several organs as papillary thyroid cancer, benign intracranial neoplasms, hepatomas and hepatoblastomas, biliary and adrenal

neoplasms and other osseous features, such as osteosarcomas and chondrosarcomas[76]. Besides the risk to develop CRC, Gardner syndrome further predisposes to duodenal, thyroid, brain, adrenal and liver cancer[77].

Figure 4. Photographs of Gardner syndrome-associated extracolonic manifestations. A. Osteoma of the forehead (black arrow); **B.** Dental anomaly due to the presence of an intrabuccal cyst (black arrow); **C.** Desmoid tumor at the right cheek; **D.** Illustration of the right chest after desmoid resection. These extracolonic lesions belong to FAP patients examined and investigated by our group.

3.4.2 Skin lesions associated with FAP

Besides the initially described cutaneous neoplasms such as epidermal cysts, fibromas and desmoids[19,74], up to now several skin lesions have been described to be associated with FAP, such as lipomas and more rarely leiomyomas, neurofibromas[78], and pilomatricomas[79,80]. Furthermore, precalcaneal congenital fibrolipomatous hamartomas (PCFH) and pigmented nevi[81], mucoepidermoid carcinoma at the parotid gland[82], and porokeratosis of Mibelli[83] have recently been reported to occur in patients with confirmed *APC* germline mutations. Some of these lesions might be coincidental.

The present study examines three particular benign cutaneous neoplasms that are associated with FAP, namely fibromas, lipomas, and epidermal cysts. The following section will give a short summary of the major characteristics of these specific FAP-associated skin lesions.

3.4.2.1 Gardner-associated fibromas

Fibromas in general are benign tumors of fibrous tissue, deriving from mesenchymal origin that mainly consists of fibrous or connective tissue[84]. The most prominent fibroma in FAP patients is the accordingly-named Gardner fibroma (GAF). GAF is a benign soft tissue lesion of 1-10 cm size that has been included in the 2002 published WHO classification[85]. Histologically it is described to consist of thick haphazardly arranged collagen bundles with interspersed bland fibroblasts and a plaque-like growth pattern with infiltration and entrapment of surrounding structures[85]. GAFs mainly affect superficial and deep soft tissues of the paraspinal region and the back, but they have a wide anatomic distribution and therefore may also occur at the chest wall, flank, head, neck and the extremities[46,85,86]. More than 69% are known to be associated with an underlying FAP disease[46].

GAFs mostly occur early in life (more than 75% occur in the first decade of life) and they therefore often precede the development of colorectal adenomas. For this, GAFs were proposed as a sentinel event for the identification of FAP before intestinal symptoms arise[86,87]. Recently, a case of GAF in a 10-week old newborn was reported that was later identified as *APC* mutation carrier[88].

In approximately 50% GAFs are associated with the otherwise FAP-related desmoid tumors that present either after excision of GAFs or in a sequential pattern[87]. GAFs have therefore also been assigned as desmoid precursor lesions[89].

3.4.2.2 Other fibroma types occurring in FAP

The occurrence of other fibroma types in FAP has extensively been discussed and a lot has been debated about their appropriate terminology. Several types of different fibromas were reported to occur in FAP patients besides the above described GAF[46,85,88,90] or Gardner-associated fibroma[86], such as nuchal fibroma (NF)[91], non-nuchal type fibroma (NNTF)[92], nuchal-type fibroma (NTF)[93-95] or extra-nuchal type fibroma (ENTF)[96]. The term “nuchal-type” fibroma was initiated as nuchal fibromas were also described to occur at other sites of the body such as at the back, on the face and extremities[93]. One report of an extra-nuchal type fibroma described a nuchal type fibroma that occurred in a patient with attenuated FAP and *MUTYH* polymorphism due to repetitive trauma and collagen degeneration[96].

Relating to their appearance and histologic presentation, nuchal type fibromas (NTFs) are very similar, if not identical to GAFs. For this, GAF has also been proposed to be integrated as a subset of NTFs occurring at multiple sites[85,86,97]. But there also exist some major differences. GAFs rather present plaque-like with rubbery texture than as hard masses, and entrap nerves only rarely. GAFs are associated to a much higher extend with FAP

(69% compared to 2% for NTFs). Furthermore, NTFs affect patients of considerable older age (between the third and firth decade of life) as well as predominantly women. GAFs in contrast occur very early in life and equally affect men and women. Besides the higher age, NTFs show in contrast to GAFs an association to diabetes mellitus type 2 (in up to 44% of patients with NTF). GAFs furthermore indicate a higher variety of different predilection sites as well as a higher size range, whereas they may be smaller than NTFs[46,93]. NTFs as well as GAFs are associated with the development of desmoids and are therefore referred to as desmoid precursor lesions[85,86,96].

3.4.2.3 Development of Gardner-associated fibromas

Relating to the development of GAFs and NTFs, no data are available about their cytogenetic or molecular genetic aspects[87]. Recent studies[46] reported positivity for CD34, and Wnt pathway proteins as β-catenin as well as its proto-oncogenic targets c-myc and cyclin-D1 in immunohistochemistry. Positivity for such Wnt pathway genes may therefore be indicative for an associated FAP disease[46,96]. Fibromas in FAP were positive for CD34 and vimentin but revealed negative reactivity in immunohistochemical examinations for muscle actin molecules, desmin, S100, EMA, GFAP, cytokeratins, and CAM5.2 (Table 1). As surgery may trigger remission of soft tissue tumors or the development of desmoids, local trauma may play also an important role in the initiation of fibromas[86,96,98].

3.4.2.4 Desmoids

Besides Gardner-associated fibromas, desmoids or aggressive fibromatosis states another benign neoplasm of mesenchymal origin affecting patients with Gardner syndrome (Figure 4). Desmoids are frequently aggressive tumors of mesenchymal origin, which arise in musculoaponeurotic structures[72]. They are benign fibromatoses consisting out of well-differentiated fibroblasts and characterized by a variable amount of collagen[99]. Desmoid tumors may arise sporadically or due to an inherited *APC* mutation (in Gardner syndrome or hereditary desmoid disease). In FAP, desmoids mainly occur in the mesentery whereas sporadic desmoids develop at various intra and extra abdominal sites[87]. The incidence of desmoids in FAP is approximately 850-fold higher than in otherwise healthy individuals. FAP-associated desmoids occur in approximately 10-25% of all FAP patients, whereas sporadic desmoids are very rare (0.03% of all neoplasms)[72,100]. Risk factors reported for desmoid development are surgical trauma, pregnancy, radiation, mutations in *APC* or *CNNB1* (*β-catenin*), and preceding GAF[87,98,101]. Immunohistochemical examinations revealed positivity for smooth muscle actin, nuclear β-actin but no reactivity for CD34 in

contrast to GAFs. Other genetic features include lack of *BCL2, RB1* and *TP53*[87,101,102]. Although non-malignant, desmoids present a major cause of morbidity and mortality among FAP patients due to their aggressive invasion into local structures and recurrence after local excision[99]. Same as GAF, desmoids may indicate the initial manifestation of FAP[86].

Table 1. Summary of immunohistochemical findings reported for Gardner-associated fibromas.

lesion (no. investigated)	**positive reactivity for**	**negative reactivity for**	**study**
GAF (10)	CD34 (8/10) vimentin (1/10)	smooth muscle actin muscle specific actin desmin	*Wehrli 2001*[86]
GAF (25)	β-catenin (16/25) cyclin D1 and c-myc (both: 25/25)		*Coffin 2007*[46]
GAF (1; patient 2)	CD34 vimentin	smooth muscle actin muscle specific actin desmin S100	*Lanckohr 2010*[90]
NTF (10)	vimentin	smooth muscle actin muscle specific actin S100, EMA (epithelial membrane antigen) GFAP (glial fibrillary acidic protein)	*Michal 1999*[93]
NNTF (1)	vimentin	Smooth muscle actin muscle specific actin desmin S100 cytokeratin	*Michal 2000*[92]
NTF+other fibroma	CD34 (NTF) vimentin (NTF+other fibroma)	CD34 (other fibroma) muscle specific actin desmin S100 cytokeratins CAM5.2	*Michal 2004*[97]
ENTF	nuclear β-catenin cyclin D1 CD99+ vimentin (spindle cells) CD34	desmin EMA Ki 67 S100 smooth muscle actin smooth muscle myosin	*Linos 2011*[96]

3.4.2.5 Lipomas

Lipomas are benign neoplasias composed of mature white adipocytes originating from mesenchymal origin. Lipomas are the most common soft tissue tumors in the general population. The majority present as small (<5cm), painless masses in superficial tissue of trunk neck and extremities. They usually present in individuals aged 40-60 years and may be multiple in 5%. Lipomas occur more often in adipose individuals, but etiology is otherwise widely unknown[103]. Lipomas are known to be possibly associated with diseases

as familial multiple lipomatosis or the autosomal dominantly (*PTEN*) inherited Bannayan-Riley-Ruvalcaba syndrome. In FAP, lipomas describe one of the extracolonic manifestations of Gardner syndrome[104].

Relating to their development, among lipomas several chromosomal aberrations are known involving particular regions on 12q13-15, 6q21-23 and 13q[103]. Furthermore, at molecular level several changes have been reported such as an affection of the high motility group gene *HMGIC* (equal *HMGA2*), the fusion of this gene with *LPP* (LIM family protein), and the involvement of the phosphatidic acid phosphatase PPAP2B in translocations[103,105]. Mutations in the tumor suppressor *menin* (*MEN1*) were further reported to cause deregulation of PPARγ and lead therefore to lipoma development[106]. An influence of Wnt signaling is present due to anti-adipogenic effects and an inhibition of white and brown adipose tissue by Wnt 10b[107,108]. Although lipomas in FAP patients are often seen (in 25-50% of all FAP patients) and reported in several case reports, little is known about their proper development in association with the FAP disease.

3.4.2.6 Epidermal cysts

Epidermal cysts were described as the most common skin manifestation in FAP with a reported prevalence of 12-53%[15,22,51,109]. Besides Gardner syndrome, epidermal cysts may also occur associated with Gorlin syndrome or pachonychia congenita type 2[110]. Epidermal cysts, same as trichilemmal cysts, display a subtype of cysts of hair follicle origin[78]. They are keratin-filled epithelial-lined cysts and present as dermal or subcutaneous mobile nodules with a central punctum, that contains eosinophilic and keratinaceous debris. In sporadic cases epidermal cysts may occur at any site on the body surface. Epidermal cysts in FAP were for the first time extensively examined in 1975 and described to occur solitary or multiple and seldom large and disfiguring and to present before the initiation of intestinal symptoms[109]. Later on, FAP-associated epidermal cysts were reported to present with a clearly distinct pattern compared to sporadic epidermal cysts. Especially if they occur multiple, familial, in young patients and at unusual sites (e.g. limbs), they may be considered as a hallmark for Gardner syndrome[78]. Furthermore, in FAP epidermal cysts often present as mixtures of epidermal and trichilemmal cysts as well as pilomatricomas[78,79]. For this, they were found to be similar to follicular stem cells of the bulge area due to these particular features[111].

The major cause for the development in sporadic epidermal cysts is the plugging of pilosebaceous units. Furthermore, they may occur due to traumatic implantation of epidermal material into deeper tissue or due to proliferation of epidermal remnants along

epidermal fusion areas[110]. A particular etiology and pathogenesis of FAP-associated epidermal cysts has not been reported up to now.

3.5 Therapy and interest of FAP-associated skin lesions

Generally, therapy for all above mentioned cutaneous neoplasia is indicated for symptomatic cases or for cosmetic reasons. Especially surgery of desmoids is very controversial, as recurrences are frequent and often more aggressive[76,78,98]. For this, neoplasms as fibromas, lipomas and epidermal cysts are usually of little concern for the patients.

Due to their early occurrence in childhood and their obligate preceding of intestinal symptoms they were recently investigated by our group as potential presymptomatic markers for especially *de novo* FAP mutation carriers. This study prospectively investigated the prevalence of particular skin lesions (fibromas, lipomas, and epidermal cysts) in 56 confirmed adult *APC* mutations carriers compared to 116 healthy controls. Almost half of all examined FAP patients were found to present with at least one skin lesion, compared to one third of controls. Overall, only single or multiple lipomas as well as combined skin lesions were revealed to occur significantly more prevalent in FAP patients than in controls. In addition, lipomas were revealed to occur three times more often at a younger age (20-49 years age range). Nevertheless, due to their low diagnostic sensitivity (7-26%) such skin lesions were further dismissed as possible presymptomatic markers for FAP[22]. Based on such results, the question was raised if such skin lesions are actually FAP-specific.

The present work, in a second step, was supposed to deal with the basic understanding of the underlying molecular mechanisms of such skin neoplasms. This question was followed mainly for skin lesions occurring in FAP patients. However, this study could also reveal insights into the development of FAP lipomas compared to lipomas occurring in the general population.

4 MATERIAL AND METHODS

4.1 FAP patients and samples

The study included in total 18 skin biopsies (nine fibromas, six lipomas, and three epidermal cysts) that were taken from 16 FAP patients (63% males (10/16) and 37% females (6/16), mean age 55 years ranging from 26-75 years) (Table 2). These patients were members of one big Swiss cohort of FAP patients that have been clinically described before[22,54,112]. This large cohort included in total 56 adult FAP patients from 18 unrelated families, wherefrom 28 patients were members of one big family (family 1981) with germline mutation in exon 18n. Another 28 patients belonged to totally 17 unrelated families with germline mutations ranging from exon 7 to exon 18u. All 56 patients underwent whole-body examination with special regard to FAP-associated skin lesions by the same dermatologist, as well as ophthalmologic inspection to reveal the status of FAP-specific ophthalmic fundus lesions (CHRPE) by the same ophthalmologist. Diagnosis of cutaneous lesions was based upon clinical findings by a clinically experienced dermatologist. From 16 of the totally 56 FAP patients, skin biopsies have been taken and were chosen to be further examined in the present study. These 16 FAP patients were members of eight unrelated families with confirmed germline mutations ranging from *APC* exon 7 to exon 18u. Seven patients belong to the big 1981 family (Figure 5) and another four patients indicated direct relatives within two families (Figure 6). Another five patients were members of independent families.

Skin lesions have been excised by a 4mm punch from different parts of the body by the same dermatologist. Fibromas were mostly localized at the neck (56%, 5/9) but also at the back (22%, 2/9) or the retroauricular region (22%, 2/9). Lipomas were biopsied mostly from the arm (50%, 3/6) but also from the back, lumbar region and thigh (17% each, 1/6). The three epidermal cysts were localized at the axilla (33%, 1/3) or at the back (66%, 2/3). Photographs of examined skin lesions are illustrated in Figure 7. From all FAP patients, biopsies have also been taken from healthy skin, directly adjacent to the skin lesion, as well as blood samples.

Properties of FAP patient and control samples that were used for analyses are listed in Table 2 and Table 3. Control samples were taken from healthy individuals, that neither had anamnestic evidence for FAP nor had a personal history of colorectal cancer, that were commonly consulting the surgical facility of our dermatology department. Four control skin samples of epidermal and dermal tissue were included (ED25, ED22, D21, D25) that were biopsied in addition next to the underlying neoplasm. Five other control samples included lipoma samples of otherwise healthy patients (non-FAP patients that were 60% males (3/5)

and 40% females (2/5), with mean age of 52 years, ranging from 35-68 years). These lipoma samples were localized at the arm (60%, 3/5) or at the shoulder (20%, 1/5); one sample was a pooled sample of different lipomas localized at the arm, thorax and thigh (20%, 1/5). All control skin samples were also diagnosed based upon clinical findings by a dermatologist. Finally, two blood samples have been included (RNA1 and RNA4) that were also taken from otherwise healthy (non-FAP) individuals. From all individuals, written informed consent was obtained according to the guidelines of the Ethical Committee of Basel (EKBB), Switzerland (EK258/05 and EK15/08).

Table 2. Properties of FAP patients and biopsies included in analyses.

patient ID	biopsy analyzed	localization	sex	age	germline mutation nucleotide change	germline mutation amino acid change
28 - 2008	fibroma	neck	female	71	c.1682_1683insA	p.Lys561fs*19
33 - 2008	fibroma	neck	female	26	c.5942delA	p.Asn1981fsX62
36 - 2008	fibroma	retroauricular	male	64	c.4778delA	p.Lys1593Serfs*57
41 - 2008	fibroma	back	male	46	c.2925_2926delAA	p.Lys975fs*9
43 - 2008	fibroma	retroauricular	female	70	c.5942delA	p.Asn1981fs*62
47 - 2008[a]	fibroma lipoma	neck lumbal	male	46	c.531+2_531+3insT	p.Arg141Ser*7
02 - 2009	fibroma	back	male	55	del ex 13-18	[?][b]
26 - 2009	fibroma	neck	female	53	c.5942delA	p.Asn1981fs*62
30 – 2008[a]	fibroma epidermal cyst	neck upper back	male	34	c.5942delA	p.Asn1981fs*62
29 - 2008	lipoma	thigh	female	42	c.1682_1683insA	p.Lys561fs*19
37 - 2008	lipoma	arm	female	38	c.1370C>G	p.Ser457*
22 - 2009	lipoma	arm	male	66	c.5942delA	p.Asn1981fs*62
35 - 2009	lipoma	back	male	73	c.5942delA	p.Asn1981fs*62
55 - 2010	lipoma	arm	male	75	c.531+2_531+3insT	p.Arg141Ser*7
21 - 2009	epidermal cyst	axilla	male	65	c.5942delA	p.Asn1981fs*62
38 - 2009	epidermal cyst	back	male	50	c.7932_7935delTTAT	p.Ile2644fs*7

[a]patients 47-2008 and 30-2008 had two different skin lesions removed (fibroma and lipoma, fibroma and epidermal cyst, respectively); [b]large submicroscopic deletion

Table 3. Properties of control biopsies included in analyses.

sample ID	biopsy	underlying skin lesion	localization	sex	age
ED25	healthy epidermis	BCC[a]	forehead	n.a.	n.a.
ED22	healthy epidermis	BCC	n.a.	n.a.	n.a.
D21	healthy dermis	SCC[b]	n.a.	n.a	n.a.
D25	healthy dermis	BCC	forehead	n.a	n.a.
40-2012	lipoma	lipoma (same)	arm, thorax, thigh (pooled)	male	60
43-2012	lipoma	lipoma (same)	arm	male	42
44-2012	lipoma	lipoma (same)	arm	male	35
2013-003	lipoma	lipoma (same)	arm	female	68
2013-014	lipoma	lipoma (same)	shoulder	female	53
RNA 1	blood control non-FAP	-	-	n.a.	n.a.
RNA 4	blood control non-FAP	-	-	n.a.	n.a.

[a]BCC: basal-cell carcinoma; [b]SCC: squamous-cell carcinoma; n.a.: not available

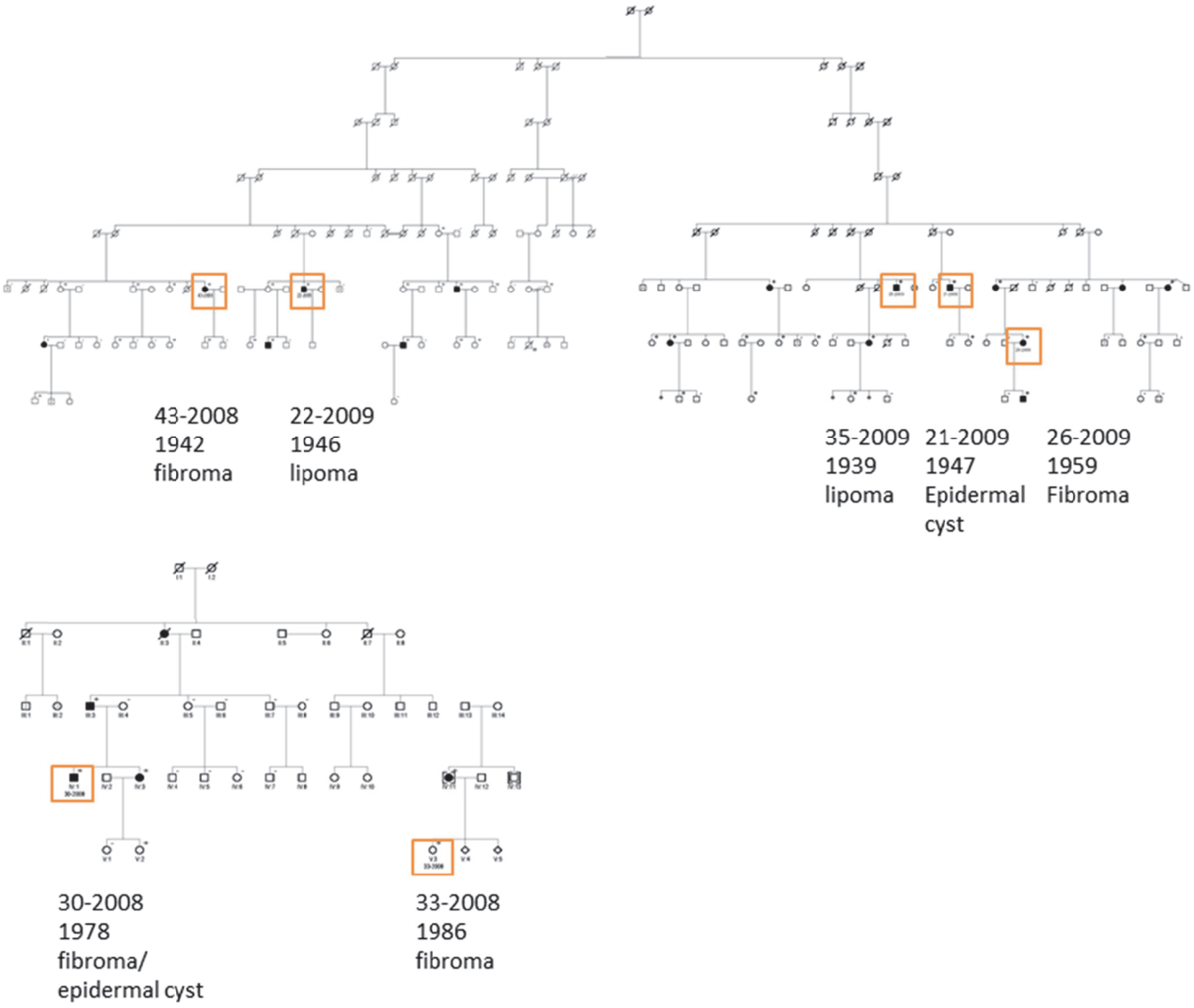

Figure 5. Extracts of 1981 FAP pedigree. Illustration shows members of a big FAP family pedigree that are all affected by the same germline mutation at codon 1981. Seven members of this kindred that were included in the present study are indicated by an orange frame with annotations of patient ID, year of birth, and type of examined skin lesion. Patients affected by colorectal polyposis are indicated by black squares (males) or circles (females); superscript $^{+}$ indicates known *APC* mutation carriers.

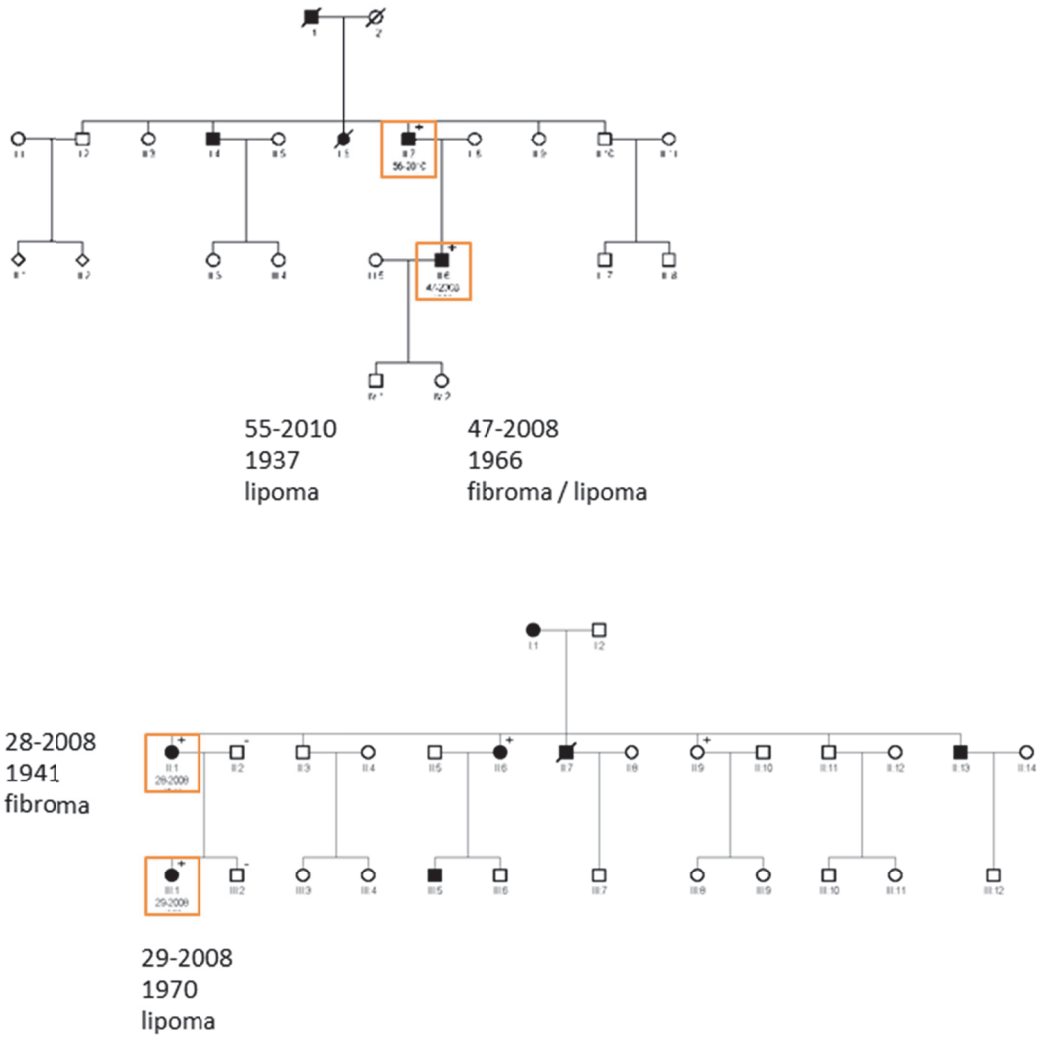

Figure 6. Pedigrees of FAP patients with germline mutations at codon 141 and within intron 7. Illustration depicts members of two FAP family pedigrees with affected germline mutation at codon 141 or within the intervening sequence next to exon 7. Both pedigrees account for direct relatives that were included in the present study. Those patients are indicated by an orange frame and are annotated with patient ID, year of birth, and type of examined skin lesion. Patients affected by colorectal polyposis are indicated by black squares (males) or circles (females); superscript $^{+}$ indicates known *APC* mutation carriers.

Figure 7. Photographs of examined fibromas (1-7)**, lipomas** (8-12)**, and epidermal cysts** (13-15). Pictures are sorted from left to right and top to bottom; localization is indicated in brackets. **1.** 28-2008 fibroma (nuchal, paramedian right), **2.** 36-2008 fibroma (retroauricular right), **3.** 41-2008 fibroma (back), **4.** 43-2008 fibroma (retroauricular), **5.** 47-2008 fibroma (nuchal), **6.** 02-2009 fibroma (back), **7.** 30-2008 fibroma (nuchal), **8.** 47-2008 lipoma (lumbal), **9.** 29-2008 lipoma (thigh), **10.** 22-2009 lipoma (arm), **11.** 35-2009 lipoma (back), **12.** 55-2010 lipoma (arm), **13.** 30-2008 epidermal cyst (upper back), **14.** 21-2009 epidermal cyst (shoulder), **15.** 38-2009 epidermal cyst (upper back). No pictures were available for 33-2008 fibroma (nuchal), 26-2009 fibroma (nuchal), and 37-2008 lipoma (arm).

4.2 Sample preparation

Skin biopsies were manually separated by scalpel in their dermal and epidermal parts before nucleic acids were isolated. Importantly to remark is, that by this method it was not possible to totally exclude the presence of small amounts of dermis within the epidermal part. Dermis samples were supposed to be pure dermal. This separation was done to enable a specific application for the particular skin neoplasm. Therefore, relating to the origin of the specific skin lesion, we applied dermis samples for fibromas and epidermis samples for epidermal cysts. For lipomas either dermal (FAP patients) or lipoma lipid tissue (non-FAP lipoma controls) was applied, according to the particular type of lipoma biopsy. Directly after biopsies have been taken, fresh skin samples were put into RNAlater® (Ambion®, Carlsbad, CA) a RNA stabilization solution for short storage at 4-8°C before nucleic acids were isolated.

4.3 Nucleic acid isolations

For FAP patients, RNA and DNA were isolated from lesional and healthy skin biopsies as well as from blood. Control samples revealed only lesional and healthy skin biopsies. RNA was isolated from all fresh human skin biopsies using mirVana™ miRNA isolation kit according to the manufacturer`s instructions (Ambion®, Carlsbad, CA). RNA samples were treated by the TURBO DNA-free™ Kit (Ambion®, Carlsbad, CA) to remove possible DNA contaminations. The DNA was sequentially isolated using the remaining lysate from the RNA isolation following specifications of the TRI Reagent® DNA/protein isolation protocol (Ambion®, Carlsbad, CA). For FAP patients, DNA was also isolated from fresh blood samples (EDTA) by the salting-out method[113]. RNA control samples (RNA1 and RNA4) of leukocytes from two independent, healthy probands have been provided by Karl Heinimann (Research Group Human Genetics, Department of Biomedicine and Division of Medical Genetics, University Hospital Basel, Switzerland). These samples have been isolated using Trizol and Chloroform, followed by purification according to specification of the RNeasy® Plus Mini Kit (Quiagen, Germany).

4.4 Analyses of second hits in *APC*

4.4.1 Direct sequencing of the mutation cluster region of *APC*

For verification of the patient specific *APC* germline mutation, DNA samples of FAP skin biopsies were examined by direct sequencing. All samples were further analyzed for mutations within the *APC* mutation cluster region (MCR; Figure 8) covering sections f-i of exon 18 (codons 1139-1640). Primer sequences for PCR reactions are as previously described[27]. All used primer sequences are listed in Supplementary Table 1 to Supplementary Table 3. PCR reactions were performed following specifications of the KAPA2G™ Fast HotStart PCR kit (Kapabiosystems, Woburn, MA) with fast PCR cycling conditions (initial denaturation 94°C 3min; 35 cycles denaturation 95°C 30s, annealing 15s and elongation 72°C 10s; and final extension 72°C, 10min) or the *Taq* PCR Core Kit (Qiagen, Germany) with stardard conditions (initial denaturation 94°C 5min; 35 cycles denaturation 94°C 45s, annealing 45s and elongation 72°C 45s-1min; and final extension 72°C, 10min) and primer-adjusted annealing temperatures. Purified PCR products (NucleoSpin® Gel and PCR Clean-up, Macherey-Nagel, Germany) were subjected to bidirectional sequencing using the BigDye® Terminator v3.1 Cycle Sequencing Kit and ABI PRISM® 3130xl Genetic Analyzer (Applied Biosystems, Foster City, CA) or were sent for sequencing (Microsynth AG, Switzerland). Sequences were analyzed using Mutation Surveyor® software v3.24 (Softgenetics®, State College, PA) and were illustrated by FinchTV v1.4.0 (Geospiza Inc.; Seattle, WA).

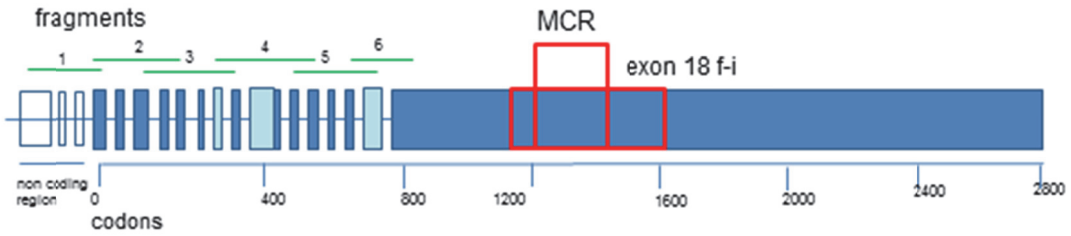

Figure 8. Illustration of *APC* with MCR and fragments used for cDNA analysis. The *APC* gene consists of 18 exons with 3 non-coding exons at the 5' end (white boxes) and 15 exons of the consensus coding sequence (blue boxes). Exons colored light blue as well as exons of the non-coding region are known to be alternatively expressed. Mutation cluster region (MCR, red box) and region covered by direct sequencing (exon 18 f-i, red box) and 6 exon-overlapping fragments used for *APC* cDNA analysis (green lines) are shown.

4.4.2 *APC* cDNA analysis

RNA samples were reverse transcribed by the Verso™ cDNA kit (Thermo Fisher Scientific, Waltham, MA) or by the Ovation® Pico WTA System (NuGEN Technologies, Inc., San Carlos, CA) according to manufacturers' protocol. Analysis of *APC* cDNA was performed with six exon-overlapping PCR fragments covering the full length gene (Figure 8). Primers were designed with Primer 3[114,115] and were received from Microsynth (Microsynth AG, Switzerland). Primer sequences are listed in Supplementary Table 4. PCR reactions were performed following specifications of the *Taq* PCR Core Kit (Qiagen, Germany). Amplified PCR products were separated on 2% agarose gels, and additional bands were sequenced directly after purification.

4.4.3 Microsatellite analysis

Microsatellite analysis was done using the dinucleotide marker D5S346 (localized 31.7kb 3' of *APC* at chromosome position 5q22.2, Figure 9), and mononucleotide markers BAT25 (intron 16 of *c-kit* oncogene) and BAT26 (intron 5 of *MSH2* mismatch repair gene). Initially, blood samples of all FAP patients were checked for a heterozygous allele pattern of D5S346 before skin lesions were investigated. PCR reactions were performed with FAM- (D5S346, BAT26) or HEX-labeled (BAT25) primers (Supplementary Table 5). Reactions were following specifications of the *Taq* PCR Core Kit (Qiagen, Germany) with microsatellite standard cyling protocol: initial denaturation 94°C 2min, 10 cycles 94°C 15s, 55°C 15s, 72°C 30s, another 20 cycles 89°C 15s 55°C 15s, and 72°C 30s, and a final extension step 72°C 10min. Primers for D5S346 were designed by Primer 3 software and received by Microsynth (Microsynth AG, Switzerland), primers for BAT25 and BAT26 were kindly provided by Karl Heinimann (Research Group Human Genetics, Department of Biomedicine and Division of Medical Genetics, University Hospital Basel, Switzerland). For fragment separation, PCR products with standard dye GeneScan™-500 ROX™ (Applied Biosystems, Foster City, CA) were loaded on an ABI PRISM® 310 Genetic Analyzer (Applied Biosystems, Foster City, CA) following standard protocol. Fragment patterns were analyzed and illustrated using GeneMarker® software (Softgenetics®, State College, PA). Loss of heterozygosity (LOH) was determined by calculating the ratio between allele peak areas in lesional and healthy tissue. A reduction of >50% in relative intensity of one allele was regarded as LOH[116].

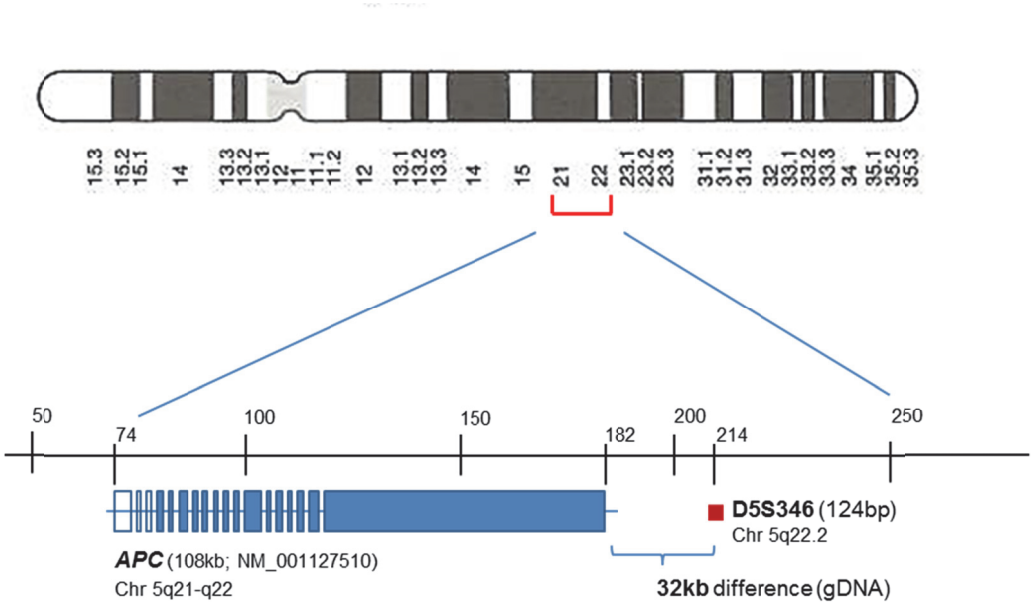

Figure 9. Localization of *APC* and microsatellite marker D5S346 at chromosome 5q. Illustration of the 108bp long *APC* gene (NM_001127510.2, var2) in relation to microsatellite marker D5S346 on human chromosome 5 gDNA. Scale in 112'000Kb gDNA. *Chromosome 5 adopted from Strachan and Read, 4th edition, 2011.*

4.5 Gene expression analyses

4.5.1 Patient setup

Differentially expressed genes (DEGs) in skin samples of benign tumors versus healthy skin were analyzed in four different groups, referring to the particular skin lesion occurring in FAP patients. Table 4 illustrates the different samples applied for each group. Grey indicated samples were only included either for microarray or qPCR analyses, but not both. Red indicated samples were excluded from array analysis (28-2008 healthy dermis of group 1, and 38-2009 healthy epidermis of group 4) due to differing Quality Assessment/Quality Control (QA/QC) histogram profiles compared to other samples within the same group (Supplementary Figure 1). Furthermore, for patient 29-2008 in group 2, no healthy sample could have been included as a pure dermis sample was not available. The first group considered gene expression differences between five fibroma and seven healthy dermis samples of totally seven FAP patients. For microarray analysis, paired fibroma and healthy samples were included from four FAP patients (30-2008, 41-2008, 47-2008, 02-2009) together with the fibroma sample of patient 28-2008. The healthy sample of 28-2008 was excluded due to differing QA/QC histogram profile compared to the other samples. The number of healthy dermis samples was expanded by two additional samples revealed from independent FAP patients (22-2009 and 35-2009) in terms of significance.

Quantitative real time PCR (qPCR) was run for all five paired FAP patients (28-2008, 30-2008, 41-2008, 47-2008, 02-2009). The healthy skin sample of 28-2008, not usable for calculation of microarray data was assumed to be suitable for qPCR analysis due to fine RNA quality (RIN: 7.3). The second group considered gene expression differences between six lipoma and five healthy dermis samples of totally six FAP patients. For microarray runs, paired lipoma and healthy samples were included for five FAP patients together with the lipoma sample of patient 29-2008. The healthy sample of 29-2008 was not included in neither of the two expression analyses as a pure dermis sample was not available. qPCR runs focused on the five paired lipoma and healthy samples . In the third group, gene expression of the same six FAP lipoma samples were compared to three lipoma samples revealed from non-FAP individuals (40-2012, 43-2012, 44-2012). qPCR runs on FAP vs. non-FAP lipoma samples were based upon highest changed targets revealed for group 2 (FAP lipoma vs. FAP healthy). These runs included two additional non-FAP lipoma samples (2013-003, 2013-014) that have not been received until later during the study. Lipoma sample 29-2008 could not be included for qPCR analyses due to lack of material. Important to mention is that the type of lipoma biopsy tissue derived from FAP patients compared to such gained from non-FAP patients differed from each other. Lipomas from FAP patients were mostly dermis isolates whereas lipoma samples from non-FAP individuals were isolated from pure lipid tissue (pure lipoma). This observation leads to the suggestion that different lipoma types exist in FAP and non-FAP individuals. The last group related to differential gene expression between three epidermal cyst and three healthy epidermis samples of totally four different FAP patients. For microarray runs, paired lesional and healthy samples could be included for two FAP patients (30-2008, 21-2009) together with the epidermal cyst of 38-2009. The healthy sample of 38-2009 was excluded due to differing QA/QC histogram profile compared to the other samples. For this, another suitable healthy sample was additionally included revealed from an independent FAP patient (26-2009). For this group no qPCR runs were performed.

Table 4. Patient samples applied for gene expression analyses. Patient samples selected for calculations of differential gene expression between lesional and healthy skin of FAP patients are illustrated in the following table. Calculations on differential gene expression between benign skin tumors and healthy were done for 4 different groups: **1.** fibroma vs. healthy dermis (all FAP), **2.** lipoma vs. healthy dermis (all FAP) **3.** lipoma from FAP patients vs. lipoma from non-FAP controls and **4.** epidermal cyst vs. healthy epidermis (all FAP). Arrays were determined to be suitable for analyses considering QA/QC histograms. Samples excluded due to differing histograms are marked in red. Samples indicated in grey were only applied for either microarray or qPCR runs (see text). Runs relating to fibroma and lipoma samples, applied samples isolated from pure dermal tissue (or pure lipid tissue for lipoma controls), whereas runs relating to epidermal cyst samples applied samples isolated from epidermis.

1. FAP fibroma samples	FAP healthy dermis samples
28-2008 fibroma dermis	28-2008 healthy dermis*
30-2008 fibroma dermis	30-2008 healthy dermis
41-2008 fibroma dermis	41-2008 healthy dermis
47-2008 fibroma dermis	47-2008 healthy dermis
02-2009 fibroma dermis	02-2009 healthy dermis
-	22-2009 healthy dermis
	35-2009 healthy dermis

2. FAP lipoma samples	FAP healthy dermis samples
29-2008 lipoma dermis	-
37-2008 lipoma dermis	37-2008 healthy dermis
47-2008 lipoma dermis	47-2008 healthy dermis
22-2009 lipoma dermis	22-2009 healthy dermis
35-2009 lipoma dermis	35-2009 healthy dermis
55-2010 lipoma dermis	55-2010 healthy dermis

3. FAP lipoma samples	non-FAP lipoma samples
29-2008 lipoma dermis	40-2012 lipoma
37-2008 lipoma dermis	43-2012 lipoma
47-2008 lipoma dermis	44-2012 lipoma
22-2009 lipoma dermis	2013-003 lipoma
35-2009 lipoma dermis	2013-014 lipoma
55-2010 lipoma dermis	

4. FAP epidermal cyst samples	FAP healthy epidermis samples
30-2008 EC epidermis	30-2008 healthy epidermis
21-2009 EC epidermis	21-2009 healthy epidermis
38-2009 EC epidermis	38-2009 healthy epidermis
-	26-2009 healthy epidermis

*28-2008 healthy was included in qPCR runs (fine bioanalyzer profile with RIN: 7.3)

4.5.2 Whole genome expression analysis

4.5.2.1 RNA sample preparation and hybridization to Affymetrix microarrays

Isolated RNA samples were quantitatively measured by the Qubit™ RNA Assay with the Qubit® 2.0 Fluorometer (Life Technologies™, Carlsbad, CA) according to manufacturer's protocol. RNA quality was determined using Agilent RNA 6000 Pico Kit running on the Agilent 2100 Bioanalyzer (Agilent Technologies, Santa Clara, CA). Integrity of the RNA was visualized by the ratio of the ribosomal 18S and 28S subunits and determined by the RNA integrity number (RIN). Generally RIN numbers of 7 and higher and/or acceptable electrophoretic trace were determined to be adequate for array load. However, also some RNA samples of lower RIN numbers were included and were later specially considered in array integrated quality check (QA/QC histogram).

RNA samples were each amplified and reverse transcribed with starting amounts of 30ng by the Ovation Pico WTA System V1 or V2 (NuGEN Technologies, Inc., San Carlos, CA) reaching final concentrations of around 400ng/ul. Complementary DNA was biotinylated using amounts of 4.5ug cDNA each, by the Encore™ Biotin Module. Resulting biotin labeled cRNA fragments were hybridized to the GeneChip® Human Gene 1.0 ST or 2.0 ST Array (Affymetrix Ltd., UK) on the GeneChip® Hybridization Oven 645 (Affymetrix Ltd., UK). Unspecific fragments were removed by washing off the arrays. Arrays were stained by streptavidin-phycoerythrin (SAPE) and biotinylated anti-streptavidin antibody. Washing and staining operations were performed on the GeneChip® Fluidics Station 450 (Affymetrix Ltd., UK). Labeling was further done with a SAPE (StreptAvidin PhycoErythrine) complex that binds to the biotin molecules. Arrays were scanned on a GeneChip® Scanner 3000 7G (Affymetrix Ltd., UK). An overview of the expression assay process as well as an image of the particular Affymetrix GeneChips® which were applied in the present study may be seen in Figure 10. These arrays are synthetic oligonucleotide microarrays in which DNA probes (applying only perfect match (PM) probes) with lengths of 25bp (25-mer probes) are produced by photolithographic synthesis on a silica substrate. They cover the whole human transcript with totally over 36 000 and 40 000 RefSeq transcripts for the HG 1.0 ST, and HG 2.0 ST GeneChip®, respectively[117].

All experiments have been supported by Philippe Demougin from the Life Sciences Training Facility Division of Molecular Psychology at the Biozentrum of the University of Basel.

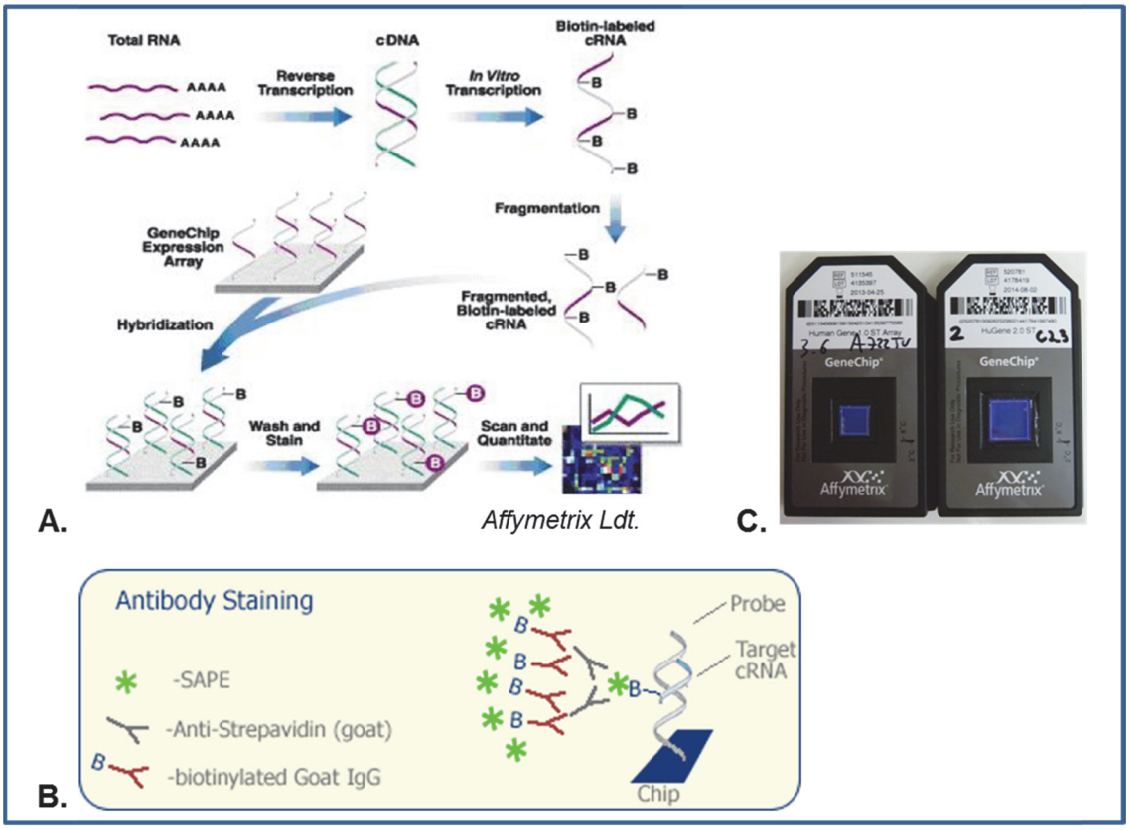

Figure 10. Steps of the expression assay and Affymetrix GeneChips®. Isolated RNA is reverse transcribed to cDNA. Before loading the array, cDNA is back transcribed to cRNA, biotinylated and fragmented to pieces between 30 to 400bp. The sample is then loaded on the array and unspecific fragments are washed away (**A.**). For visualization with laser scanning, fragments are stained with SAPE (StreptAvidin PhycoErythrine), that bind through streptavidine to the biotin molecules, augmented by anti-streptavidin antibodies, that again bind streptavidine (**B.**). Picture of the two Affymetrix GeneChips® Human Gene 1.0 ST and Human Gene 2.0 ST Array which were applied in the present study (**C.**). *Illustration adopted from German Cancer Research Center (http://www.dkfz.de/gpcf/24.html) and Oregon Health and Science University (http://www.ohsu.edu/xd/research/research-cores/gene-profiling-shared-resource/project-design/array-technology/affymetrix-genechip-arrays.cfm).*

4.5.2.2 Microarray data analysis

The Affymetrix GeneChip® CEL data files were processed applying Partek® Genomics Suite™ (Partek Inc., St. Louis, MO). For normalization of the raw data, the Robust Multi-Array Averaging (RMA) method was applied. **RMA** performs background correction only on probe intensities of perfect match (PM) probes followed by quantile normalization and multichip summarization, a summarization at the probe set level. **Background correction** aims to adjust for optical background noise and for unspecific binding (intensity not related to hybridization). For this, it applies the median intensity of specific background probes to estimate the background signal for each probe set. **Quantile normalization** was used to correct for systematic array differences (non-biological variation) within and between arrays. This method adjusts the probe level intensities in a way that they are identically distributed for all arrays. For this, it forces the distribution of the PM values to be the same for every array in an experiment[118,119]. **Quality assessment** of the gene chips was done with Partek® Genomic Suite™ by means of three different graphical representations. First, the scanned pseudo array image was inspected to identify any low-quality arrays (artefacts) or outliers. In a second step, array normalization was checked by observing box plots that represent the array intensity distribution before and after normalization. And last, a histogram plot was inspected, that shows the distribution of gene intensities across all samples and the distribution of the array intensities across all genes. Latter was also used to identify any outliers. As a first complex visualization overview of the final chip data in relation to each other and in relation to the whole human genome, we applied **Principal components analysis (PCA**) scatter plot. This exploratory multivariate statistical technique for simplifying complex data reduces dimensionality by performing a covariance analysis between factors. PCA “summarizes” overall data and is used to uncover unknown trends in gene expression data (to identify predominant gene expression patterns) and to explore correlations between samples[120]. **Calculations of DEGs** between benign skin lesion and healthy skin were run in different groups, separating the particular neoplasms, namely fibromas, lipomas and epidermal cysts as can be seen in Table 4. Differential gene expression was assessed by analysis of variance (**2-way ANOVA**) applying methods of moments for balanced data sets of same size (epidermal cyst) and restricted maximum likelihood (REML) for unbalanced data sets with different sample sizes in the lesional and healthy group (fibroma, lipoma). ANOVA is a multivariate statistic tool, that calculates the overall variability of a multi-group experiment by employing multiple estimates of a population’s variance. For each group, two estimates of variance are taken, namely the standard deviation of each group and the variability between means of each group. Probability values are then calculated by deviding the population variance estimate of the

means by the population variance estimate of the standard deviations[121,122]. The **False discovery rate (FDR)** indicates an additional multiple comparison correction for multi-hypotesis testing analyses such as microarray experiments. FDR is generally recommended to be of at least 0.1, indicating a false positive rate of 10%[123,124]. Fisher's Least Significant Difference (LSD) was used as a linear contrast method, doing pairwise comparisons of the means, for calculation of the levels in gene expression difference (**-fold changes**) between lesional and healthy skin samples. Based on these data, gene lists are established for the different groups by setting a minimum (FDR)-unadjusted p-value <0.05 and a minimum -fold change of at least 1.5. For further data processing, stringency of significance cut-offs and -fold changes were gradually increased. Established gene lists were analyzed in terms of hierarchical clustering by Partek® Genomic Suite™. **Gene ontology (GO) and pathway analyses** on significant DEGs were done with the Database for Annotation, Visualization and Integrated Discovery (DAVID) v6.7[125] and Ingenuity pathway analysis software (IPA®; Ingenuity Systems, Inc.; Redwood City, CA). These analyses were used to validate the received data regarding their biological relevance.

4.5.3 Reverse transcription quantitative PCR (qPCR) analysis

4.5.3.1 Sample preparation and qPCR run setup

Selected RNA samples for fibroma, lipoma and corresponding healthy skin samples were reverse transcribed by the Verso™ cDNA kit (Thermo Fisher Scientific, Waltham, MA) using equal amounts of 180ng RNA per 20µl reaction. qPCR was run with SYBR® green chemistry following specifications of the Power SYBR® Green PCR Master Mix (Life Technologies™, Carlsbad, CA). For each reaction, 10µl 2x Power SYBR® Green PCR Master Mix were mixed with 1ul 5uM primer dilutions (250nM final primer concentration), and 1ul of the respective cDNA sample solution added with deionized water ad 20µl total reaction. Three technical replicates and one negative control with water instead of template cDNA were applied for each target. Reactions were run on MicroAmp® Optical 96-Well Reaction Plates (Life Technologies™, Carlsbad, CA). qPCR reactions were run on the ABI 7500 Fast Real-time PCR System (Life Technologies™, Carlsbad, CA) applying convenient cycle conditions of the system: 95°C preheating for 10min to activate polymerase, followed by 40 cycles of sample denaturation at 95°C for 15s for annealing and elongation at 60°C for 1min. At the end of every run, a dissociation-curve was established to detect possible unspecifics products by recording the decrease in fluorescence of the SYBR® Green dye due to the dissociation of double stranded DNA during melting.

4.5.3.2 Standard curve reactions for primer establishment

Primers for targets and house keeping genes (HKGs) were designed by Primer 3 software and NCBI Primer-BLAST based on human mRNA sequences (Table 5, Table 6). To prevent amplification of genomic DNA, primers were designed to overlap exon-intron junctions whenever possible. Primers were received by Microsynth (Microsynth AG, Switzerland). To check for primer efficiency and presence of unspecific products, standard curves were initially established for each target. For this, five dilutions (1:2) of pooled control samples with cDNA amounts of 0.056ng, 1.125ng, 2.25ng, 4.5ng and 9ng were applied. Efficiency for each target was calculated by means of linear regression using ABI 7500 software v.2.0.6 (Life Technologies™, Carlsbad, CA). Primer concentrations were calibrated and set to an optimal concentration of 250nM per reaction. As control samples, pooled samples consisting of equal amounts of dermis controls D21 and D25, or out of the three non-FAP lipoma controls 43-2012, 44-2012, 2013-003 (Table 3) were applied to establish the fibroma runs or the lipoma runs, respectively.

Table 5. Properties of established qPCR primer sets for fibroma qPCR runs. Primers for validation of selected mRNA targets for FAP fibroma vs. healthy dermis, with target IDs colored in black (HKGs), red (expected up-regulated targets) or blue (expected down-regulated targets). Primers were designed to overlap exon-intron junctions whenever possible. C_T values at threshold 0.2 were applied for further calculation. Efficiency was calculated by means of linear regression based on standard curve results. R^2 values refer to the target specific stability. Values of at least 0.95 were determined as acceptable. *CHL1* was accepted despite lower R^2 value (stable qPCR runs, nice melting curves).

gene ID	type	product size	primer no (fwd/rev)	exon overlap	threshold	primer conc	R^2	efficency (%)
HPRT1	HKG	63	279/280	no (ex 3)	0.2	250nM	0.996	103
TBP	HKG	57	281/282	no (ex 1)	0.2	250nM	0.99	99.27
GAPDH	HKG	60	273/274	yes (ex 5-6)	0.2	250nM	0.995	87.52
GUSB	HKG	81	31/32	yes (ex 11-12)	0.2	250nM	0.971	108
S100B	target	86	463/464	no (ex 3)	0.2	250nM	0.988	113
CDH19	target	90	479/480	yes	0.2	250nM	0.952	93.31
HMCN1	target	78	495/496	yes (ex 19-20)	0.2	250nM	0.996	100.5
CHL1	target	125	483/484	yes (ex 14-15)	0.2	250nM	0.898	106.08
SERPINE2	target	130	485/486	yes (ex 8-9)	0.2	250nM	0.957	109
SPRR2E	target	126	563/564	no (ex 2)	0.2	250nM	0.995	100.345
CST6	target	108	461/462	yes (ex 1-2)	0.2	250nM	0.996	110
SPINK5	target	63	465/466	no (ex 1)	0.2	250nM	0.986	99.64
CARD18	target	74	487/488	yes (ex 2-3)	0.2	250nM	0.996	91.3
ABHD5	target	95	489/490	yes	0.2	250nM	0.998	92.86
CLDN1	target	93	497/498	yes (ex 1-2)	0.2	250nM	0.99	101.6
DSP	target	120	493/494	yes (ex 13-14)	0.2	250nM	0.981	127

Table 6. Properties of established qPCR primer sets for lipoma qPCR runs. Primer IDs are colored in black (HKG) or red (expected up-regulated targets). Primers were designed to overlap exon-intron junctions whenever possible. C_T values at threshold 1 were applied for further calculation. *SLPI* was separately calculated for threshold 0.2 (with HKGs set accordingly to threshold 0.2). Efficiency was calculated by means of linear regression based on standard curve results. R^2 values refer to the target specific stability. Values of at least 0.95 were determined as acceptable.

gene ID	type	product size	primer no (fwd/rev)	exon overlap	threshold	primer conc	R^2	efficency (%)
HPRT1	HKG	63	279/280	no (ex 3)	1	250nM	0.995	99.536
GAPDH	HKG	60	273/274	ex 5-6	1	250nM	0.998	94.171
GUSB	HKG	81	31/32	ex 11-12	1	250nM	1	97.109
LRP10	HKG	81	539/540	ex 6-7	1	250nM	0.999	98.565
CLN3	HKG	148	557/558	ex 14-15	1	250nM	0.996	101.47
NELFB	HKG	114	543/544	ex 9-10	1	250nM	0.996	93.059
TMEM47	target	122	505/506	ex 2-3	1	250nM	0.988	100.504
RBP7	target	118	507/508	ex 1-2	1	250nM	0.988	100.983
DDX5	target	77	509/510	ex 12-13	1	250nM	0.995	100.957
MXRA5	target	125	511/512	ex 2-3	1	250nM	0.996	98.181
FABP4	target	95	513/514	ex 3-4	1	250nM	0.991	104.142
SFRP2	target	85	515/516	ex 1-2	1	250nM	0.998	107.184
SHOC2	target	129	547/548	ex 7-8	1	250nM	0.996	120.2
HIST1H1C	target	109	523/524	ex 1	1	250nM	0.993	84.405
UBE2R2	target	116	525/526	ex 1-2	1	250nM	0.994	113.146
SMARCA1	target	126	529/530	ex 17-18	1	250nM	0.985	112.681
SLPI	target	577/578	577/578	ex 1-2	0.2*	250nM	0.969	93.31

**SLPI* was separately calculated for threshold 0.2 (calculation and normalization with HKGs set accordingly to threshold 0.2).

4.5.3.3 Calculation of relative gene expression applying qbasePLUS software

For accurate normalization of the qPCR runs qbasePLUS software (Biogazelle, Belgium) was applied. This software uses a generalized model of the delta-delta-C_T approach that enables normalization of relative quantities with multiple reference genes and gene specific amplification efficiencies. Ideal housekeeping genes (HKGs) were selected based on their stability M-values, the average pairwise variation of a particular reference gene with all other reference genes. As the lower the M-values, the more stable the reference gene stability; housekeepig genes with higher stability M-values were subsequently excluded. Another stability measure, the coefficient of variation of the normalized reference gene expression levels (CV) was used to identifiy the ideal number of reference genes for normalization. For calculation of normalized gene expression values, qbasePLUS first calculated average quantity values of a sample for a given target across all samples for that given target (relative quantities, RQ) followed by normalization to the selected HKGs (calibrated normalized relative quantities, CNRQ)[126]. Those CNRQ values were illustrated as lesional relative to healthy samples and were further statistically evaluated using GraphPad Prism® software (GraphPad Software Inc., La Jolla, CA). Statistical analysis of differential regulation of target genes was done on the one hand between paired lesional and healthy samples of FAP patients by applying a 2-way ANOVA (fibroma group). On the other hand by applying Wilcoxon rank sum test, for unpaired samples to assess statistical significance for differentially regulated targets in FAP lipoma vs. FAP healthy skin and in FAP lipoma vs. control lipoma. ANOVA and Wilcoxon rank sum test were calculated based on sample means or medians, respectively. Wilcoxon rank sum test assumes non-parametric distribution of the expression data. Data are expressed as means (ANOVA) or medians (Wilcoxon rank sum test) and standard deviation.

5 RESULTS

5.1 *APC* second hit mutation analysis on skin biopsies of FAP patients

The survey of 15 FAP-associated skin lesions from confirmed *APC* mutation carriers for somatic alterations in *APC* revealed changes in two (13.3%) samples (Table 7). Bi-directional Sanger sequencing identified a heterozygous frameshift mutation in the epidermal cyst sample of patient 30-2008. This epidermal cyst sample as well as the lipoma of 29-2008, revealed both LOH at microsatellite marker D5S346 located close to *APC* as well as novel alleles for D5S346 indicating microsatellite instability (MSI).

Table 7. Overview of examined FAP patients, skin lesions, and observed somatic second hits. Somatic changes (including mutations in the MCR and microsatellite instability for D5S346) as well as the SNP rs41115 (c.4479G>A) are shown in the last column on the right with same results for skin and leukocytes, if not assigned differently. The tissue samples with the identified second hits are accentuated in bold.

patient ID	skin biopsy analyzed	sex	age	*APC* germline mutation		SNP rs41115 somatic second hit
28-2008	fibroma	female	71	c.1682_1683insA	p.Lys561fs*19	SNP heterozygous
33-2008	fibroma	female	26	c.5942delA	p.Asn1981fsX62	SNP heterozygous
36-2008	fibroma	male	64	c.4778delA	p.Lys1593Serfs*57	SNP homozygous A
41-2008	fibroma	male	46	c.2925_2926delAA	p.Lys975fs*9	SNP n/a
43-2008	fibroma	female	70	c.5942delA	p.Asn1981fs*62	SNP n/a
47-2008	fibroma	male	46	c.531+2_531+3insT	p.Arg141Ser*7	SNP heterozygous
02-2009	fibroma	male	55	del ex 13-18	[?][a]	SNP n/a
26-2009	fibroma	female	53	c.5942delA	p.Asn1981fs*62	SNP heterozygous
30-2008	fibroma	male	34	c.5942delA	p.Asn1981fs*62	SNP heterozygous/ homozygous G[b]
30-2008	**epidermal cyst**	male	34	c.5942delA	p.Asn1981fs*62	SNP heterozygous/ homozygous G[b] **second hit c.4778delA MSI + LOH for D5S346**
21-2009	epidermal cyst	male	65	c.5942delA	p.Asn1981fs*62	SNP heterozygous
38-2009	epidermal cyst	male	50	c.7932_7935delTTAT	p.Ile2644fs*7	SNP homozygous G
29-2008	**lipoma**	female	42	c.1682_1683insA	p.Lys561fs*19	SNP heterozygous **MSI + LOH for D5S346**
22-2009	lipoma	male	66	c.5942delA	p.Asn1981fs*62	SNP homozygous G
35-2009	lipoma	male	73	c.5942delA	p.Asn1981fs*62	SNP heterozygous

[a]large submicroscopic deletion; [b]polymorphism difference in patient 30-2008 for SNP rs41115: SNP heterozygous in cutaneous tissue (fibroma, epidermal cyst, healthy skin), and SNP homozygous G in leukocytes.

5.1.1 Bi-directional sequencing of the mutation cluster region of *APC*

For each skin biopsy (benign neoplasms and healthy skin) from FAP patients, particular frameshift germline mutation was confirmed by sequencing of the mutated region of the *APC* gene. Sanger sequencing of the MCR on 13 FAP skin lesions revealed no mutation in sections f-h (codons 1139-1499) of exon 18. In section i (codons 1471-1640), we identified

one second hit mutation (c.4778delA; Figure 11) in the epidermal cyst of patient 30-2008 that leads to a frameshift with a predicted premature stop codon occurring 57 amino acids downstream (p.Lys1593Serfs*57).

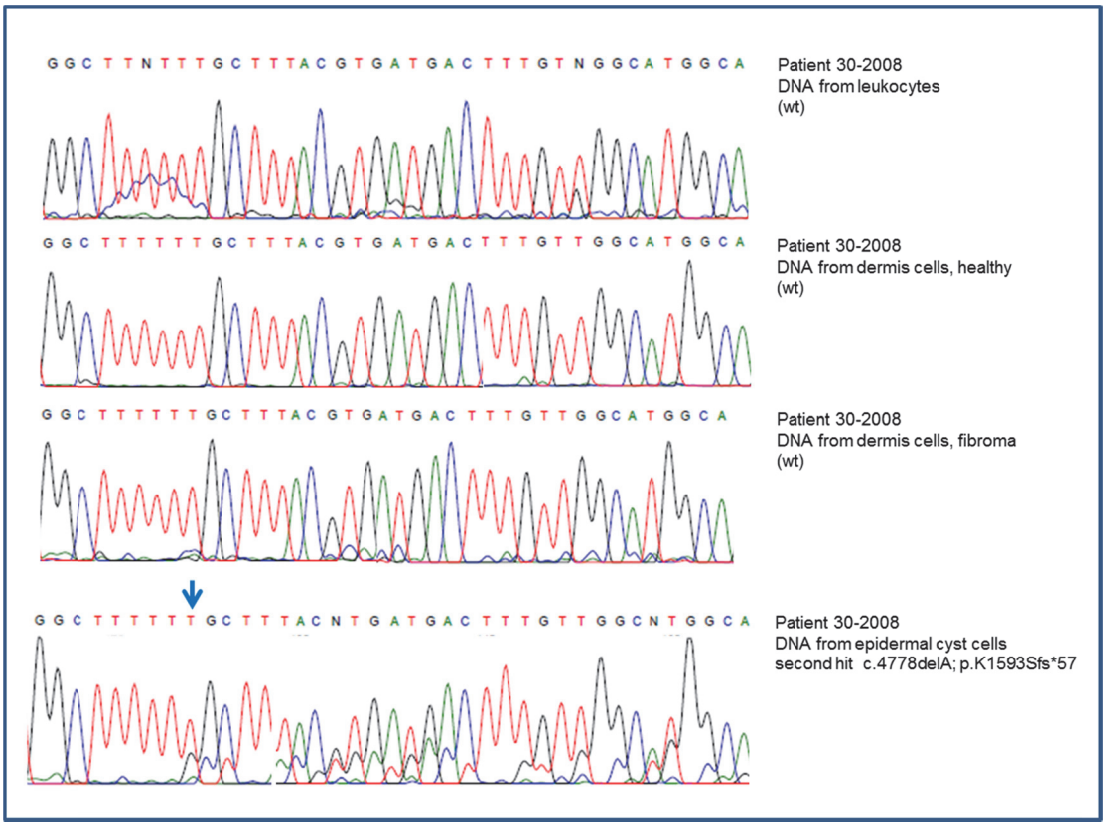

Figure 11. Direct sequencing results of exon 15i for different tissues of 30-2008. Direct sequencing of *APC* exon 15i in different tissues from patient 30-2008 revealed wildtype sequence in gDNA from leukocytes, healthy dermis, and fibroma dermis. The epidermal cyst tissue showed a heterozygous deletion of an adenine at codon position c.4778 resulting in a frameshift. The blue arrow indicates the start of the one base pair deletion c.4778delA for the genomic DNA sample derived from epidermal cyst tissue. This heterozygous deletion is predicted to lead to a frameshift with premature stop codon after 57 amino acids.

5.1.1.1 Genomic variability for SNP rs41115 in exon 18i

Within the region of exon 18i, a particular SNP rs41115 (c.4479G>A) is known to be localized. This SNP has been reported by another study to be correlated with a lower risk of localized prostate carcinoma[127]. In the present survey, a genetic variation for this SNP among the examined FAP patient samples was observed coincidentally by sequencing of the MCR. Relating to gDNA samples derived from skin, altogether 8 patients were heterozygous for this SNP, one patient revealed a homozygous pattern, and 2 other patients showed the wildtype sequence (MAF/minor allele count: A=0.454/10). Interestingly, for patient 30-2008 somatic mosaicism for SNP rs41115 (c.4479G>A) was observed in the patient's leukocytes (homozygous G) compared to cutaneous tissue

samples such as healthy dermis, fibroma dermis, and epidermal cyst tissue (heterozygous G/A; Figure 12). A profiling analysis for several samples of this patient confirmed the results and excluded a possible confusion of patient samples. In addition, for the epidermal cyst sample of this patient, SNP rs41115 was identified to be laid on the same allele as the second hit c.4778delA (Figure 12B). Furthermore, the c.4778delA mutation was also present as a germline alteration in another patient (36-2008; Table 7). Possible DNA sample mix-up could be excluded by DNA profiling and analysis of the corresponding tissue samples (data not shown).

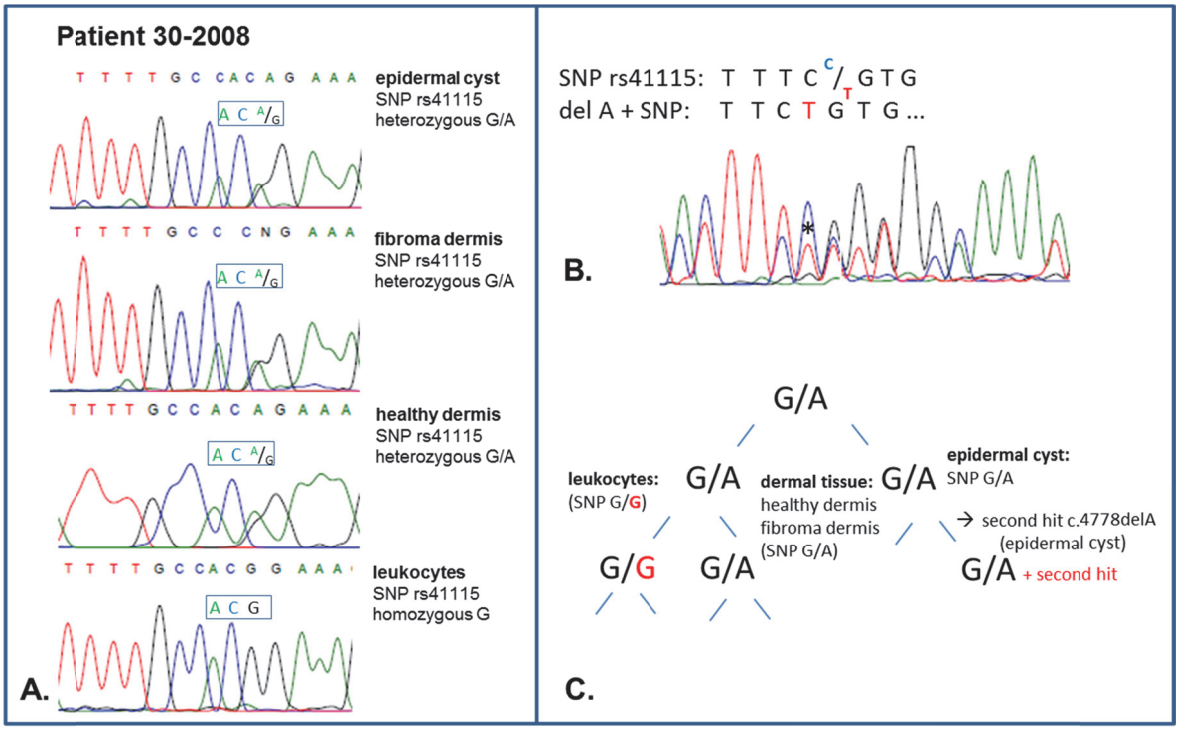

Figure 12. Sequencing results for the region around SNP rs41115 (c.4479G>A) in exon 15i. **A.** For patient 30-2008, cutaneous tissue samples revealed a heterozygous G/A pattern for the SNP (first three sequences), whereas leukocytes revealed homozygous G. **B.** Result from direct sequencing of 30-2008 epidermal cyst, illustrating that the SNP lies on the same allele as the second hit mutation. Illustrated reverse sequence indicates the shifted allele caused by c.4778delA, together with the SNP rs41115 (c.4479G>A) located at the same (shifted) allele (black asterisk). The shifted allele displays the mutated A nucleotide (T in the reverse sequence) of the SNP, that overlays the regular C nucleotide of the wt allele. The colocalization of all three (C, G, and T) nucleotides for the right peak besides the asterisk-marked C/T is the result of the additional presence of cells with the SNP on the wt allele. **C.** Cartoon of a possible development of somatic mosaicism in 30-2008 with the genotype G/G arisen in leukocytes and G/A in dermis and epidermal cyst tissue.

5.1.2 Exon-overlapping analysis revealed several *APC* isoforms in skin

Transcript analysis of *APC* should result in six fragments spanning the total cDNA. For all 15 included skin lesion samples (nine fibromas, three lipomas, and three epidermal cysts) in total five fragments with expected full-length could be identified (Table 8, Figure 13 to Figure 18). In place of the first expected fragment, covering exons 1-4 (626bp), we identified two smaller products generated by deletion of exons 2 and 3, and additionally of the 3' part of exon 1 (Figure 13). In addition, eight further alternative products were detected with six of them for all samples analyzed and two of them for a particular patient due to his germline mutation (Figure 14 and Figure 15), resulting from alternative splicing. Most of these alternatively spliced products (6/10) originated from deletions of parts of or entire exons whereas a minority (3/10) resulted from an insertion. Another product arose from the combination of the insertion and deletion also identified independently in two other products for fragment 4 (Figure 16D).

Table 8. Transcripts resulting from *APC* cDNA analysis.

fragment	*APC* region exons	expected transcript	splice products	caused by	reference
1	1-4	626bp[a]	451bp 218bp	deletion exons 2 and 3 deletion ex1 (233bp 3'), ex 2 and 3	Thliveris *et al,* 1994[128] Thliveris *et al,* 1994[128]
2	4-8	609bp	686bp 500bp[b]	insertion exon 4A deletion exon 7	De Rosa *et al*, 2007[129] Neklason *et al*, 2004[130]
3	6-11	629bp	520bp[b]	deletion exon 7	Neklason *et al*, 2004[130]
4	10-14	666bp	720bp 420bp 363bp	insertion exon 13A insertion exon 13A + deleted 303bp of 5' exon 12 deletion 303bp of 5' ex 12	Sulekova and Ballhausen, 1995[131]; Xia *et al*, 1995[132] Sulekova *et al*, 1995[133] Groden *et al*, 1991[27]
5	13-17	506bp	560bp	insertion exon 13A	Sulekova and Ballhausen, 1995[131]; Xia *et al*, 1995[132]
6	16-18	565bp	350bp	deletion exon 17	Sulekova *et al*, 1995[133]

[a]the full length 626bp transcript could not be detected in any sample because of skipping of exons 2 and 3; [b]only for patient 47-2008

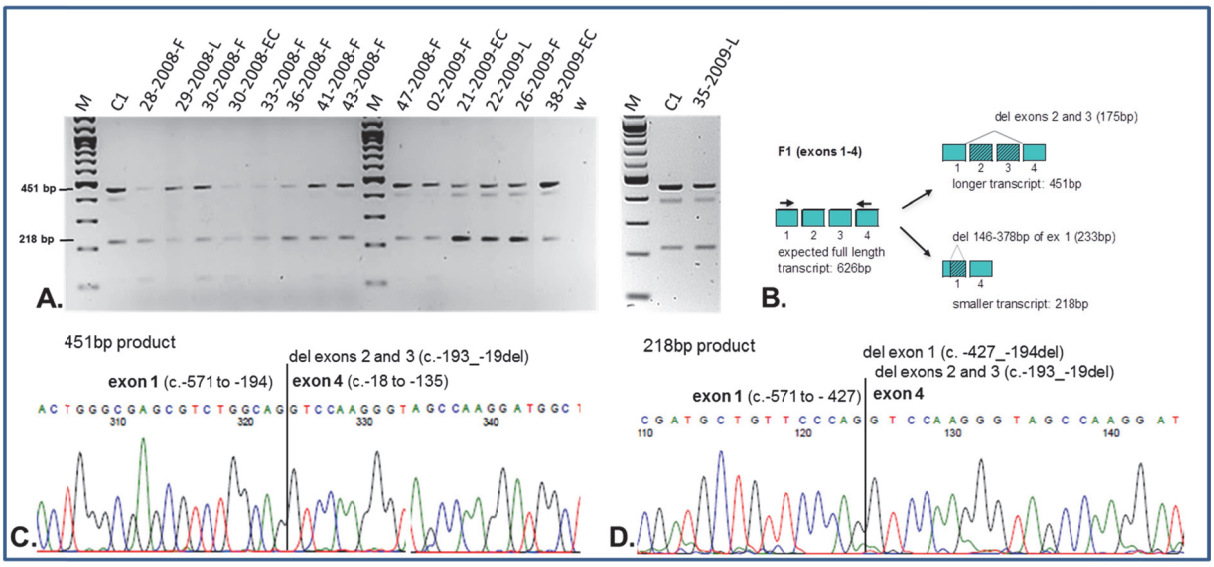

Figure 13. Gel image and schematic representation of splice products in fragment 1. A. PCR results for fragment 1 revealed different splice products of 451bp and 218bp length for all FAP skin samples and two controls from epidermal tissue and leukocytes (only epidermal tissue control C1 is shown). 35-2009-L was repeated with a new cDNA sample because of degradation (separate gel). The expected full-length transcript was not observed in any sample. The weak band at approximately 400bp was identified as a hybrid sequence joining the 451bp and the 218bp product. **B.** Illustration of the composition of the expected and aberrant transcripts. **C.** Sequencing result of the 451bp product indicates a deletion of exons 2 and 3 (c.-193_-19del) **D.** Sequencing result for the shorter 218bp product revealed an additional deletion of the 3' 233bp of exon1 (c.-427_-194del).

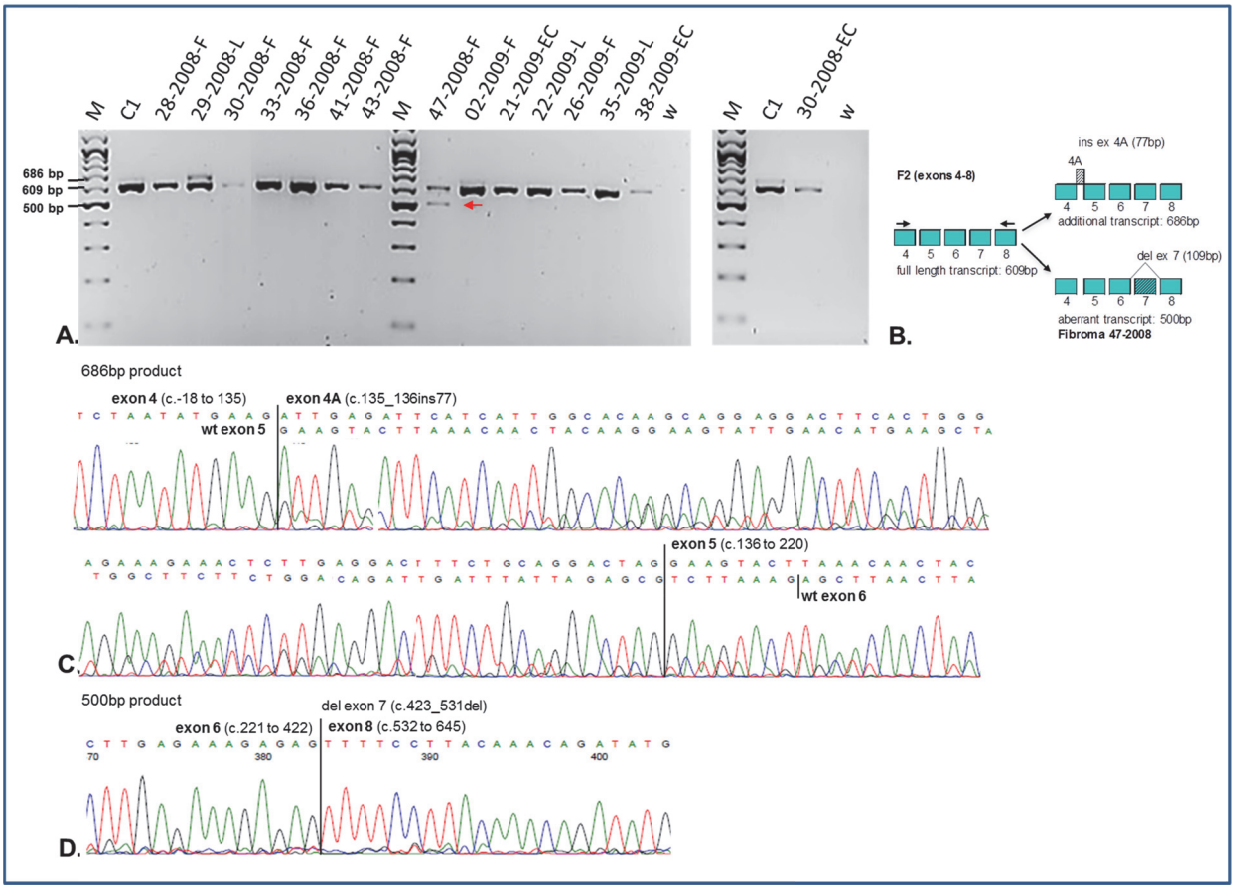

Figure 14. Gel image and schematic representation of splice products in fragment 2. A. Expected full-length product (609bp) consisting of exons 4-8 was observed in all samples. Also a longer product (686bp) was weakly but commonly present in all samples. One single additional bond at 500bp (red arrow) was observed for the fibroma sample of patient 47-2008 only. **B.** Illustration of the composition of the expected and aberrant transcripts. **C.** Sequencing results of the 686bp band revealed an inserted exon 4A (c.135_136ins77). **D.** The shorter 500bp product (red arrow) was only present for the fibroma sample of patient 47-2008. Sequencing of this product revealed a deletion of exon 7 (c.423_531del), the consequence of the patient's germline splice site mutation.

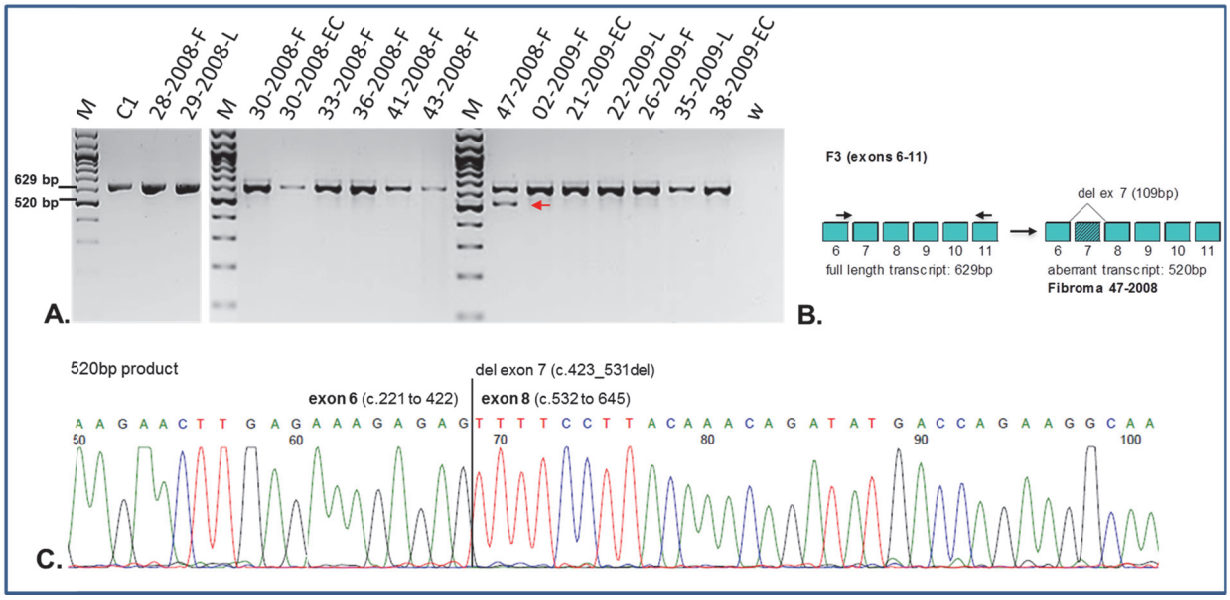

Figure 15. Gel image and schematic representation of splice products in fragment 3. A. Full-length 629bp product covering exons 6-11 was present in all skin samples. One single additional bond at 520bp (red arrow) was observed for the fibroma sample of patient 47-2008 only. **B.** Illustration of the composition of the expected and aberrant transcript **C.** Sequencing result of this shorter 520bp band indicates a total deletion of exon 7 that confirmed the patient's germline splice site mutation (c.531+2_531+3insT). The same result was also revealed by fragment 2, covering the same region (Figure 14).

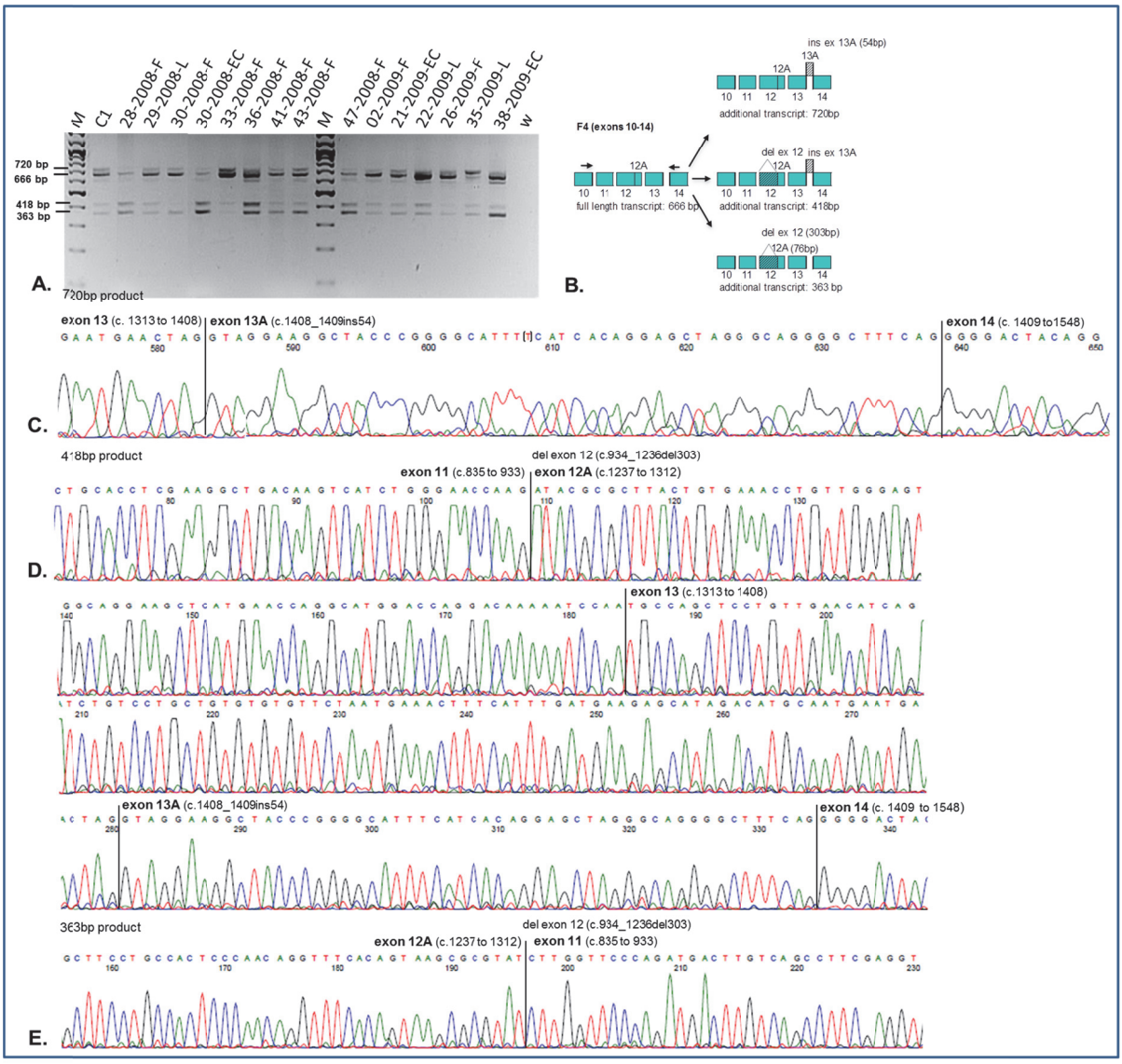

Figure 16. Gel image and schematic representation of splice products in fragment 4. A. PCR results for fragment 4 revealed the expected full-leng product (666bp) together with three different additional products (720bp, 418bp, 363bp) present in all skin samples. **B.** Illustration of the composition of the expected and aberrant transcripts. **C.** Sequencing result of the longest 720bp band revealed an insertion of exon 13A (c.1408_1409ins54). **D.** Sequencing result of the 418 product indicated the same deletion of exon 13A in addition with a deletion of 303bp 5' exon 12 (c.934_1236del303). **E.** Sequencing result of the 363bp band revealed the same deletion of 5' exon 12 (c.934_1236del303).

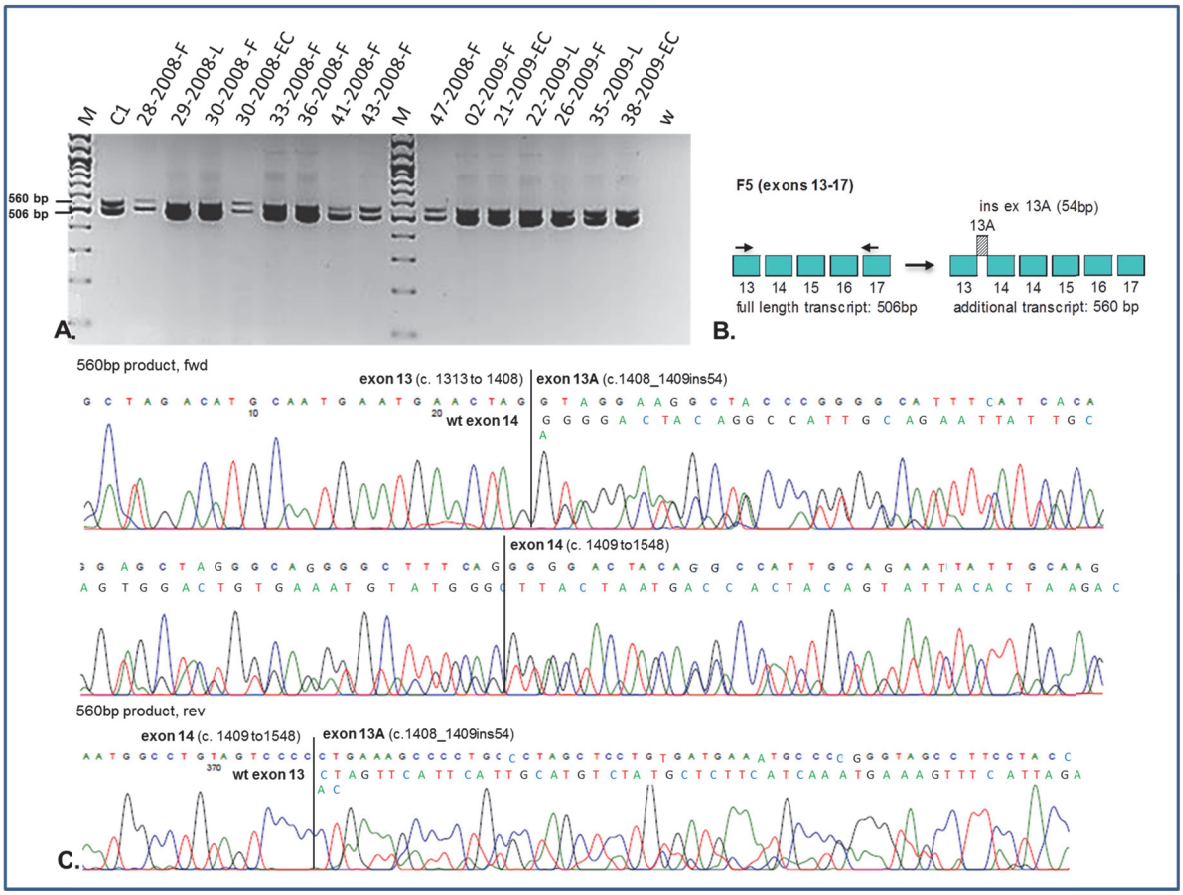

Figure 17. Gel image and schematic representation of splice products in fragment 5. A. PCR results for fragment 5 revealed for all samples two products: the expected 506bp product covering exons 13-17 and an additional product indicated by a band at 560bp length. **B.** Illustration of the composition of the expected and aberrant transcript. **C.** Sequencing results of the 560bp band indicated an insertion of exon 13A (c.1408_1409ins54). The same result was also revealed by fragment 4, covering the same region (Figure 16).

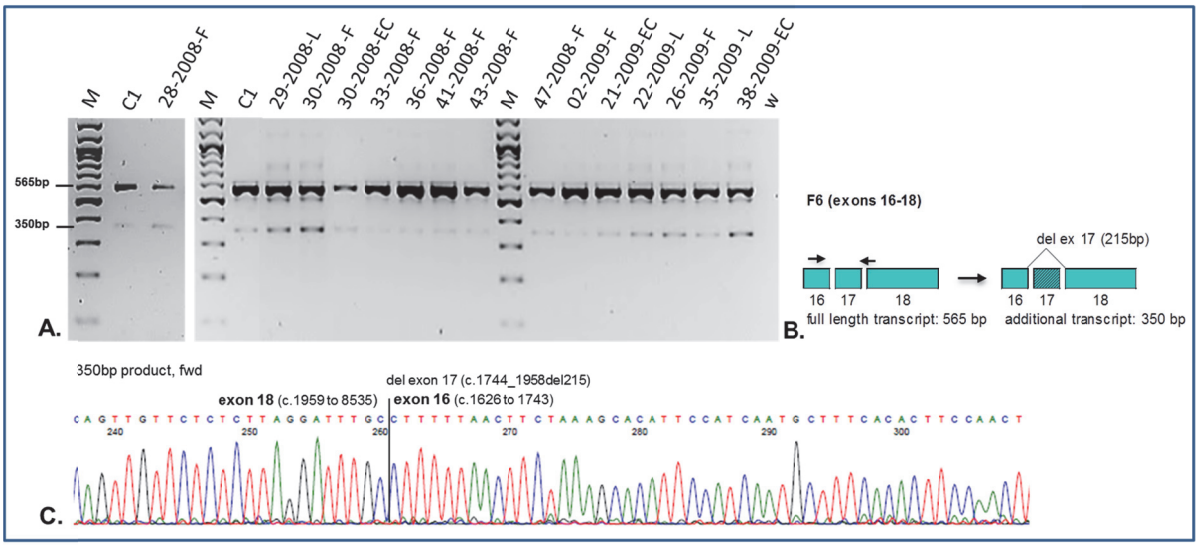

Figure 18. Gel image and schematic representation of splice products in fragment 6. A. For fragment 6, all samples revealed the expected 565bp full-length product covering exons 16-18 as well as a shorter additional product of 350bp length. **B.** Illustration of the composition of the expected and aberrant transcript. **C.** Sequencing results for the shorter 350bp band indicated a deletion of exon 17 (c.1744_1958del215).

5.1.3 Microsatellite analysis of marker D5S346 revealed LOH and instability patterns in two patient samples

For microsatellite analysis 12 skin lesion samples (six fibromas, three lipomas, three epidermal cysts) were analyzed. In two of them, one lipoma (29-2008) and one epidermal cyst (30-2008), evidence for LOH as well as MSI at marker locus D5S346 was found (Figure 19). To check for MSI in general, we additionally analyzed the mononucleotide markers BAT25 and BAT26 which are particularly sensitive in the detection of MSI. No evidence for MSI at BAT25 or BAT26 was found. Marker analysis of blood and healthy skin samples of these patients revealed normal heterozygous patterns, as observed in all other FAP patient samples (Figure 20, Figure 21).

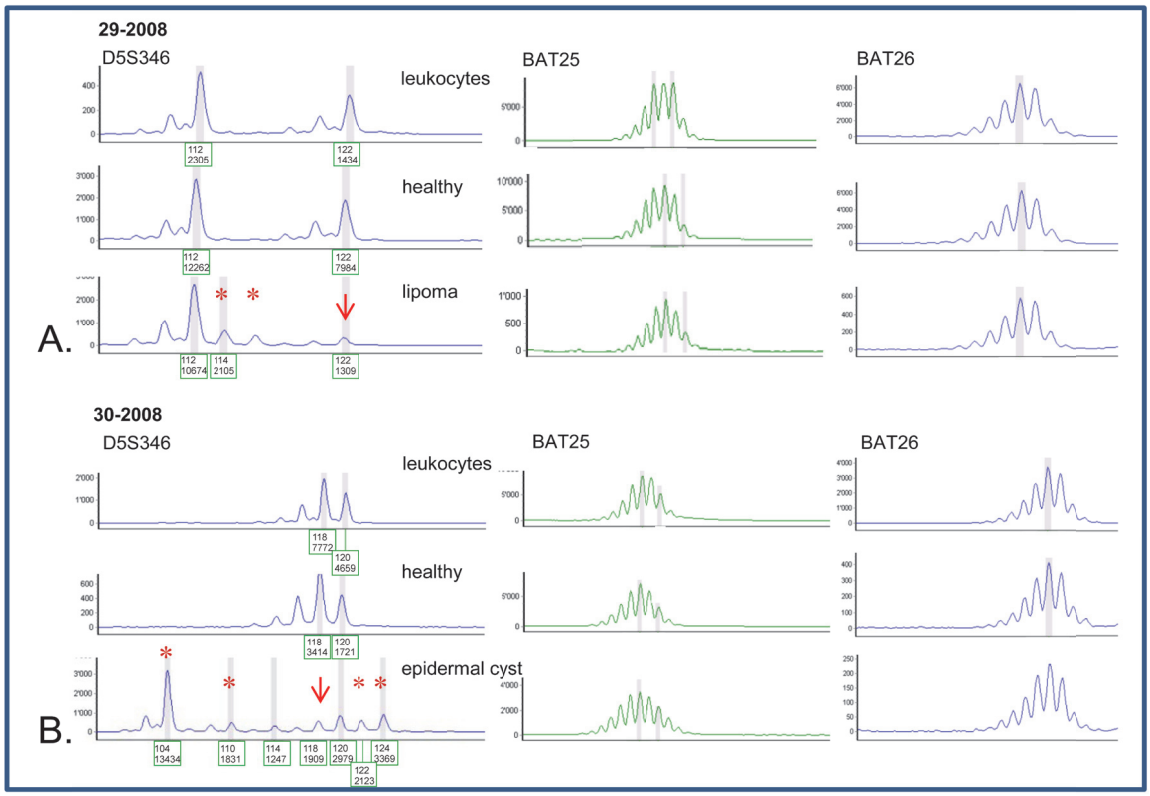

Figure 19. Patterns of microsatellite markers D5S346, BAT25, and BAT26 in 29-2008 lipoma and 30-2008 epidermal cyst as well as their respective leukocyte and healthy skin tissues. Allele peaks are marked by their size and area. In both lesions aberrant allele patterns for marker D5S346 were observed: the lipoma (**A.**) and the epidermal cyst (**B.**) showed allelic loss (marked by red arrows) of approx. 80% and 50%, respectively, indicating loss of heterozygosity. In addition, both lesions displayed novel alleles (marked by red asterisks) indicative for microsatellite instability; analysis of mononucleotide markers BAT25 and BAT26, however, revealed stable allele patterns.

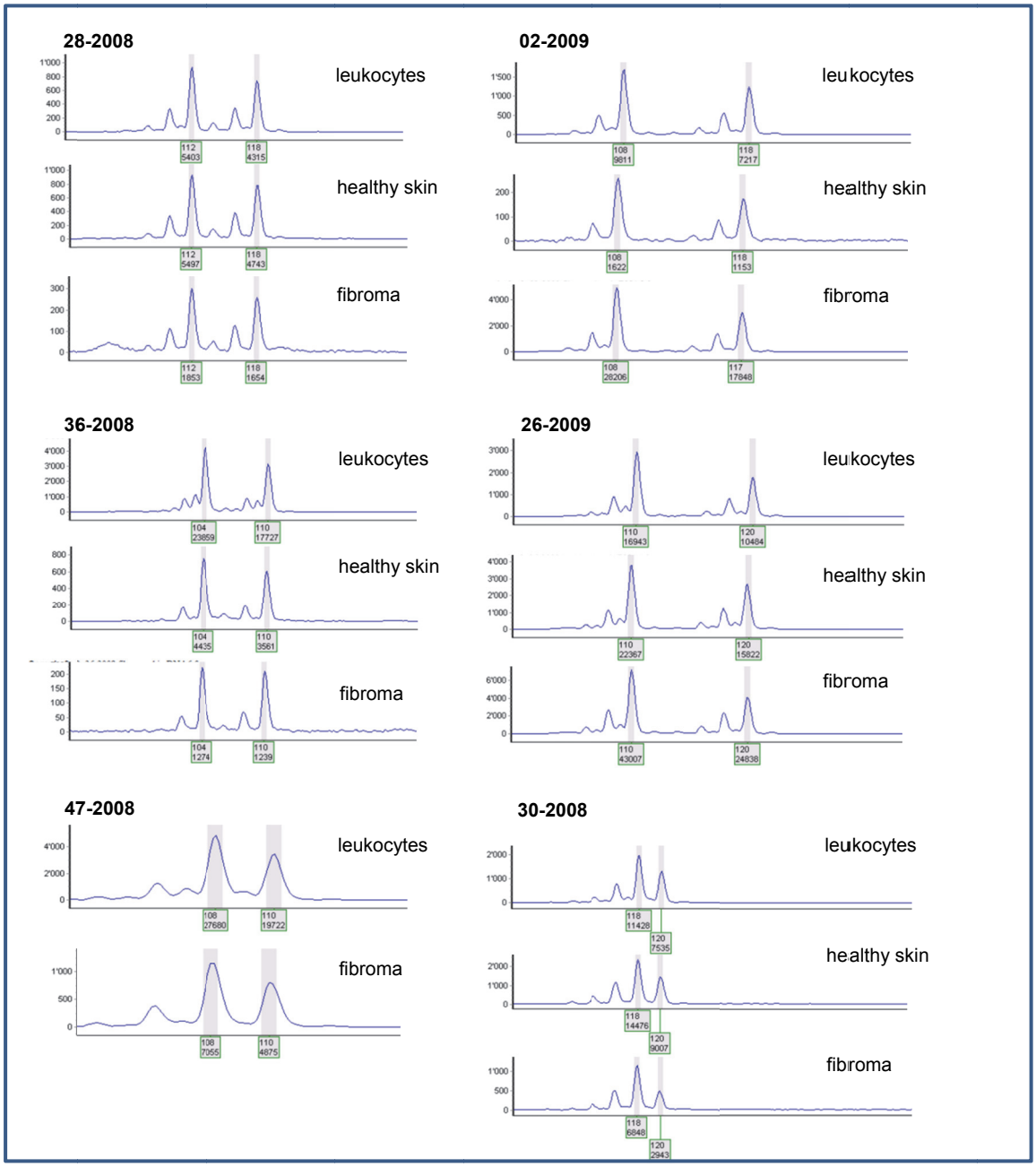

Figure 20. Illustration of normal heterozygous patterns of microsatellite marker D5S346 for all fibroma samples and their respective leukocyte and healthy skin tissues. Allele peaks are marked by their size and area. Results for 47-2008 healthy dermis were not suitable.

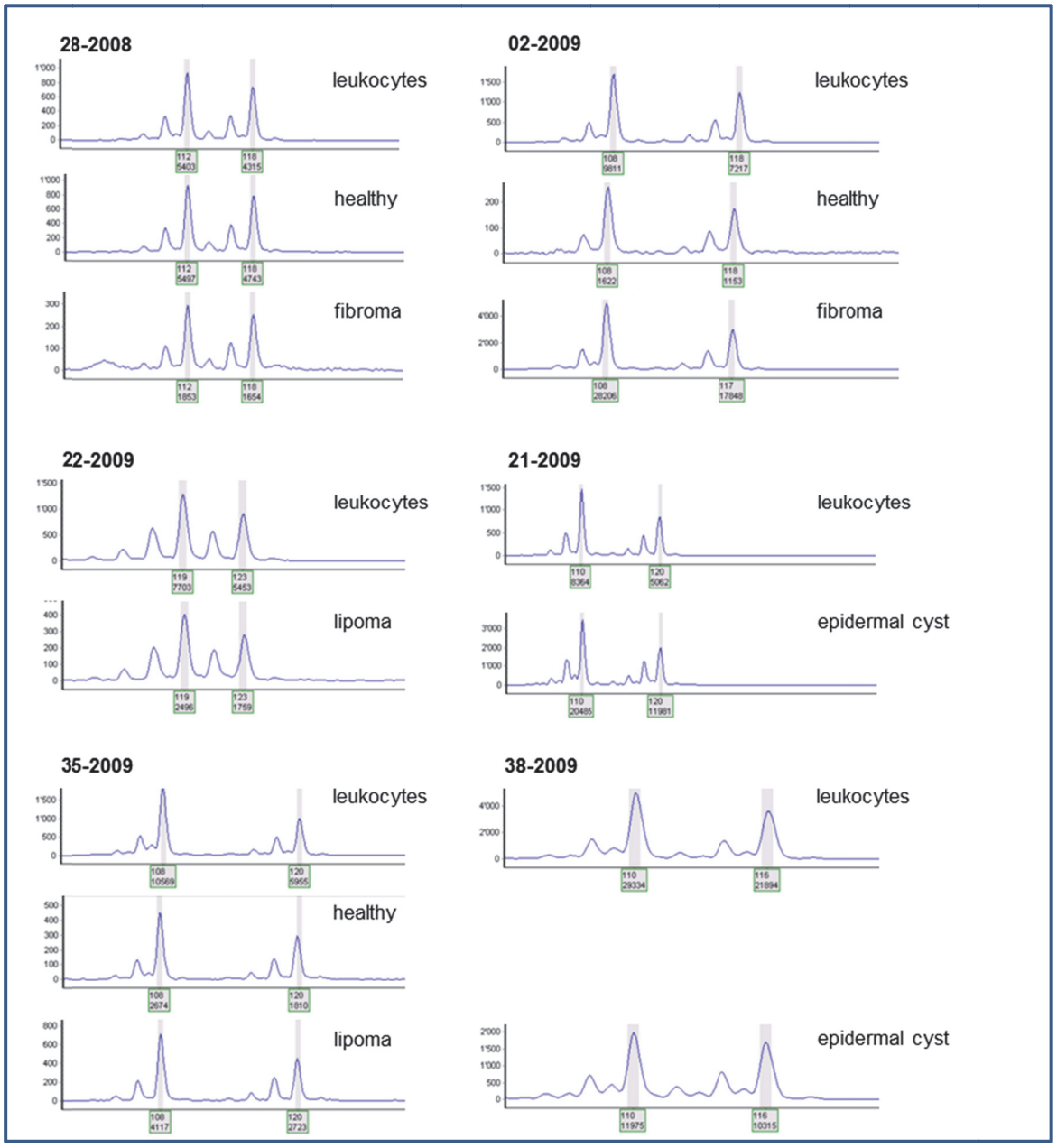

Figure 21. Illustration of normal heterozygous patterns of microsatellite marker D5S346 for all other lipoma and epidermal cyst samples and their respective leukocyte and healthy skin tissues. Allele peaks are marked by their size and area. Results for 22-2009, 21-2009, and 38-2009 healthy skin were not suitable.

5.2 Gene expression analysis

5.2.1 FAP fibroma vs. FAP healthy dermis

5.2.1.1 Whole genome expression analysis

Gene lists of differentially expressed genes (DEGs) in FAP fibroma vs. FAP healthy dermis were established based on expression intensities of **five fibroma and six healthy samples of seven FAP patients** that reached quality criteria as already described (Table 4). In total, 816 up- and 554 down-regulated genes were found to reveal differential gene expression concerning an FDR-unadjusted p-value <0.05. Since we could only analyze a small sample size, our datasets calculated from adjusted p-values will reach very high FDR values of 0.9 (for comparison of FAP fibroma vs. healthy skin), 0.35 (for FAP lipoma vs. healthy skin) or 0.8 (for FAP lipoma vs. control lipoma) if we would include a sufficient amount of genes. Therefore, the use of uncorrected p-values was decided to be practical for all analyses. Attention was also laid on a sufficient expression difference of at least 50% (relating to -fold changes of 1.5) and further approaches, such as GO- and pathway analysis, that were used to validate the received data regarding their biological relevance. Table 9 indicates the number of DEGs for -fold changes and significance levels.

Table 9. Numbers of DEGs in FAP fibroma vs. FAP healthy dermis. The table shows the number of DEGs for -fold changes and significance levels. Differences of expression intensities were indicated by -fold changes (fch). Detailed analyses were focused on gene expression differences of at least 2-fold (red frame).

	p-value <0.05	fch 1.5	fch 2	fch 3	p-value <0.01	fch 1.5	fch 2	fch 3
No. genes detected	(816↑, 554↓)	(77↑, 168↓)	(26↑, 70↓)	(8↑, 12↓)	164↑, 81↓)	(7↑, 36↓)	(3↑, 13↓)	-

As a first illustration of the total expression data of each chip, we used **Principal Components Analysis (PCA) scatter plot**. This plot shows the entire final chip data in relation to each other and in relation to the whole human genome. In PCA, by covariance analysis of the different factors, the high-dimensionality of the array data is reduced to a three dimensional grid illustrating the human genome. Within this grid each point represents a single chip. Points localized nearer to each other are supposed to have a similar overall gene distribution covering the whole human genom. Fibroma (red points) as well as healthy dermis samples (blue points) seemed to be scattered across the grid and do not show any clustering (Figure 22A). This means that samples of same tissue type (fibroma or healthy dermis) were likely not to show similar overall intensities, except of three healthy samples located at the center of the grid. In Figure 22B the same sample distribution is seen but labeled by *patient ID*. As can be seen, none of the corresponding

patient samples showed similar overall gene expression. The two grids indicated a homogenous scattering without obvious outliers. Furthermore, it refered to a **high inter-sample variation** which is well tolerable considering the source of human material and the low sample number examined.

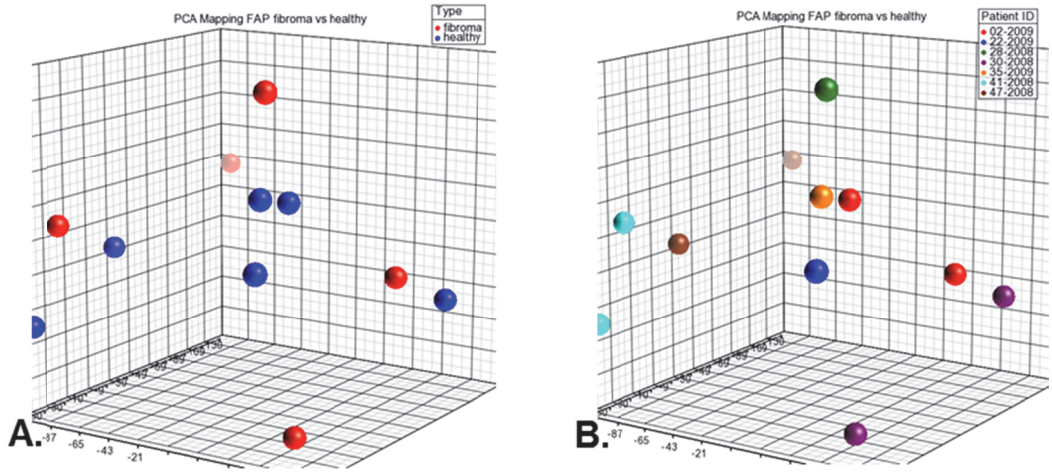

Figure 22. PCA scatter plot illustrating microarray chips of fibroma and healthy dermis samples from FAP patients. The grid shows the whole human genome and points represent single arrays. **A.** illustrates the distribution of fibroma (red points) and healthy skin samples (blue points). **B.** indicates the same distribution but assigns *patient IDs* to the chip samples. Axes represent the three components of the gene expression intensities.

5.2.1.1.1 Hierarchical clustering of mRNA expression data

We focused for further analyses on gene lists with FDR-unadjusted p-values <0.05 and expression differences of 2-fold and 3-fold, to ensure enough high expression changes between FAP fibroma and healthy dermis. Hierarchical clustering was calculated for totally 96 genes (26 up- and 70 down-regulated, Supplementary Table 6) with 2-fold expression change and FDR-unadjusted p-value <0.05. The heat map (Figure 23) indicated a **consistent clustering** of up- or down-regulated genes in fibroma vs. healthy skin. Gene expression patterns consistently appeared for all samples except for two fibroma samples (patients 30-2008 and 47-2008). Their patterns were either differing in genes generally up-regulated in fibroma (30-2008) or in genes that were generally down-regulated in fibroma (47-2008). Localization of these samples at the highest or lowest row position refers to a similarity sorting by internal algorithms. Overall, cluster analysis illustrates a **clearly different expression pattern between fibroma and healthy samples** of FAP patients.

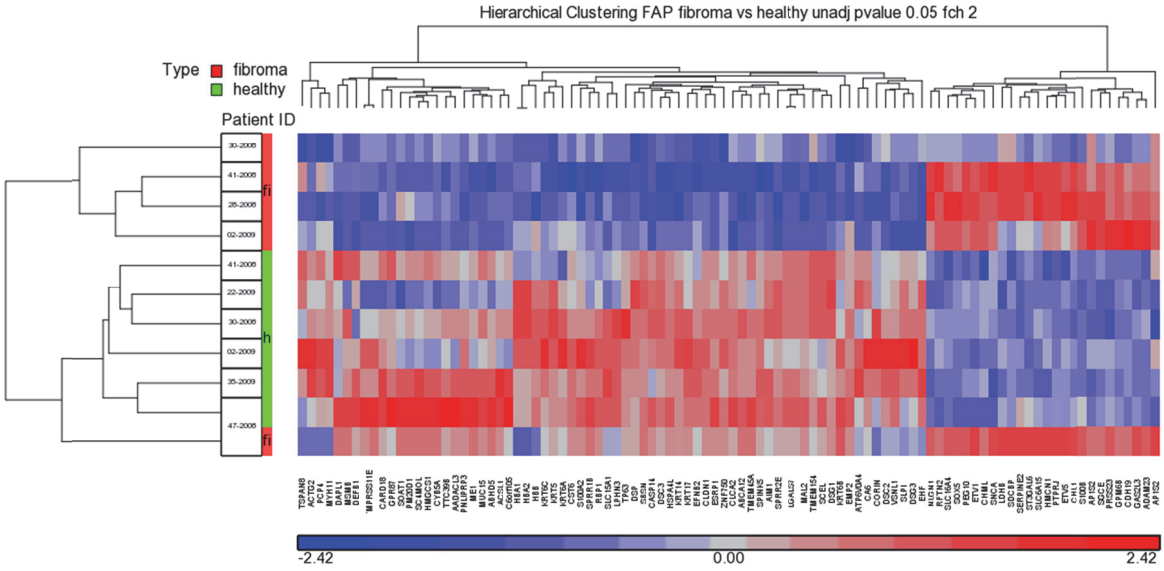

Figure 23. Hierarchical clustering of differentially expressed mRNAs in fibroma vs. healthy dermis. The heat map displays gene expression levels of all examined genes for each sample. Here it was generated for significantly regulated genes with 2-fold expression difference and unadjusted p-values <0.05 at least. Each row indicates a single patient sample whereas genes are depicted by independent columns. Up-regulated genes are represented by red and down-regulated genes by blue areas. Grey areas assign genes of unchanged expression between fibroma vs. healthy dermis. The dendrograms represent similarities in mRNA expression intensitites between different patients or between different genes.

5.2.1.1.2 Gene ontology analysis for DEGs in FAP fibroma vs. FAP healthy dermis

GO analysis was performed with DAVID v6.7 using the same 96 genes (26 up- and 70 down-regulated) with 2-fold expression difference as illustrated in hierarchical clustering. Several common biological processes were revealed and illustrated in Figure 24. Up-regulated genes (Figure 24A) are mainly involved in adhesion and transport processes, in cellular processes and signaling. The group of neurological processes is supposed to be included due to the involvement of several genes that are also expressed in cells of the nervous system (such as *S100B*, *neuroligin 1* (*NLGN1*), *synthenin* (*SDCBP*), or *hemicentin* (*HMCN1*)). Down-regulated genes (Figure 24B) are mostly involved in differentiation and developmental processes of epithelia in general, the epidermis and ectoderm, as well as in cell adhesion.

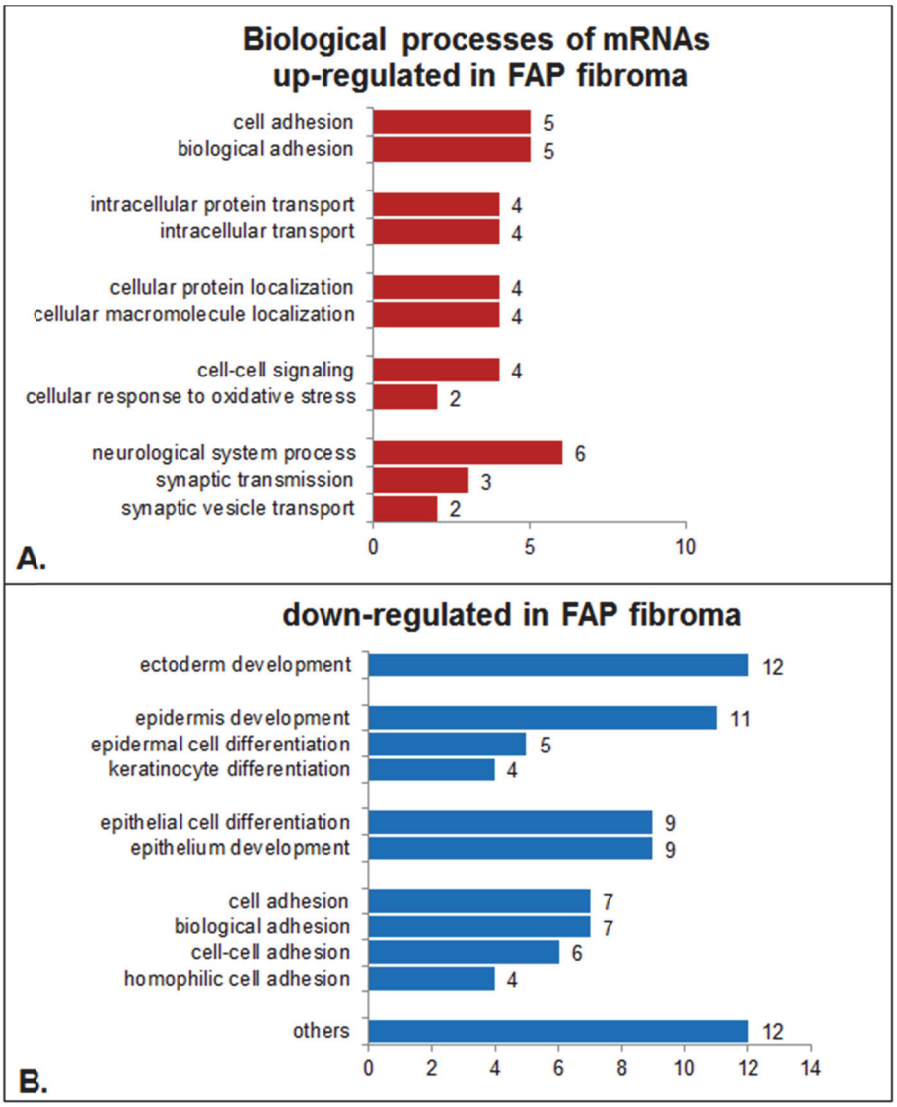

Figure 24. GO annotations for biological processes of changed mRNAs. GO analysis revealed several biological processes for up- (**A.**) and down-regulated (**B.**) mRNAs in fibroma vs. healthy dermis. Numbers indicate quantity of genes involved in particular biological processes. Illustrations were based on gene lists with significance cut-off of unadjusted p-values <0.05 and expression changes of 2-fold with 25 (**A.**) and 68 detected genes (**B.**). Biological processes named *"others"* (**B.**) include processes with less than 4 genes which were considered not to be relevant in the present fibroma study (sterol metabolic process (3), regulation of blood pressure (3), oxygen transport (2), gas transport (2) and peptide cross-linking (2)).

5.2.1.1.3 Ingenuity Pathway Analysis (IPA®)

Analysis of the same gene list with IPA® resulted in several functional networks mainly involving functions related to **dermatological disease and development** (Table 10). Identified high DEGs were not involved in one or more prevailing pathways.

Table 10. Functional IPA® networks detected for genes with expression changes of 2-fold. In total 96 genes were divided into network groups considering their particular gene function. Networks with **interesting functions (skin and development processes)** are marked in yellow. Strongly changed genes with -fold changes of at least 3 are indicated in bold and marked by arrows indicating their higher or lower regulation in fibroma vs. healthy dermis. They will be illustrated in more detail (5.2.1.1.4).

Top Functions	Molecules in Network
Dermatological Diseases and Conditions, Developmental Disorder, Organismal Injury and Abnormalities	*ACSL1, ADTRP, Alpha catenin, CASP14, caspase, Cg, CYB5A, Cytokeratin, DSC2, DSG1, DSG3,* ***DSP*****↓***, EFNB2, ERK1/2, ETV1, Focal adhesion kinase, HBA1/HBA2, HBB, hemoglobin, KRT5, KRT14, KRT17, KRT6A, KRT6B, KRT6C, P38 MAPK, PTPRJ, RBP1,* ***S100B*****↑***, SBSN, SDCBP, Sos,* ***SPINK5*****↓***, TP63, TSPAN8*
Drug Metabolism, Molecular Transport, Embryonic Development	*ACTG2, Actin, Ap1, CD3,* ***CDH19*****↑***, DEFB1 (includes EG:1672), EHF, EMP2, estrogen receptor, GAS2L3, Histone h3, Histone h4,* ***HMCN1*****↑***, HMGCS1, Insulin, Jnk, LGALS7/LGALS7B, Mapk, ME1, MUC15, MYH11, NFkB (complex), PDGF BB, PI3K (complex), Ras,* ***SERPINE2*****↑***, SLC15A1,SLPI, SNCA, SOAT1, SOX5 ,SRC (family), trypsin, Vegf, VSNL1*
Reproductive System Development and Function, Gene Expression, Organismal Injury and Abnormalities	*ADAM8, ADAM10, ADAM23, AEN, AP1S2, ATP6AP1, ATP6V0A4,* ***CLDN1*****↑***, CXCR6, DHRS7, DPH1, DSC3, EI24, ETV5, Gpcr, GPR87, GRM6, HSPA4L, KRT6B, LPHN3, NPRL3, ODF2L, PCP4, PDDC1, PEG10, PHF23 ,PRSS23, RBM38, RNA polymerase II, SEZ6L2, TMEM222, TNF, TP53, TRAPPC4, UBC*
Lymphoid Tissue Structure and Development, Cellular Development, Reproductive System Development and Function	*AHNAK, ANO1, ASPM, ATP13A2, CDC42EP3, CDC42SE1, CDK1, CDK17, CDK18, CLCA2, DSC3, DSG2, ECM1, EPAS1, ESRP1, GSC, KRT72 ,LDHB, PKP4, plasminogen activator, S100A2, S100A11, SERPINE1, SGCB, SGCE, SLC16A4, SLC6A15,* ***SPRR2E*****↓***, TGFB1, THEM6, TMEM45A, TMPRSS11E, TOR1A, TTC39B, UBC*
Embryonic Development, Hair and Skin Development and Function, Organ Development	*ABCA12, ADAM8, AIM1, AKAP12, Akt, ANXA6, C1S, CA6, CARD8,* ***CARD18*****↓***, CD6, ceramidase, ceramide,* ***CHL1*****↑***, CHML, CLDN4, CORIN, CTSL1, DSG1, DSG3, EGFR, EMP1, FOSL1, FSH, GPM6B, GSK3B, GZMK, IgG, IL17a dimer, JUN, KLK7, KRT17, KRT6B, KRT34, LGI1, LGMN, MAL2, MAPK1, MSMB, MSMO1, MYC, NCAM1, NLGN1, OLIG2, OSM, PIGR, PPARG, PPP1CA, PPP1R13L, RAB5A,* ***S100B*****↑***, SCEL, SDCBP, SGMS, SLA, SPRR1B, ST3GAL6, TLR7, TNF, TMEM154, TPD52, TPD52L1, UGCG, ULBP2, ZFP36L1*
Lipid Metabolism, Small Molecule Biochemistry, Molecular Transport	*AADAC,* ***ABHD5*****↓***, CEL, Ces1d, cholesterol, HDL, LIPA, LIPC, LIPE, LIPF, LIPG, LPL, PNLIP, PNLIPRP1, PNLIPRP2, PNLIPRP3, PNPLA2, PNPLA3, PNPLA4, PPARA, triacylglycerol lipase*
Dermatological Diseases and Conditions, Hereditary Disorder, Inflammatory Disease	*KLF4, ZNF750*

5.2.1.1.4 Most interesting genes selected for qPCR validation

Among the DEGs, 12 most interesting genes (five up- and seven down-regulated in FAP fibroma) were selected for further analyses (qPCR) showing a differential regulation of at least 3-fold (Table 11). Those genes were selected after *in silico* investigation for interesting annotations (Pubmed and gene database NCBI). Criteria for selection based on the respective cutaneous affection and the underlying FAP disease with association to Wnt signaling. For this purpose, particular focus was set to:

- the general gene function
- the gene function in skin
- a possible involvement in cell proliferation and apoptosis
- a possible association to Wnt signaling.

Genes up-regulated in FAP fibroma are involved in **general processes** affecting the entire organism (metal ion binding (*S100B*), cell adhesion (*CDH19, CHL1*), signal transduction (CHL1), extra cellular matrix junction formation (*HMCN1*), and modulation of cell growth (*SERPINE2*)). Some of them specifically relate to the epidermal part of the skin (junction formation (*HMCN1*) or hair follicle growth (*SERPINE2*)). Almost all up-regulated genes were associated with **particular skin diseases** as well as with **cell proliferation dysfunction** (*S100B, CDH19, CHL1, SERPINE2*). One of them (*CHL1*) was found to relate to Wnt signaling. Genes down-regulated in fibroma were found to be mainly involved in processes concerning the **epidermal part of the skin** such as epidermis development and skin barrier formation (*SPRR2E, CST6, DSP*), formation of intercellular junctions (*CLDN1, DSP*), and hair morphogenesis (*SPINK5, DSP*). Almost all of them were found to relate to skin diseases mainly affecting the epidermal part of the skin (*SPRR2E, CST6, SPINK5, ABHD5, CLDN1, DSP*). **Cell proliferation or tumor suppressive functions** were noted for *CARD18, CLDN1, DSP*, and *CST6*. Two of them (*DSP, CLDN1*) were noticed to be associated with Wnt signaling. Selected genes were localized on different chromosomal positions.

The same selected genes were also illustrated in Figure 25. Regarding their **influence on cell proliferation**, their oncongenic or tumorsuppressive potential was assigned. Two proto-oncogenes (*S100B, SERPINE2*) as well as one tumorsuppressor gene (*CDH19*) were up-regulated, whereas the role of *CHL1,* which was likewise up-regulated, was contrarily described. Within the group of down-regulated genes one proto-oncogene (*CLDN1*) and two tumorsuppressor genes (*DSP*, *CST6*) could be identified as well as a gene (*CARD18*) which may play a role in apoptosis and in cancer growth. Overall, among

the DEGs in fibroma vs. healthy dermis, proto-oncogenes as well as tumor suppressor genes were differentially regulated.

Table 11. High significantly changed mRNA expression in fibroma vs. healthy dermis. In total, 12 possibly relevant genes (five up- and seven down-regulated) were selected that have reached a significant change in mRNA expression of 3-fold in fibroma vs. healthy dermis. Known gene functions and known influences on cellular processes (selected annotations) are summarized. Latter mainly focused on *gene functions in skin, proliferation, apoptosis and possible association with Wnt signaling pathway*. Statistical analysis has been done by a 2-way ANOVA after microarray technology based whole genome expression analysis. Chromosomal positions are indicated. Up-regulated genes are sorted top down by decreasing -fold change. In contrast, down-regulated genes are sorted top down by decreasing negative -fold change.

Up-regulated in fibroma vs. healthy dermis

gene ID	gene description and selected annotations	localization	fch	p-value
S100B	**S100 calcium binding protein B** - calcium ion binding, axonogenesis - marker for malignant melanoma[134] - expressed in chondromyxoid fibroma[a, 135] - contributes to cancer progression by down-regulation of tumorsuppressor p53[136]	21q22.3	**5.26**	0.03
CDH19	**cadherin 19, type 2** - calcium dependent cell-cell adhesion - down-regulated in cholesteatoma[b] (associated with *S100A7A, SERPINB, SPRR1B*)[137] - loss of cadherins associated with cancer formation -*CDH1* (*E-cadherin*) involved in Wnt signaling pathway[138]	18q22.1	**4.78**	0.05
HMCN1	**hemicentin 1** - fibulin family of extracellular matrix (ECM) proteins - extracellular member of immunoglobulin superfamily - cell-cell and cell-matrix junctions - epidermal-dermal junction formation - epidermal organization of hemidesmosomes[139,140]	1q25.3-q31.1	**3.98**	0.03
CHL1	**cell adhesion molecule with homology to L1CAM** - cell adhesion, neural recognition, signal transduction - altered expression in several human cancers including melanoma and SCC[141] - involved in cancer growth and metastasis - β-catenin target gene[142]	3p26.1	**3.73**	0.04
SERPINE2	**serpine peptidase inhibitor, clade E, member 2** - inhibitor of growth-modulating serine proteases (thrombin, urokinase and tissue plasminogen activator) - overexpressed in sclerodermal fibroblasts[c,143] - involved in the development of several cancers[144-148] - target of ERK signaling in colorectal cancer[148]	2q36.1	**3.39**	0.04

[a]chondromyxoid fibroma: rare benign bone neoplasm (< 1% of all bone tumors) with abundant myxoid or chondroid intercellular material[149]; [b]cholesteatoma: epidermal inclusion cysts of the middle ear or the mastoid[137]; [c]scleroderma: accumulation of extracellular matrix material in skin and internal organs[143].

Down-regulated in fibroma vs. healthy dermis

gene ID	gene description and selected annotations	localization	fch	p-value
SPRR2E	**small proline-rich protein 2E** - protein binding, structural molecular activity - involved in epidermal development, keratinization and keratinocyte differentiation - primary constituent of the cornified cell envelope[150] - functional candidate gene (SPRR family) for psoriasis[151]	1q21-q22	**-4.43**	0.01
CST6	**cystatin E/M** - cysteine proteinase inhibitor with tumor suppressor activity - involved in skin barrier formation and epidermal terminal differentiation[152,153] - overexpression suppresses melanoma invasiveness[154]	11q13	**-4.09**	0.04
SPINK5	**serine peptidase inhibitor, Kazal type 5** - role in skin and hair morphogenesis - mutations cause Netherton syndrome[d,155] and atopic dermatitis[156]	5q32	**-3.81**	0.02
CARD18	**caspase recruitment domain member 18** - cysteine-type endopeptidase activity - apoptotic function[157] - inhibition of inflammatory cytokine IL-1 beta[158] - not reported in skin - up-regulated in gastric cancer[159]	11q22.3	**-3.55**	0.01
ABHD5	**abhydrolase domain containing 5** - lipid metabolic process - mutations associated with secondary ichthyosis due to triglyceride storage disease[160]	3p21	**-3.14**	0.02
CLDN1	**claudin 1** - cell adhesion, integral membrane protein - component of tight junctions - mutated in ichthyotic skin disease[161] - highly expressed in colorectal cancer[162] - β-catenin target gene[163]	3q28-q29	**-3.13**	0.01
DSP	**desmoplakin** - intercellular junctions, cytoskeletal linker of desmosomes - mutations cause woolly hair and palmoplantar keratoderma[e, 164] - tumor suppressive function by Wnt modulation[165]	6p24	**-3.08**	0.02

[d]Netherton Syndrome: severe autosomal recessive disorder with congenital ichthyosis, defective cornification, specific hair shaft defect and severe atopic manifestations[155]; [e]keratoderma: hyperproliferation of stratum corneum

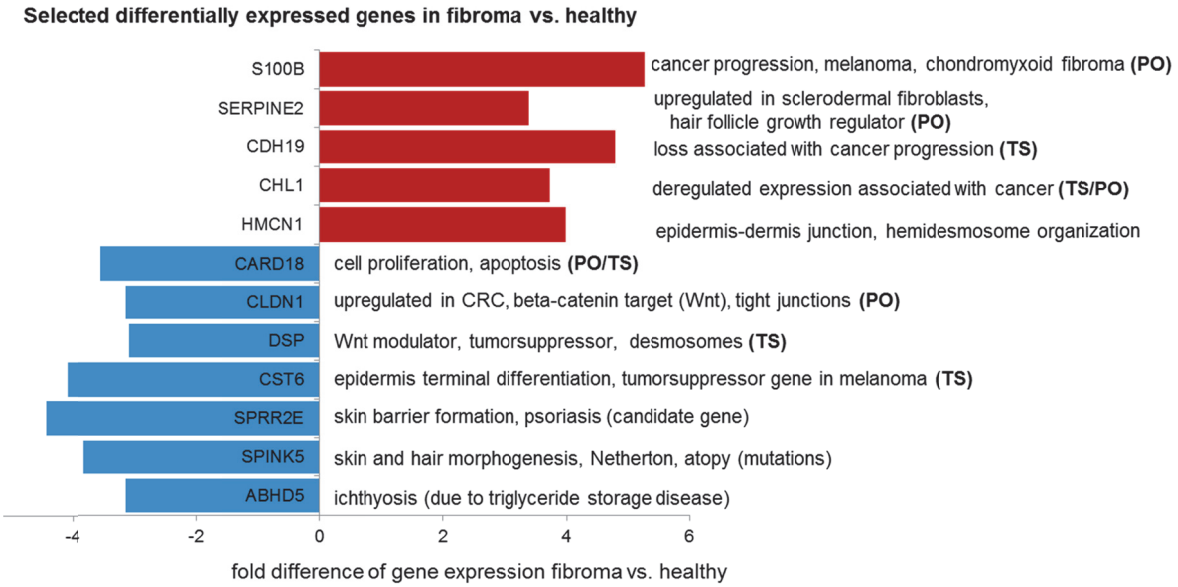

Figure 25. Overview of selected genes relating to cell proliferation function. The 12 genes (five up- and seven down-regulated in fibroma) finally chosen for qPCR validation are sorted according to their specific annotation. Red bars indicate gene expression changes of genes overexpressed in fibroma vs. healthy skin, whereas blue bars indicate -fold differences of down-regulated genes. Known proto-oncogenes (PO) or tumor suppressor genes (TS) are indicated. Gene expression -fold difference is illustrated on the x-axis. Genes are depicted on the y-axis.

5.2.1.2 Results of qPCR FAP fibroma vs. healthy skin

After whole genome expression analysis of the fibroma samples, 12 significantly DEGs (5.2.1.1.4) were validated by qPCR. Selection of presumably not regulated reference genes (*HPRT1*, *GUSB*, *GAPDH*, *TBP*)[166-168] for normalization followed the stability criteria correlated over all samples (4.5.3.3). Two genes (*HPRT1*, *GUSB*) were identified to be consistently expressed in all samples (fibromas and healthy skin). For normalization C_T values at threshold 0.2 were applied. qPCR has been successfully performed for four FAP patients (28-2008, 02-2009, 41-2008, 47-2008), one sample (30-2008) had to be excluded as the healthy sample did not reach exponential curve shape and behaved very unstably and variably during repeated runs for all targets (Supplementary Figure 2). The healthy skin of 28-2008, although not usable for calculation of microarray data, was assumed to be suitable for qPCR analysis due to fine RNA quality (RIN: 7.3). Figure 26 illustrates the ratio of mRNA expression levels between fibroma and healthy skin samples applied on average. The wide SD resulted from large variance between different patient samples (Figure 27). Almost all 12 targets, analyzed in FAP fibroma vs. healthy skin, confirmed the expression regulation relating to microarray data. After statistical analysis (2-way ANOVA) changed expression of totally six (*S100B*, *CDH19*, *CHL1*, *SERPINE2*, *CST6*, *CARD18*) out of 12

targets was significantly supported. Highest significant results (***p<0.001) were reached for the up-regulated genes *S100B* and *CHL1*, followed by *CDH19*, *SERPINE2* and the down-regulated *CARD18* (**p<0.01), as well as the down-regulated *CST6* (*p<0.05).

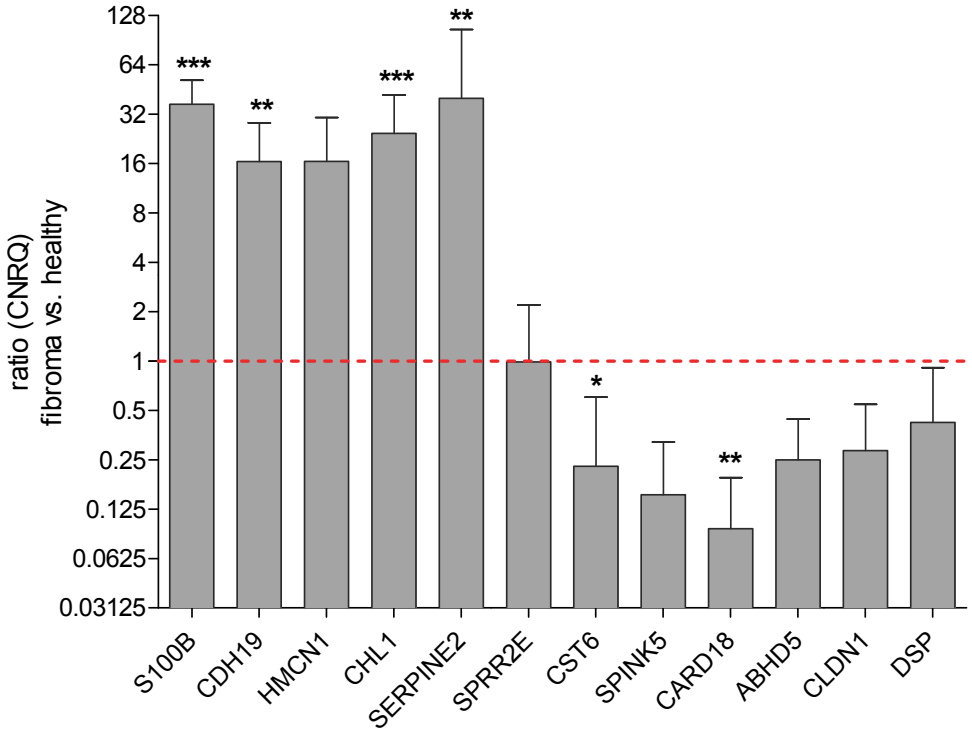

Figure 26. Relative mRNA expression levels between FAP fibroma and healthy dermis after qPCR. Ratio of target genes, selected after microarray expression analysis of FAP fibroma and FAP healthy skin samples. Genes are sorted according to their corresponding expression in microarray analysis. Bars indicate ratios of relative mRNA expression between averaged normalized intensities of FAP fibroma and healthy dermis samples, whereas healthy dermis samples were set to one (indicated by red dashed line). Y-axis is illustrated log2 transformed. Values are presented as mean of the qbasePLUS calibrated normalized relative quantities (CNRQ) + SD. CNRQ values were reached after normalization to *HPRT1* and *GUSB*. Statistical analysis was done using a 2-way ANOVA. Calculation was performed on four fibroma and corresponding healthy samples, except *SPRR2E* (n=3 lacking 41-2008) *p< 0.05; **p<0.01; ***p<0.001.

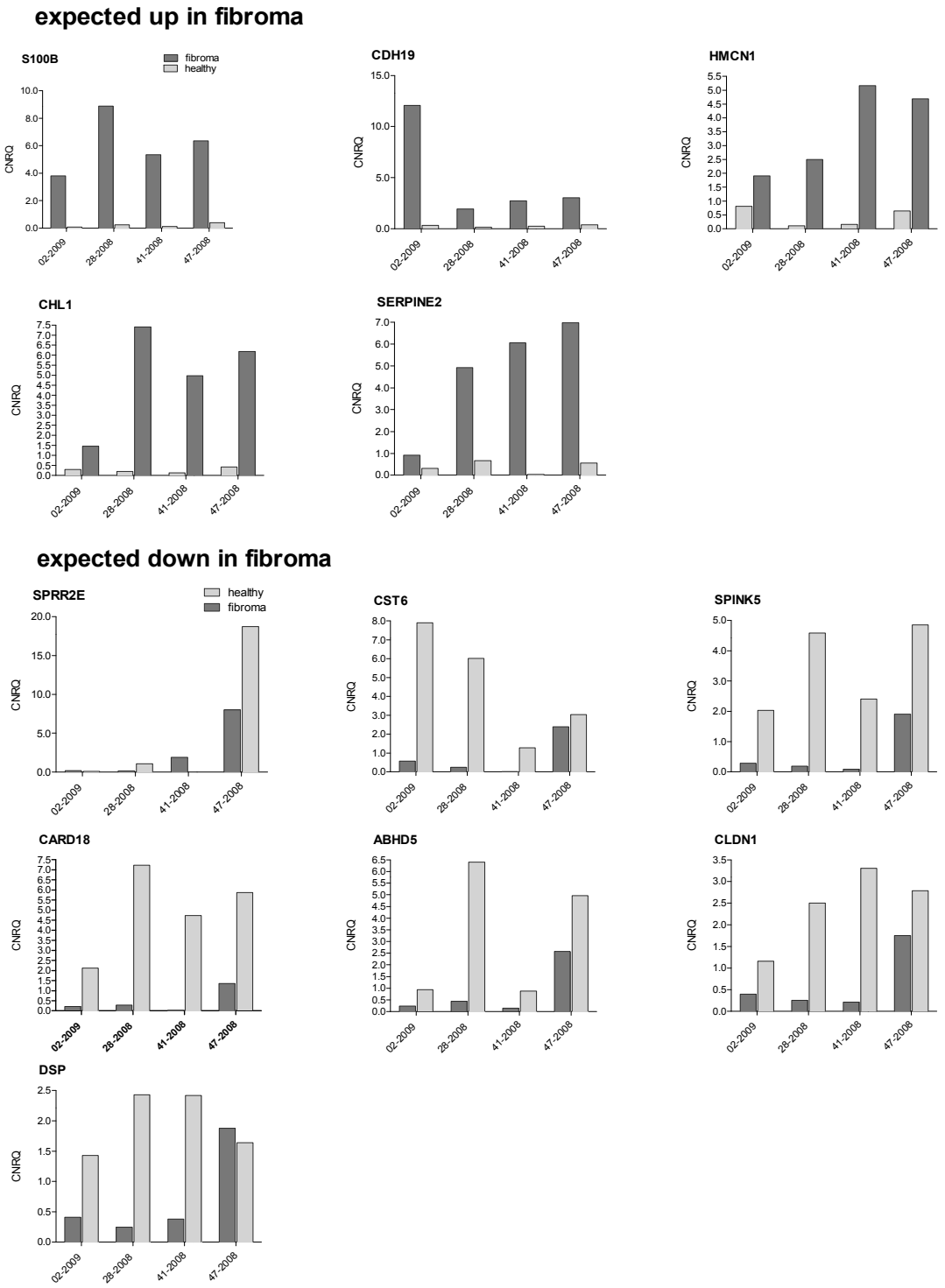

Figure 27. Illustration of normalized mRNA expression levels of single patient samples. Targets are indicated as expected up- or down-regulated in fibroma vs. healthy skin based on microarray results. Bars indicate calibrated mRNA expression values (CNRQ; y-axis) after normalization with ideal reference genes *HPRT1* and *GUSB* for each patient sample (x-axis) (dark bars are fibroma; bright bars indicate healthy skin samples). For *SPRR2E*, no reliable results (sigmoid curve) could be achieved for sample 41-2008 healthy skin. CNRQ values for *SERPINE2*, *CST6*, and *CARD18* were very low for 41-2008 healthy skin or fibroma, respectively, compared to other samples.

5.2.2 FAP lipoma vs. FAP healthy dermis

5.2.2.1 Whole genome expression analysis

For the FAP lipoma group, gene lists were established based on expression intensities of totally **six lipoma and five healthy dermis samples of six FAP patients**, that reached defined quality criteria (Table 4). In total 886 up- and 1699 down-regulated genes were found to reach differential gene expression concerning an FDR-unadjusted p-value <0.05. Table 12 shows the number of DEGs for -fold changes and significance levels.

Table 12. Numbers of DEGs in FAP lipoma vs. healthy dermis. The table shows the number of DEGs for -fold changes (fch) and significance levels. Detailed analyses were focused on gene expression differences of 2.5-fold and higher (red frame).

	p-value <0.05	fch 1.5	fch 2	fch 2.5	fch 3	p-value <0.01	fch 1.5	fch 2
No. genes detected	(886↑, 1699↓)	(527↑, 304↓)	(204↑, 22↓)	62 (59↑, 3↓)	17 (16↑, 1↓)	(45↑, 178↓)	(20↑, 9↓)	-

The PCA scatter plot indicated a **distribution tendency** between lipoma (blue points) and healthy dermis (red points) samples (Figure 28A). Nevertheless, overall gene expression of single samples different in both tissue types and single points tended to be distributed across the diagonals of the grid. Regarding paired lipoma and healthy samples of same patients (Figure 28B), similar overall distribution was seen for patients 37-2008 (purple points), 35-2009 (green points), and 55-2010 (turquois points). In contrast, paired samples of patients 47-2008 (orange points) and especially 22-2009 (red points) differed much more. For patient 29-2008, only the lipoma sample could have been included in analyses. Remarkably, this lipoma sample differed the most from all other samples in its overall gene expression profile.

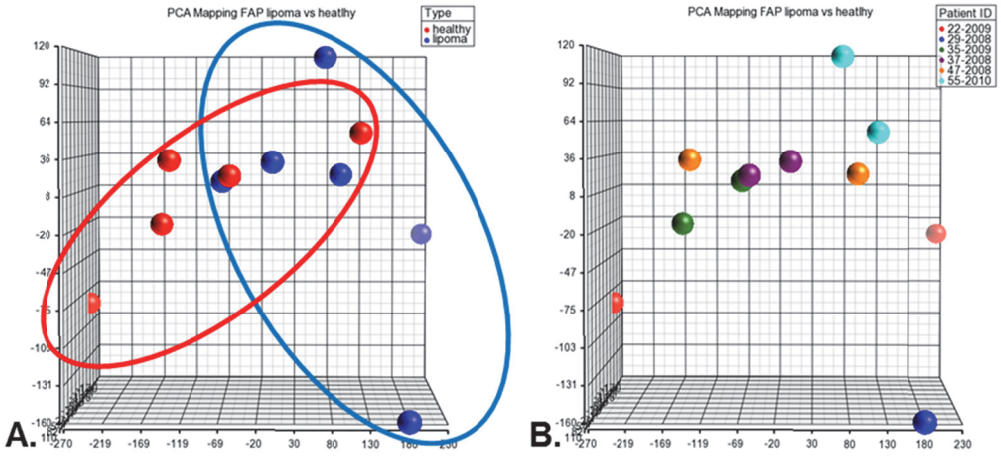

Figure 28. PCA scatter plot illustrating microarray chips of lipoma and healthy dermis samples from FAP patients. The grid shows the whole human genome and points represent single arrays. **A.** illustrates the distribution of lipoma (blue points) and healthy (red points) samples. Red

and blue ellipsoids enclose the particular tissue types by indicating their distribution tendencies. **B.** depicts the same distribution but assigns *patient IDs* to the chip samples. Axes represent the three main components of the gene expression intensities.

5.2.2.1.1 Hierarchical clustering of the mRNA expression data

Hierarchical clustering was calculated for totally 62 genes (59 up- and three down-regulated, Supplementary Table 7) with 2.5-fold expression differences and FDR-unadjusted p-values <0.05. The heat map (Figure 29) indicated **consistent clustering** of DEGs in lipoma compared to healthy skin samples of FAP patients. Two lipoma samples (35-2009 and 37-2008) showed a rather neutral expression pattern. Furthermore, the healthy dermis sample of **patient 55-2010** revealed a pattern different to all other healthy dermis samples, and may therefore be considered as an outlier. This pattern rather resembled expression distribution of lipoma samples. The pattern of the corresponding lipoma sample of patient 55-2010 did not show any peculiarities but fitted finely together with the expression distribution of the other lipoma samples.

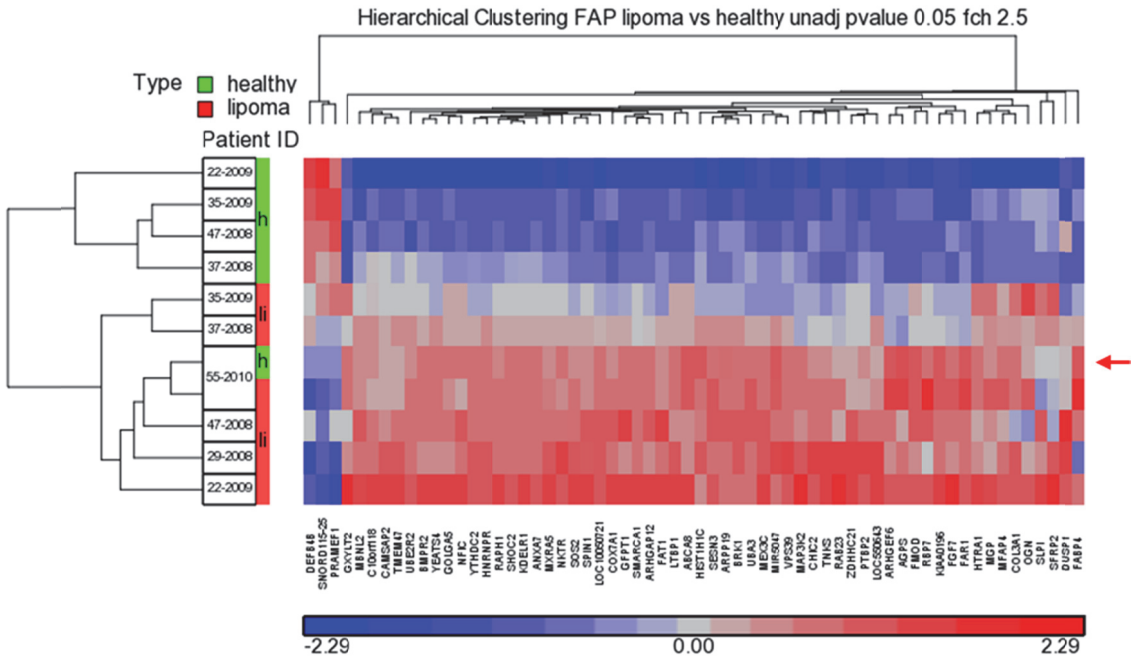

Figure 29. Hierarchical clustering of differentially expressed mRNAs in FAP lipoma vs. FAP healthy dermis. The heat map displays gene expression levels of all 62 genes (59 up- and 3 down-regulated) for each sample. It was generated for significantly regulated genes with 2.5-fold expression difference and FDR-unadjusted p-values <0.05. Each row indicates a single patient sample whereas genes are depicted by independent columns. Up-regulated genes are represented by red areas and down-regulated genes by blue areas. Grey areas assign genes of unchanged expression in FAP lipoma vs. FAP healthy dermis. The dendrograms represent similarities in mRNA expression intensities between different patients or between different genes. The red arrow marks the healthy dermis sample of patient 55-2010 with differing expression pattern compared to all other healthy dermis samples.

5.2.2.1.2 Gene ontology analysis FAP lipoma vs. FAP healthy dermis

GO analysis was performed with DAVID v6.7 using the same 62 genes (59 up- and three down-regulated) with 2.5-fold expression difference as illustrated in hierarchical clustering. Several common biological processes were revealed and illustrated in Figure 30. Up-regulated genes were mainly involved in the regulation of biosynthetic processes, cell cycle, signaling pathways, and response to abiotic and extracellular stimuli. Other processes (lung development and bone formation) were determined not to be of major interest for the present study. To enable GO analysis for down-regulated genes, 22 genes with 2-fold down-regulated expression change in FAP lipoma were analyzed. Only one single process (immune response) was found that included four of the down-regulated genes.

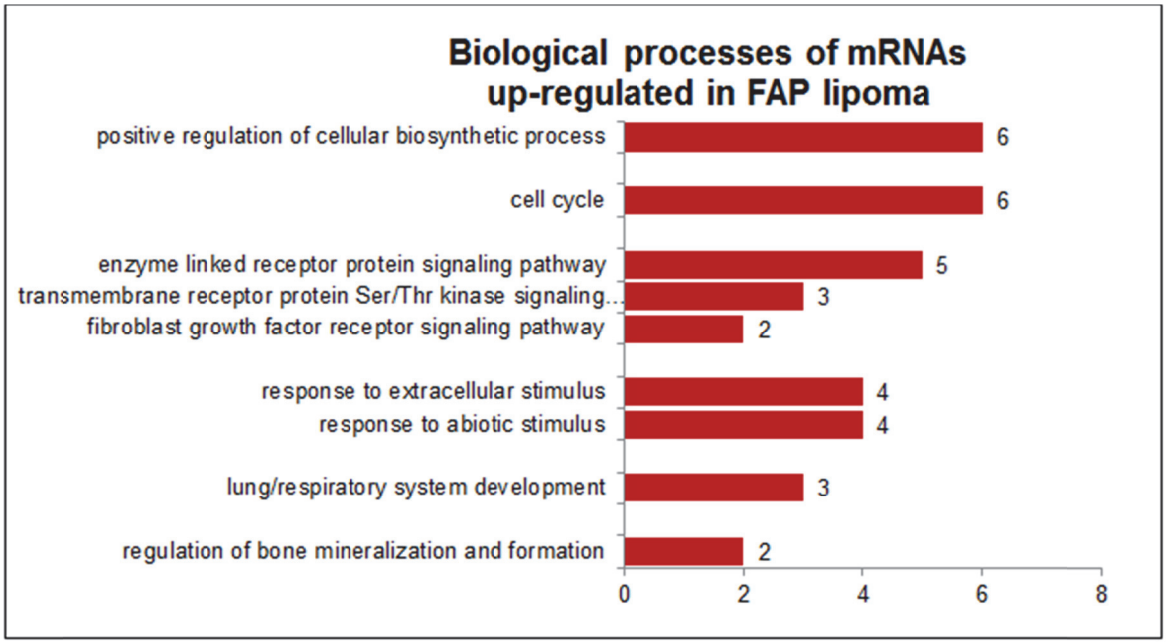

Figure 30. GO annotations for biological processes of changed mRNAs. GO analysis revealed several biological processes for up-regulated mRNAs in FAP lipoma vs. FAP healthy dermis. Numbers indicate quantity of genes involved in particular biological processes. Illustration was based on gene lists with significance cut-off of unadjusted p-values <0.05 and expression changes of 2.5-fold with 41 detected up-regulated genes.

5.2.2.1.3 Ingenuity pathway analysis

Analysis of the same gene list with IPA® resulted in several functional networks with functions in **development, cancer and hereditary disorders**. Such networks included severals of the highest changed genes with 3-fold expression difference (Table 13). Identified high DEGs were not involved in one or more prevailing pathways.

Table 13. Functional IPA® networks detected for genes with expression changes of 2.5. In total, 49 genes were divided into network groups considering their particular gene function. Networks with **interesting functions (development, hereditary disorder, cancer)** are marked in yellow. Strongly changed genes with -fold changes of at least 3 are indicated in bold and marked by arrows indicating their higher or lower regulation in FAP lipoma vs. FAP healthy dermis. They will be illustrated in more detail (5.2.2.1.4). Networks are sorted referring to IPA® established scores (considering numbers of genes included in particular network and relevance).

Top Functions	Molecules in Network
Cardiovascular System Development and Function, Organismal Development, Tissue Morphology	*AGPS, Alp, BMPR2, BRK1, CD3, COL3A1, Collagen type I, COX7A1, DEFB4A/DEFB4B, DUSP1, ERK1/2,* ***FABP4***↑*, FGF7, FMOD, Histoneh4, HNRNPR, IL1, Immunoglobulin, KDELR1, LTBP1, MAP3K2, Mapk, MGP, NKTR, OGN, P38, MAPK, PDGFBB, Ras,* ***SHOC2***↑*,* ***SLPI***↑*, SOS2, Sos, Tgf beta, TNKS ,YEATS4*
Cell Morphology, Inflammatory Response, Cell Death and Survival	*ALOX15B, ANXA7, ARHGEF6, CHIC2, FAT1, FLAD1, GFPT1, HMGXB3, IMPDH1, INF2, KIAA0196, KIAA1033, KIRREL, KLHL23/PHOSPHO2-KLHL23, MBNL2, MFAP4, NBEA, NFIC, NPRL2, PTBP2, RAPH1, SESN3, SPIN1, TGFB1, TMEM108, TOP3B, UBC, UBE2R2, VPS39, WDR73, YTHDC2, ZNF135, ZNF167, ZNF431, ZNF433*
Inflammatory Disease, Inflammatory Response, Renal Inflammation	*ABCA1, ABCA8, ACAT1, APRT, ARFGAP1 ,ARHGAP12, ARPP19, C10orf118, C20orf24, CAMSAP2, CHCHD2, CPNE2, FAR1, FNBP1, GOLGA5, HPCAL1, IKBKG, ITSN1, LIMA1, MEX3C, MXRA5, NOS3, OCRL, PACSIN3, PAK3, PLD3, PLEKHA5, PRAMEF1, RAB23, RBP1, SMYD3, SOD3, SUFU, UBC, ZDHHC21*
Embryonic Development, Organ Development, Organismal Development	*Akt, AQP5, BAZ1A, BCL2L2, BMF, Cg, CHCHD2, CHD8,* ***DDX5***↑*, ERK, FAM46A, FGF7, FSH, GPER, GSTT1, GTPBP4,* ***HIST1H1C***↑*, Histone h3, HTRA1, Jnk, LIMA1, mir-101, miR-19b-3p ,NFkB (complex) ,NuRD, POLE3, PPARA,* ***RBP7***↑*, RNA polymerase II, RNU7-1,* ***SFRP2***↑*,* ***SMARCA1***↑*, UBA3, ZBED1, ZNF622*
Hematological Disease, Hereditary Disorder, Infectious Disease	*F9, GXYLT2*
Hereditary Disorder, Neurological Disease, Cancer	*HIC1,* ***TMEM47***↑

By IPA® analysis, **eight upstream regulators** were found that regulate at least two of the high significantly changed genes with 3-fold expression difference. Among the upstream regulators are growth factors (TGFA, TGFB1, IGF1), transcription regulators (FOS, CEBPB, TP53), the cytokine WNT3A and the ligand-dependent nuclear receptor THRB. Figure 31 illustrates the connections of those up-regulated genes and their upstream regulators. Among the genes repetitively indicated are ***FABP4, SFRP2, SLPI*** and ***DDX5*** with functions in lipid metabolism, cell proliferation and Wnt signaling (5.2.2.1.4). *SLPI* was additionally included despite slightly lower expression change of 2.6-fold in FAP lipoma vs. FAP healthy dermis.

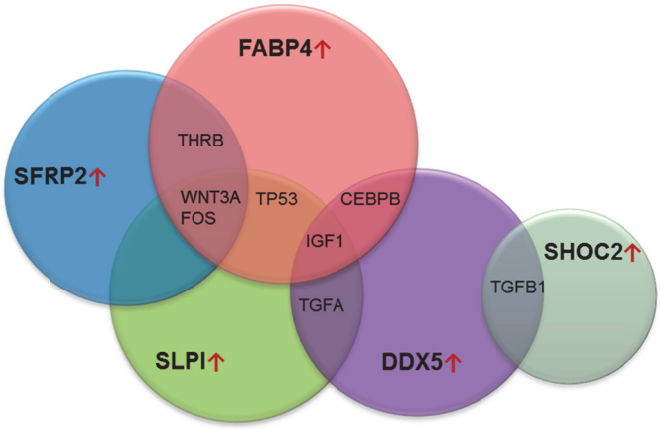

Figure 31. Venn diagram depicting common upstream regulators of DEGs. Upstream regulators of at least two of the most important up-regulated genes were selected and depicted at the connection position of the particular genes. *SLPI*, with a 2.6-fold expression difference, was additionally included due to similar regulation. Upstream regulators are the growth factors transforming growth factor α (TGFA), and β1 (TGFB1), and the insulin-like growth factor 1 (IGF1); the three transcriptional regulators FBJ murine osteosarcoma viral oncogene homolog (FOS), the CCAAT/enhancer binding protein β (C/EBPβ), and the tumor protein p53; as well as the cytokine Wnt integration site 3A (WNT3A), and the nuclear receptor thyroid receptor β (THRB).

5.2.2.1.4 Most interesting genes selected for qPCR validation

Among the DEGs, 10 most interesting genes (all up-regulated in FAP lipoma) with differential regulation of at least 3 were selected for further analyses by qPCR (Table 14). Those genes were selected after *in silico* investigation for interesting annotations (Pubmed and gene database NCBI). Selection criteria were based on the particular cutaneous affection and the underlying FAP disease with association to Wnt signaling. For this purpose, particular focus was set to:

- the general gene function in skin
- the specific function relating to lipoma or lipid metabolism
- a possible involvement in cell proliferation and apoptosis
- a possible association to Wnt signaling.

Several targets were found to realize distinct functions in skin, with most of them concerning the epidermal part *(TMEM47, DDX5, SFRP2, SHOC2, SMARCA1*) or adipose tissue (*FABP4*). Two targets were found with functions in **lipid metabolism and adipocyte differentiation** (*RBP7, FABP4*). Several genes revealed functions in **cell proliferation** (*TMEM47, DDX5, MXRA5, SFRP2, SMARCA1*), whereas two of them (*SFRP2, SMARCA1*) were involved in **Wnt signaling**. Two other targets were found with specific functions in chromatin compaction (*HIST1H1C*) and ubiquitin-mediated proteasomal degradation (*UBE2R2*). Selected genes are localized on different chromosomal positions with three of them localized on the X chromosome (*TMEM47, MXRA5, SMARCA1*).

The same genes were also illustrated in Figure 32. Regarding their **influence on cell proliferation**, their oncongenic or tumorsuppressive potential was assigned. Two proto-oncogenes (*DDX5, MXRA5*) and three tumorsuppressor genes (*TMEM47, SFRP2, SMARCA1*) were up-regulated in FAP lipoma. Two tumor suppressors (*SFRP2, SMARCA1*) were found to be known modulators of Wnt signaling. Furthermore two other genes were found with anti-proliferative effects that are achieved by transcriptional repression (*HIST1H1C*) and ubiquitine mediated degradation at the proteasome (*UBE2R2*). Overall, among the DEGs in FAP lipoma vs. healthy dermis, proto-oncogenes as well as tumor suppressor genes were differentially regulated, whereas tumor suppressive and anti-proliferative functions tend to prevail among the highest DEGs.

Table 14. High significantly changed mRNA expression: up in FAP lipoma vs. FAP healthy dermis. In total, 10 possibly relevant genes (all up-regulated) were selected that reached a significant 3-fold mRNA expression change in FAP lipoma vs. FAP healthy dermis. Known gene functions and known influences on cellular processes (selected annotations) are summarized. Latter mainly focused on *gene functions in skin, lipoma, lipid metabolism, cell proliferation, and Wnt signaling pathway.* Chromosomal positions are indicated. All genes were up-regulated in FAP lipomas and are sorted top down by decreasing -fold change.

gene ID	gene description and selected annotations	localization	fch	p-value
TMEM47	**transmembrane protein 47** - member of claudins (tight junctions) - possible tumor suppressor in malignant melanoma[169]	Xp11.4	**4.20**	0.03
RBP7	**retinol binding protein 7, cellular** - stabilization, transport, and metabolism of vitamin A - lipid metabolism (PPARgamma target gene)	1p36.22	**3.82**	0.03
DDX5	**DEAD (Asp-Glu-Ala-Asp) box polypeptide 5** - RNA helicase; alteration of RNA secondary structure - controls keratinoctye proliferation in wound healing[170] - overexpressed in colorectal carcinoma[171]	17q21	**3.79**	0.03
MXRA5	**matrix-remodelling associated 5** - ECM remodeling and cell-cell adhesion[172] - involved in lung and colorectal cancer as oncogene[172,173]	Xp22.33	**3.60**	0.02
FABP4	**fatty acid binding protein 4, adipocyte** - uptake, transport, and metabolism of fatty acids - marker of adipocyte differentiation[174] - expressed in lipomas and hibernomas[175]	8q21	**3.53**	0.02
SFRP2	**secreted frizzled-related protein 2** - involved in the formation of hypertrophic scars[176] - methylation associated with colorectal cancer[177] - soluble modulator of Wnt signaling	4q31.3	**3.32**	0.04
SHOC2	**soc-2 suppressor of clear homolog** (C. elegans) - protein-protein interactions - mutations associated with Noonan-like syndrome with loose anagen hair[178] - RAS scaffold protein in ERK1/2 signaling pathway[179]	10q25	**3.14**	0.04
HIST1H1C	**histone cluster 1, H1c** - chromatin compaction into higher order structures - involvement in p53-dependent DNA damage response pathways[180]	6p21.3	**3.12**	<0.05
UBE2R2	**ubiquitin-conjugating enzyme E2R2** - component of ubiquitin dependent proteolytic pathway - involved in β-catenin degradation[181]	9p13.3	**3.12**	0.04
SMARCA1	**SWI/SNF related, matrix associated, actin dependent chromatin regulator** - ATPase, nucleosome remodeler, transcription regulator - down-regulated in melanoma - modulator of Wnt signaling[182]	Xq25	**3.05**	0.04

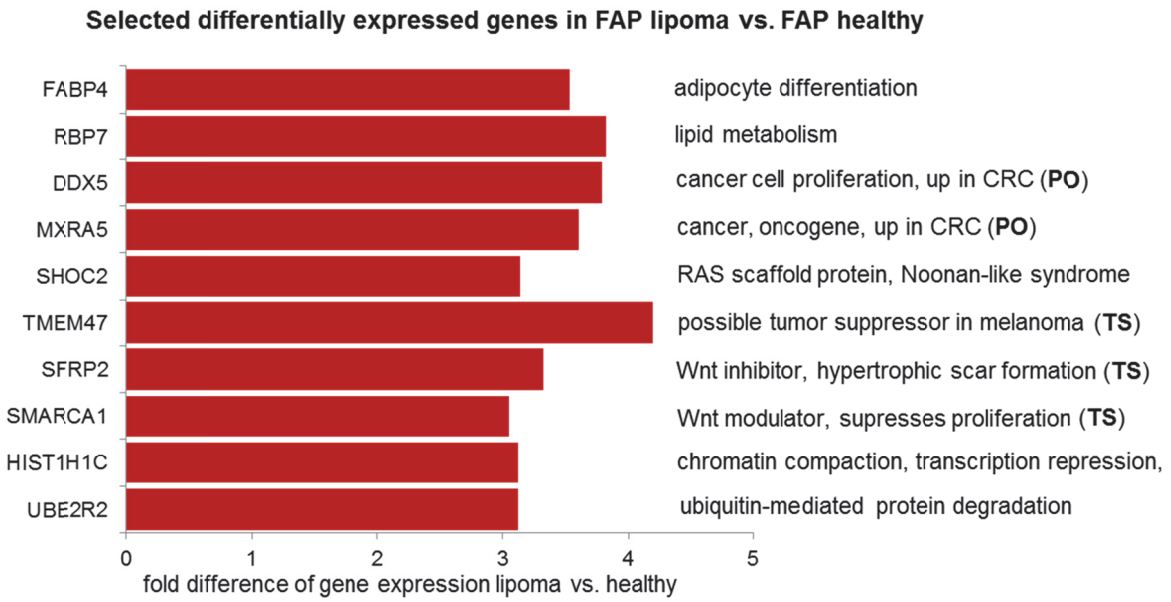

Figure 32. Overview of selected genes relating to cell proliferation function. The ten genes (all up-regulated in FAP lipoma vs. healthy dermis) finally selected for qPCR validation. These genes are sorted relating to their specific annotation. Red bars indicate up-regulated expression change of genes overexpressed in FAP lipoma compared to FAP healthy dermis. Known proto-oncogenes (PO) or tumor suppressor genes (TS) are indicated. Gene expression -fold difference is illustrated on the x-axis. Genes are depicted on the y-axis.

5.2.2.2 Results of qPCR FAP lipoma vs. FAP healthy skin

After whole genome expression analysis of the lipoma samples ten significantly DEGs (5.2.2.1.4) were validated by qPCR. For normalization, in total six reference genes were validated, three of them (*HPRT1, GUSB, GAPDH*) already included in fibroma runs (5.2.1.2) as well as three (*CLN3, LRP10, NELFB*) based on previous work on adipose tissue[183]. Selection of presumably not regulated reference genes followed the stability criteria correlated over all samples (4.5.3.3). Two genes (*HPRT1, LRP10*) were identified to be consistently expressed in all samples (lipoma and healthy skin). For normalization, C_T values at threshold 1 were applied. qPCR validation was overall successful for four FAP patients (37-2008, 22-2009, 35-2009, 55-2010). One patient (47-2008) was initially excluded, because the lipoma sample revealed sigmoid curves (Supplementary Figure 3). Furthermore, several healthy dermis samples must have been excluded as they either resulted in sigmoid curves, no results at all, curves that did not reach exponential phase, or because they behaved very unstably and variably during repeated runs. For this, the healthy skin sample of 35-2009 must has been excluded for all targets. For single targets, 37-2008 healthy skin (*TMEM47, RBP7, MXRA5*), and 22-2009 healthy skin (*UBE2R2*) were excluded. Figure 33 illustrates the ratio of mRNA expression levels between lipoma and

healthy dermis samples. This illustration was achieved by initial calculation of the averages of all suitable lipoma and healthy dermis samples. The wide SD resulted from large variance between different patient samples (Figure 34). The majority (6/10) of targets analyzed in FAP lipoma vs. healthy skin, confirmed the expression regulation relating to microarray data. Statistical analysis (Wilcoxon rank sum test for unpaired samples) could not support significant expression changes for any target.

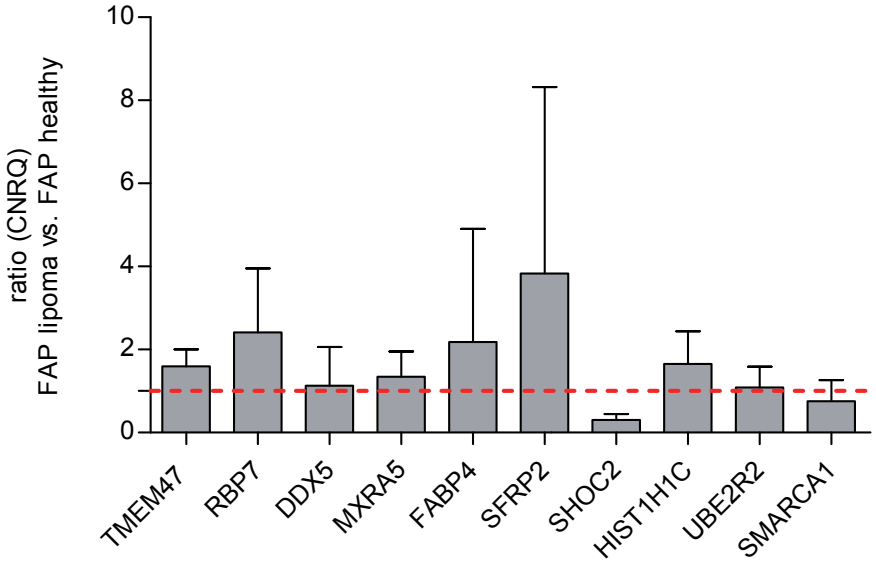

Figure 33. Relative mRNA expression levels between FAP lipoma and FAP healthy dermis after qPCR. Ratio of target genes, selected after microarray expression analysis of FAP lipoma and FAP healthy dermis samples. Genes are sorted according to their corresponding expression in the microarray. Bars indicate unpaired ratios of relative mRNA expression between averaged normalized intensities of FAP lipomas and healthy dermis samples, whereas healthy dermis samples were set to one (indicated by red dashed line). Values are presented as mean of the qbasePLUS calibrated normalized relative quantities (CNRQ) + SD. CNRQ values were reached after normalization to *HPRT1* and *LRP10*. Statistical analysis was done using Wilcoxon rank sum test (for unpaired samples, assuming non-parametric distribution of the expression data). Calculation was performed on four lipoma (37-2008, 22-2009, 35-2009, 55-2010) and three healthy dermis samples (37-2008, 22-2009, 55-2010) samples, except *TMEM47, RBP7, MXRA5* (healthy dermis n=2, lacking 37-2008), and *UBE2R2* (healthy dermis n=2, lacking 22-2009).

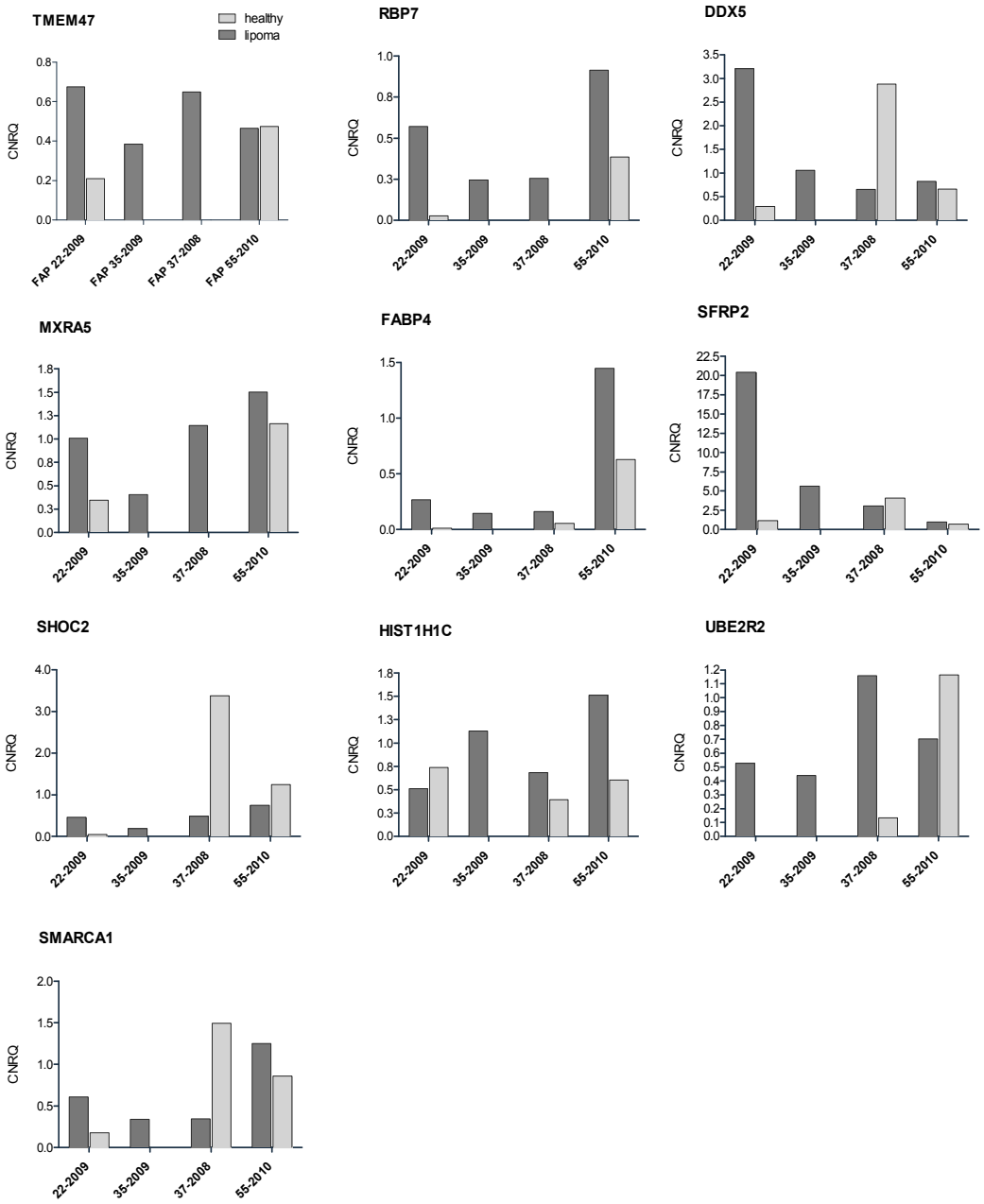

Figure 34. Illustration of normalized mRNA expression levels of single patient samples for each target. Targets are indicated as expected up-regulated in FAP lipoma vs. FAP healthy dermis based on microarray results. Bars indicate calibrated mRNA expression values (CNRQ; y-axis) after normalization with ideal reference genes *HPRT1* and *LRP10* for each patient sample (x-axis) (dark bars are lipoma; bright bars indicate healthy dermis samples). For all targets, no reliable results could be achieved for sample 35-2009 healthy dermis (no results at all, very late amplification). For *TMEM47, RBP7, MXRA5,* 37-2008 healthy dermis (sigmoid curve or very late amplification), as well as for *UBE2R2,* 22-2009 healthy dermis (very unstable and variable in run repeats) did not reveal reliable results.

5.2.2.3 Results of qPCR FAP lipoma vs. non-FAP lipoma

By qPCR analysis, the same mRNA targets selected for the FAP lipoma samples (5.2.2.1.4) were in a second step validated for differential expression in FAP lipoma compared to control (non-FAP) lipoma samples. In addition, *SLPI* with differential gene expression of 2.6-fold between FAP lipoma vs. healthy dermis (Supplementary Table 7) was included because it was also found to be highly changed in array results for FAP lipoma vs. control lipoma (5.2.3.1.4) and due to its regulation by common upstream regulators (Figure 31). For normalization, C_T values at threshold 1 were applied and normalized to previously selected reference genes (*HPRT1, LRP10*). qPCR runs for target *SLPI* with reference genes (*HPRT1, LRP10*) were separately run and calculated based on C_T values of threshold 0.2. qPCR analyses were successfully performed for all four FAP lipoma samples (37-2008, 02-2009, 35-2009, 55-2010) as well as for all five control lipoma samples (40-2012, 43-2012, 44-2012, 2013-003, 2013-014). Averaged normalized mRNA expression levels for FAP lipoma and control lipoma samples for significantly confirmed targets are illustrated in Figure 35A,B. Results for all targets and detailed expression results for single samples are illustrated in Supplementary Figure 4. Statistical analysis (Wilcoxon rank sum test) revealed significant (*$p<0.05$) results for totally eight of all 12 applied mRNA targets with six of them down-regulated (*RBP7, FABP4, SHOC2, SMARCA1, UBE2R2, TMEM47*) and two up-regulated (*SFRP2, SLPI*) in FAP lipoma vs. control lipoma. Such mRNA targets are annotated relating to lipid metabolism and cell proliferation. Genes associated with lipid metabolism (*RBP7, FABP4*) and tumor suppressive activity (*SMARCA1, UBE2R2, TMEM47)* were mainly down-regulated in FAP lipoma vs. control lipoma, whereas down-regulated genes indicated functions in modulation (*SFRP2*) as well as in promotion of cell proliferation (*SLPI*). mRNA targets differentially expressed in microarray analyses comparing FAP lipoma vs. FAP healthy dermis as well as in FAP lipoma vs. control lipoma are summarized in Figure 35C.

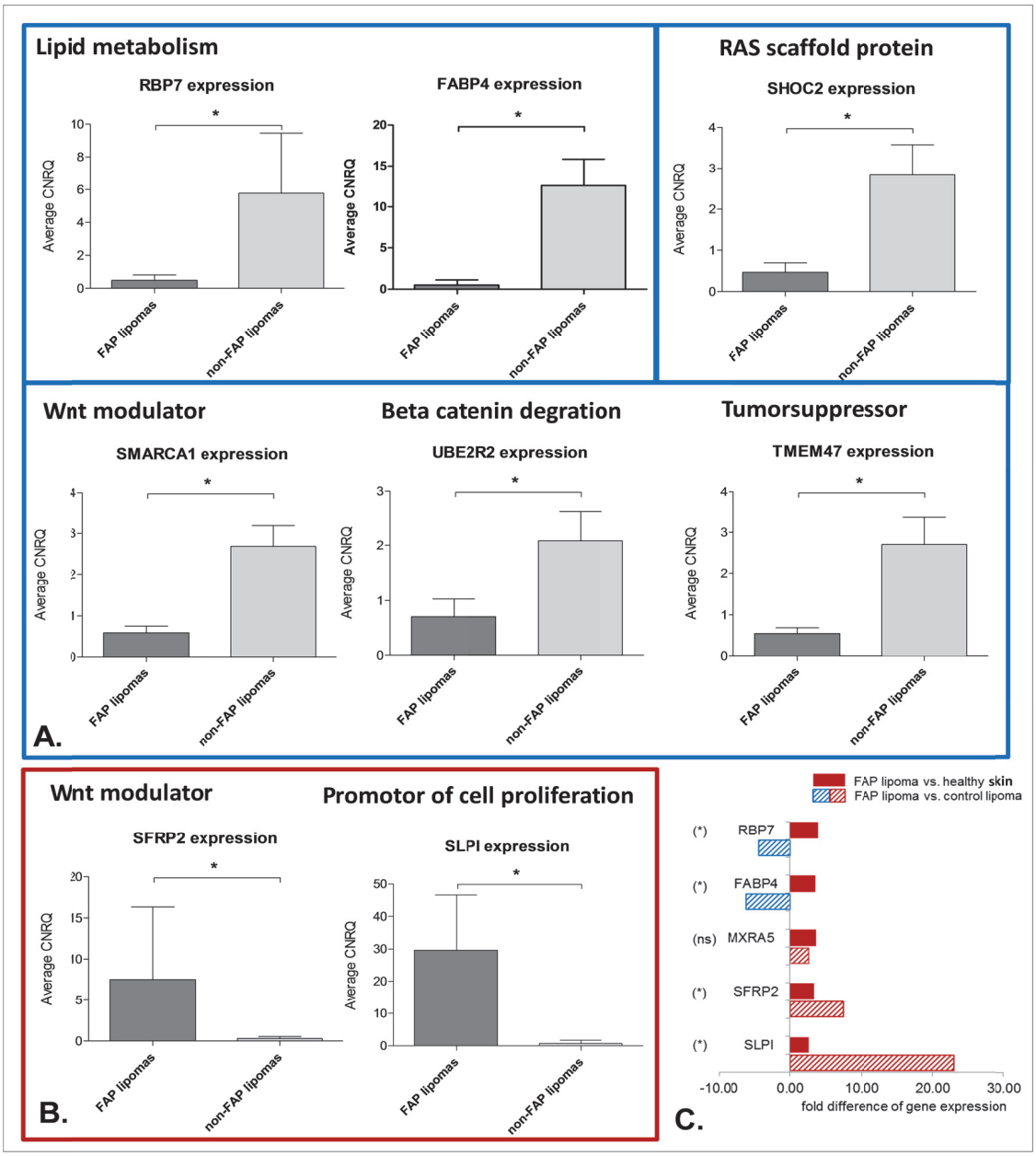

Figure 35. Averaged normalized mRNA expression levels of FAP lipoma and control lipoma samples after qPCR for significant targets. Bars indicate averaged normalized mRNA expression levels for FAP lipoma (dark bars) and control lipoma samples (bright bars) for selected targets after microarray expression analysis of FAP lipoma vs. FAP healthy skin. Values are presented as mean of the qbasePLUS calibrated normalized relative quantities (CNRQ) + SD. CNRQ values were reached after normalization to *HPRT1* and *LRP10*. Statistical analysis was done using Wilcoxon rank sum test based on sample medians. Calculation was performed on four FAP lipoma and five control lipoma samples, except *SLPI* (FAP lipoma n=3, lacking 22-2009).*p< 0.05; ns not significant. **A.** down-regulated mRNA targets in FAP lipoma are annotated with functions in lipid metabolism and cell proliferation (mainly tumor suppressive activity). **B.** up-regulated mRNA targets in FAP lipoma are annotated with functions in cell proliferation (repression and promotion). **C.** scheme summarizing microarray expression results for targets high differentially expressed in FAP lipoma vs. FAP healthy dermis (red filled bars) as well as in FAP lipoma vs. control lipoma (blue or red striated bars indicating down- or up-regulation, respectively). Significance levels of qPCR mRNA expression change are indicated in brackets for each target on the left.

5.2.3 FAP lipoma vs. control lipoma (non-FAP)

5.2.3.1 Whole genome expression analysis

The third analysis compared whole genome gene expression of FAP-associated lipomas with lipoma samples of the general population (control lipoma). Gene lists of DEGs were established based on expression intensities of totally **six FAP lipoma and three control lipoma** (non-FAP), that reached defined quality criteria (Table 4). In total, 741 up- and 1066 down-regulated genes were found to reveal differential gene expression concerning an FDR-unadjusted p-value <0.05. Table 15 indicates the numbers of DEGs for -fold changes and significance levels. By that approach, genes reached overall higher significance values than compared to the prior analyses of the FAP fibroma and FAP lipoma groups. Therefore, initial focus was set upon genes with minimum FDR-unadjusted p-values of <0.01 that included totally 120 up- and 273 down-regulated genes.

Table 15. Numbers of DEGs in FAP lipoma vs. control lipoma. The table shows the number of DEGs for -fold changes (fch) and significance levels. Detailed analyses were focused on gene expression differences of 4-fold and higher (red frame).

	p-value <0.05	p-value <0.01	fch 1.5	fch 2	fch 3	fch 4	fch 5	fch 10
No. genes detected	(741↑, 1066↓)	(120↑, 273↓)	(96↑, 184↓)	(69↑, 97↓)	(32↑, 54↓)	(14↑, 27↓)	(9↑, 19↓)	(4↑, 4↓)

The **PCA scatter plot** of the two lipoma types (Figure 36A) tend to separate at the middle of the grid to the lower left for FAP lipomas (red points) and the upper right for control lipomas (blue points). The blue ellipsoid encloses the three control lipoma samples that are less spread across the grid than the FAP lipomas samples. Among the FAP lipoma samples, a single sample (55-2010; Figure 36B) was localized on the most upper right side above the control lipoma samples. Two other FAP lipomas were spread to the two outer parts of the grid (22-2009, 29-2008). Therefore, FAP lipoma samples resulted in a higher inter-sample variation than control lipomas.

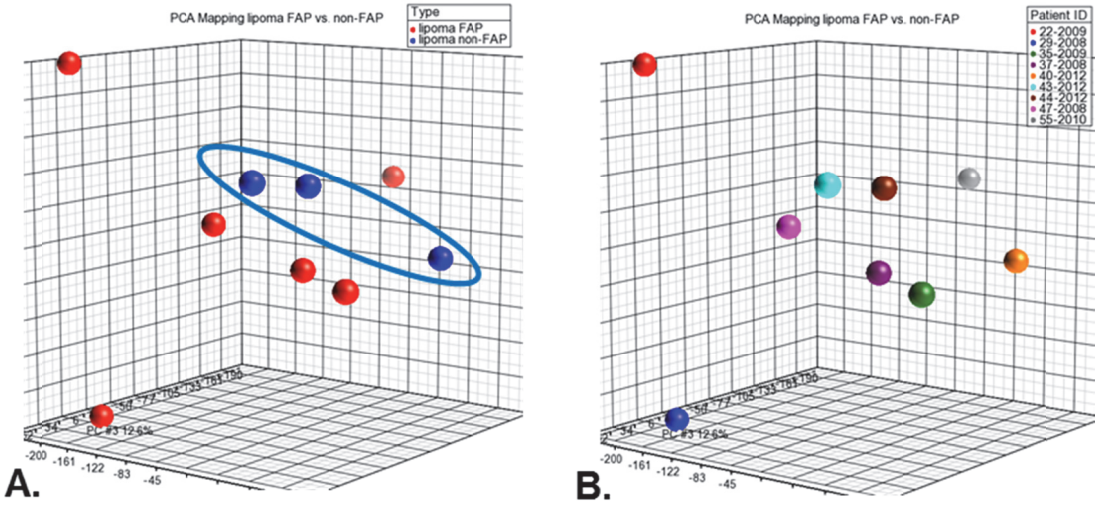

Figure 36. PCA scatter plot illustrating microarray chips of FAP lipoma and control lipoma samples. The grid shows the whole human genome and points represent single chips. **A.** illustrates the distribution of FAP lipoma (red points) and control lipoma (blue points). The blue ellipsoid encloses the three control lipoma samples. **B.** illustrates the same distribution but assigns *patient IDs* to the chip samples. Axis represent the three components of the gene expression intensities.

5.2.3.1.1 Hierarchical clustering of the mRNA expression data

We focused for further analyses on DEGs with FDR-unadjusted p-values <0.01 and a minimum 4-fold expression difference between FAP lipoma and control lipomas. Hierarchical clustering was therefore calculated for totally 41 genes (14 up- and 27 down-regulated, Supplementary Table 8). The heat map (Figure 37) indicated consistent clustering of DEGs in FAP lipoma compared to control lipoma samples. Especially for the three control lipoma samples expression profile was very consistent. One single sample (**55-2010 FAP lipoma**) revealed an overall differing expression pattern compared to all other FAP lipoma samples. Interestingly, the clustering for FAP lipoma vs. FAP healthy dermis (Figure 29) has shown a deviating pattern for the healthy sample of the same patient.

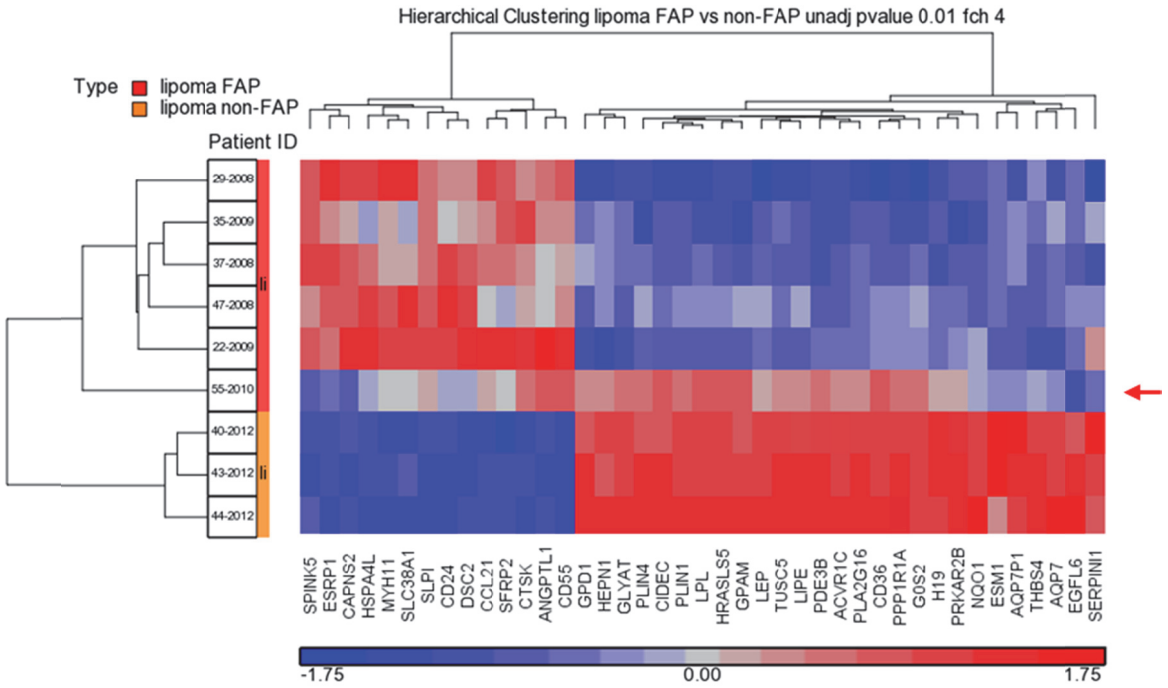

Figure 37. Hierarchical clustering of differentially expressed mRNAs in FAP lipoma vs. control lipoma. The heat map displays gene expression levels of all 41 genes (14 up- and 27 down-regulated) for each sample. It was generated for significantly regulated genes with 4-fold expression difference and FDR-unadjusted p-values <0.01. Each row indicates a single patient sample whereas genes are depicted by independent columns. Up-regulated genes are represented by red areas and down-regulated genes by blue areas. Grey areas assign genes of unchanged expression in FAP lipoma vs. control lipoma. The dendrograms represent similarities in mRNA expression intensities between different patients or between different genes. The red arrow marks the FAP lipoma sample of patient 55-2010 with differing expression pattern compared to the other FAP lipoma samples.

5.2.3.1.2 Gene ontology analysis FAP lipoma vs. control lipoma

GO analysis was performed with DAVID v.6.7 for the same 41 genes (14 up- and 27 down-regulated in FAP lipoma) with 4-fold expression difference as illustrated in hierarchical clustering. Several common biological processes were revealed and illustrated in Figure 38. Up-regulated genes are mainly involved in wounding, extracellular matrix organization, immunological processes, and calcium homeostasis. Only two or three genes are included in such processes. Processes associated with respiratory bust were suggested not to be of major interest in the present study (Figure 38A). Down-regulated genes were found to be associated with several single processes. Figure 38B illustrates those that include at least four of the down-regulated genes. Such genes are mostly involved in growth regulation, lipid metabolism, cell adhesion and response to stimuli.

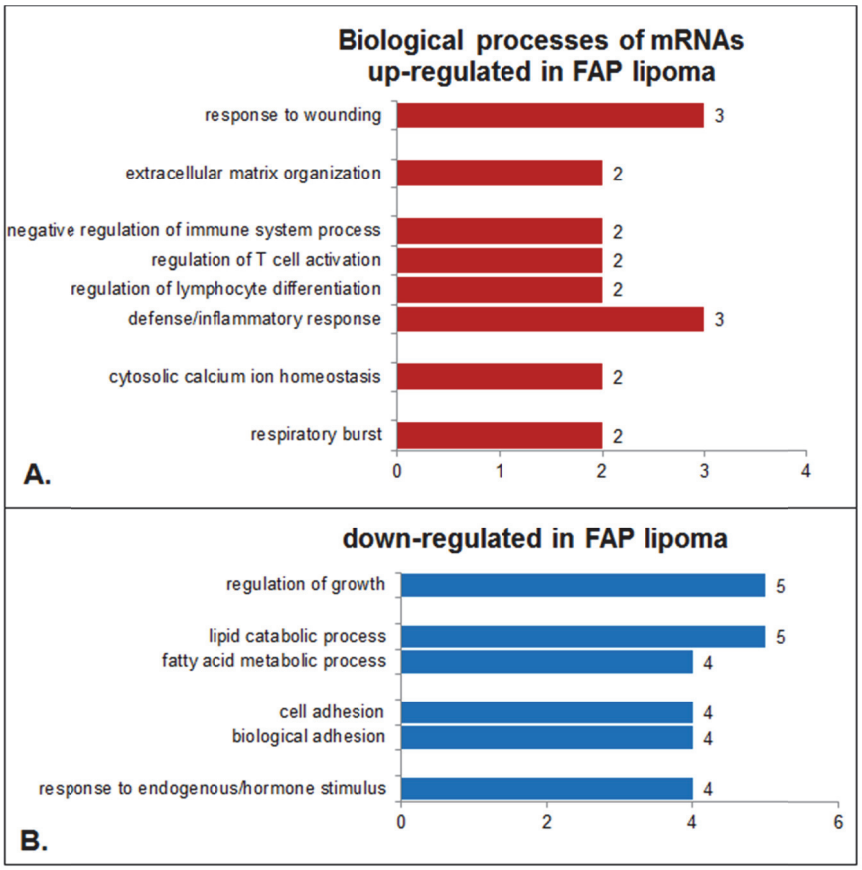

Figure 38. GO annotations for biological processes of changed mRNAs. GO analysis revealed several biological processes for up- (**A.**) and down-regulated (**B.**), including only processes with at least four down-regulated genes mRNAs in FAP lipoma vs. control lipoma. Numbers indicate quantity of genes involved in particular biological processes. Illustrations were based on gene lists with significance cut-off of unadjusted p-values <0.01 and expression changes of 4-fold with 12 (**A.**) and 22 (**B.**) detected genes.

5.2.3.1.3 Ingenuity pathway analysis

IPA® pathway analysis for the same 41 genes (14 up- and 27 down-regulated) with 4-fold expression change between FAP lipoma and control lipoma revealed totally **three pathways** that included at least 3 of the totally 41 genes (**PPARα/RXRα** activation pathway, **Leptin signaling** in obesity, and the **AMP-activated protein kinase** (AMPK)). All three pathways are known to function in lipid metabolism. Furthermore, several functional networks were found with functions in **development, lipid metabolism, and cell death and survival** (Table 16).

Table 16. Functional IPA® networks detected for genes with expression changes of 4-fold in FAP lipoma vs. control lipoma. In total 41 genes were divided into network groups considering their particular gene function. Networks with **interesting functions (development and lipid metabolism)** are marked in yellow. Strongly changed genes with –fold changes of at least 10, as well as *MYH11* and *SFRP2*, are indicated in bold and marked by arrows indicating their higher or lower regulation in FAP lipoma vs control lipoma. They will be illustrated in more detail (5.2.3.1.4).

Genes found to be regulated by common regulators (Figure 39) are indicated in bold grey. Such mRNAs are all down-regulated in FAP lipoma.

Top Functions	Molecules in Network
Connective Tissue Development and Function, Lipid Metabolism, Small Molecule Biochemistry	*AMPK, Ap1, AQP7, CCL21, CD36, CD55, **CIDEC**↓, collagen, Collagen Alpha1, Collagen(s), CPT1, Creb, CTSK, ERK1/2, ESM1, G0S2,**GPAM**↓, GPD1, H19, HDL, HDL-cholesterol, IL1, LDL, **LEP**↓, LIPE, LPL, **MYH11**↑, Nfat (family), NQO1, P38 MAPK, PDE3B, PLIN1, **PRKAR2B**, Tgf beta, THBS4*
Cell Death and Survival, Skeletal and Muscular System Development and Function, Lipid Metabolism	*ABCB11, ACAT1, ALDOB, APP, BCAT2, **CAPNS2**↑, CDSN, CS, DNAJC13, EDEM3, ESRP1, ETFDH, GLYAT, HMGCS2, HNF4A, HRASLS5, HSPA4L, KLK7, LRRC8C, MBNL1, MLX, PLA2G16, PLG, PLIN4, PNRC2, PPP1R3C, PRCP, SERPINI1, SLC38A1, **SPINK5**↑, SSFA2, TPP2, TPRA1, TUFT1, UBC*
Cellular Movement, Cardiovascular Disease, Congenital Heart Anomaly	*ACVR1C, Akt, ANGPTL1, CCKAR, **CD24**↑, **DSC2**↑, **EGFL6**↓, EMR1, ERK, estrogen receptor, FGF23, FREM1, FUT7, HRH3, Hsp70, IL12 (complex), IRAK1BP1, Jnk, Mapk, NFkB (complex), Pde3,PI3K (complex), PIK3R6, Pka, Pkc(s), PLA2G1B, PP1 protein complex group, PPP1R1A, RNF25, **SFRP2**↑, **SLPI**↑, SRC (family), TPP2, TRAFD1, ULBP2*

By IPA® analysis, several commonly present **upstream regulators** were found that regulate at least three of the high DEGs. Such upstream regulators include the cytokines TNF and WNT3A, the ligand-dependent nuclear receptors of the PPAR family, and the growth factor LEP. The Venn diagram in Figure 39 summarized the regulation of those molecules for high DEGs (bold; ***LEP, GPAM, CIDEC, SLPI***) as well as for other **lipid metabolism genes** with a minimum down-regulated expression of 4-fold (Supplementary Table 9). In addition, two further growth factors (TFGB1 and IGF1) were found to regulate genes such as *CIDEC, LEP, MYH11*, and *LEP, MYH11, SLPI*, respectively (data not illustrated). These results match finely with the three pathways detected all involved in lipid metabolism.

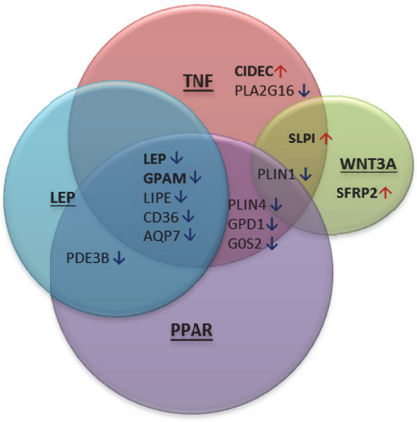

Figure 39. Venn diagram illustrating common upstream regulators of DEGs. High DEGs (bold) and others with negative -fold changes of at least 4 that are involved in lipid metabolism are depicted at the connection sites of their particular upstream regulator (bold and underlined). Upstream regulators are the tumor necrosis factor (TNF), leptin (LEP), molecules of the peroxisome proliferator-activated receptor (PPAR) familiy (namely α, β, and γ), and member 3A of the wingless-type MMTV integration site (WNT3A) a member of the WNT family.

5.2.3.1.4 Most interesting DEGs in FAP lipoma compared to control lipoma

Genes with highest supposed importance for the development in FAP lipoma compared to lipoma of the general population were selected based on their expression difference and their particular annotations (Table 17). Among the DEGs, totally eight genes (four up- and down-regulated, each) reached minimal expression difference of at least ten-fold. Such genes were investigated *in silico* for interesting annotations (Pubmed and gene database NCBI) with particular attention to:

- a possible function in skin diseases, especially in lipoma,
- a particular function in adipose tissues and lipid metabolism
- a possible involvement in cell proliferation and apoptosis, and
- a possible association to Wnt signaling (relating to the FAP disease)

Table 17 also includes *MYH11* (association with colorectal cancer) and *SFRP2* (Wnt modulator also selected in FAP lipoma vs. FAP healthy dermis) with lower -fold changes, but with interesting functions. Genes up-regulated in FAP lipoma were found to be involved in several skin manifestations (*SLPI, CD24, SPINK5, SFRP2*). Almost all of them were found to be associated with **proliferative processes** (*SLPI, CD24, MYH11, SFRP2*) with two of them (*CD24, SFRP2*) relating to **Wnt signaling**. Down-regulated genes were especially found to be **associated with lipid tissues** (*LEP, EGFL6, CIDEC*) or to function in **lipid metabolism** (*LEP, GPAM, CIDEC*). Two of them (*LEP, EGFL6*) were found to be involved in **cell proliferation** with *LEP* relating to Wnt signaling. Selected genes were found to localize different chromosomal positions. The same genes were also illustrated in Figure 40 relating to their **influence on cell proliferation**, their oncongenic or tumorsuppressive potential was assigned. Among the up-regulated genes two proto-oncogenes (*SLPI, CD24*) and one tumor suppressor (*SFRP2*) were found. Another gene with potential tumor suppressor functions (*CAPNS2*) was found to induce apoptosis if sustained activated[184]. Within the group of down-regulated genes, two proto-oncogenes were identified (*LEP, EGFL6*). Another gene (*CIDEC*) might function as a tumor suppressor as overexpression was reported to trigger apoptosis[185]. Overall, among the DEGs in FAP lipoma vs. control lipoma, proto-oncogenes as well as tumor suppressor genes were differentially regulated. However, genes mainly involved in cell proliferation predominated among the up-regulated genes, whereas genes associated with lipid tissue, adiposity, and lipid metabolism were mainly among the down-regulated genes.

Table 17. High significantly changed mRNA expression in FAP lipoma compared to control lipoma. In total eight possibly relevant genes (4 up- and 4-down-regulated) that have reached a significant change in mRNA expression of at least 10-fold and FDR-unadjusted p-value <0.01. In addition, two other genes (*MYH11* and *SFRP2*) with lower -fold changes were also listed due to their potentially interesting annotations in cell proliferation. Known gene functions and known influences on cellular processes (selected annotations) are summarized. Latter mainly focused on *gene functions in skin, lipoma, lipid metabolism, cell proliferation, and association to Wnt signaling pathway*. Statistical analysis has been done by a 2-way ANOVA after microarray technology based whole genome expression analysis. Chromosomal positions are indicated. Up-regulated genes are sorted top down by decreasing -fold change. In contrast, down-regulated genes are sorted top down by decreasing negative -fold changes.

Up-regulated in FAP lipoma vs. control lipoma

gene ID	gene description and selected annotations	localization	fch	p-value
SLPI	**secretory leukocyte peptidase inhibitor** - serine protease inhibitor - antiinflammatory, antimicrobial, imunomodulatory activity - contributes to psoriasis pathogenesis[186] - promotes cell proliferation and wound healing[187,188] - overexpressed in several cancers[189]	20q12	**22.98**	< 0.001
CD24	**cluster of differentiation 24** - cell adhesion molecule, granulocytes and B-cells - overexpressed in BCC and SCC[190] - overexpressed in cancer development and progression[191] - β-catenin target gene (Wnt signaling)[192]	6q21	**17.22**	<0.001
CAPNS2	**calpain, small subunit 2** - cysteine protease - key regulator in cellular functions - cellular signaling, remodeling, degradation and cell death (if sustained activated)[184]	16q12.2	**11.51**	0.01
SPINK5	**serine peptidase inhibitor, Kazal type 5** - multidomain serine protease inhibitor - skin and hair morphogenesis - mutations associated with Netherton syndrome[a] and atopic dermatitis[155,156]	5q32	**11.49**	0.01
MYH11	**myosin, heavy chain 11, smooth muscle** - smooth muscle myosin - major contractile protein - mutations associated with human colorectal cancer and intestinal neoplasia[193,194]	16p13.11	**8.27**	0.004
SFRP2	**secreted frizzled-related protein 2** - involved in wound healing and development of hypertrophic scars[176] - methylation associated with colorectal cancer[177] - soluble modulator of Wnt signaling	4q31.3	**7.39**	0.005

[a]Netherton Syndrome: severe autosomal recessive disorder with congenital ichthyosis, defective cornification, specific hair shaft defect and severe atopic manifestations[155] .

Down-regulated in FAP lipoma vs. control lipoma

gene ID	gene description and selected annotations	localization	fch	p-value
LEP	**leptin** - secreted by white adipocytes - regulator of body weight - expressed in several neoplasms of lipid tissue[195] - possible role in the immunopathogenesis of psoriasis[196,197] - involved in Wnt signaling and cancer progression[198]	7q31.3	**-19.17**	0.001
EGFL6	**EGF-like-domain, multiple 6** - member of epidermal growth factor (EGF) repeat superfamily - cell adhesion, and extra cellular matrix (ECM) protein - increased expression in adipose tissue with obesity[199] - expressed in hair follicle development[200] - regulation of cell cycle, proliferation, and developmental processes[201]	Xp22	**-16.27**	<0.001
GPAM	**glycerol-3-phosphate acyltransferase, mitochondrial** - synthesis of glycerolipids out of saturated fatty acids	10q25.2	**-12.87**	0.006
CIDEC	**cell death-inducing DFFA-like effector c** - regulator of lipid metabolism - predominantly expressed in adipocytes[202] - promotes lipid droplet formation in adipocytes[203] - triggers apoptosis if overexpressed in cancer[185]	3p25.3	**-11.76**	0.005

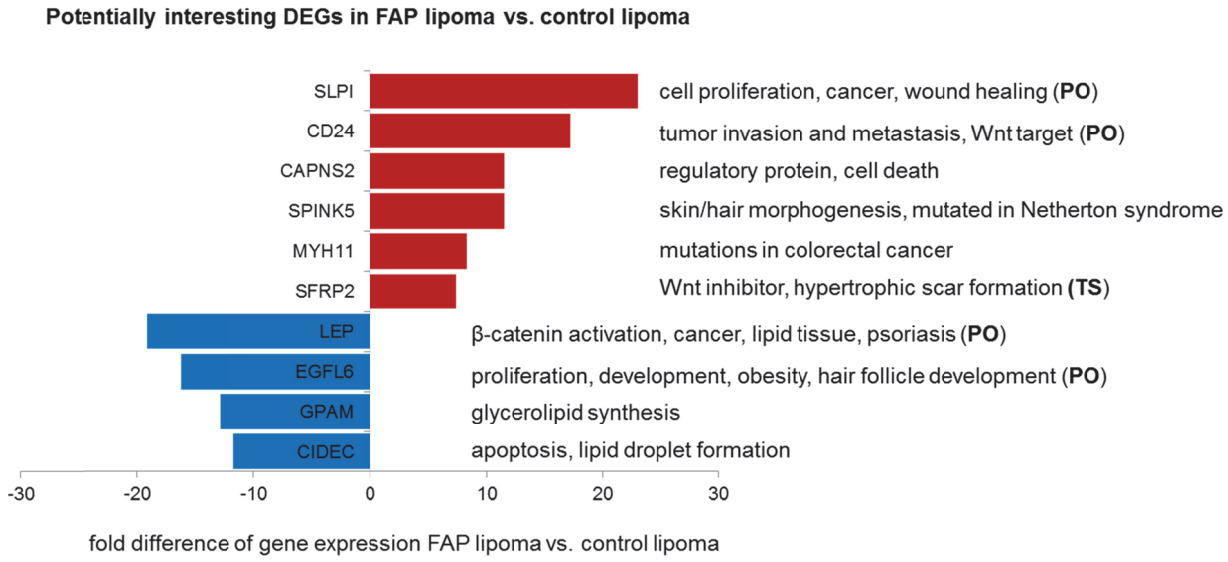

Figure 40. Overview of selected genes relating to cell proliferation function. The ten highly changed genes (six up-, four down-regulated) are sorted by their expression change and indicated by their particular annotation relating to cell proliferation. Red bars indicate gene expression changes of genes overexpressed in FAP lipoma vs. control lipoma, whereas blue bars indicate -fold differences of down-regulated genes. Known proto-oncogenes (PO) or tumor suppressor genes (TS) are indicated. Gene expression -fold difference is illustrated on the x-axis. Genes are depicted on the y-axis.

5.2.3.2 Calculation of differential gene expression in lipoma investigations without outlier 55-2010 included all selected DEGs

As expression patterns for both samples of patient 55-2010 were found to differ from other healthy skin or lipoma samples (Figure 29, Figure 37), differential gene expression has also been calculated for both groups by excluding patient 55-2010. Interestingly, an overall higher number of DEGs was reached for equal significance levels (-fch 2.5 (p-value <0.05) for FAP lipoma vs. healthy dermis and -fch 3 (p-value <0.01) for FAP lipoma vs. control lipoma). This was supposed to be achieved due to a higher accuracy reached after exclusion of patient 55-2010. But most importantly, the high DEGs discussed in detail, were also revealed by such calculations with same significance levels and -fold changes. However, why both samples of 55-2010 revealed a different pattern compared to other corresponding samples is not clear. A possible exchange or double loading of the same samples during calculations could be excluded, as calculations were based on sample IDs that were set right after array load and were not changed anymore afterwards. Moreover, the lipoma and the healthy sample of 55-2010 indicated a slight but distinct difference in the heat map (Figure 29). In quality control and PCA analysis both samples were rather inconspicuous. Finally, samples of patient 55-2010 differed only little in their whole genome expression compared to other patient samples. Therefore this patient contributed less to the differential expression patterns. Due to the low sample number and the source of human material this difference might also be explained and tolerated by the inter-individual differences.

5.2.4 FAP epidermal cyst vs. FAP healthy epidermis

The last analysis compared whole genome expression of FAP-associated epidermal cysts with healthy epidermal skin of FAP patients. Gene lists of DEGs were established based on expression intensities of totally **three epidermal cysts and three healthy skin samples of four FAP patients** that reached defined quality criteria (Table 4). Very few DEGs were detected with a minimum expression change of at least 1.5 and FDR-unadjusted p-value <0.05, with only six genes (three up- and three down-regulated in FAP epidermal cysts, Supplementary Table 10). Table 18 indicates the number of DEGs for -fold changes and significance levels.

Table 18. Numbers of DEGs in FAP epidermal cyst vs. FAP healthy epidermis. The table shows the number of DEGs for -fold changes and significance levels. Differences of expression intensities were indicated by -fold changes (fch). Gene lists have been created by a 2-way ANOVA applying methods of moments for statistical analysis and Fisher's Least Significant Difference (LSD) as contrast method using Partek® Genomic Suite™.

	p-value <0.05	fch 1.5	fch 2	p-value <0.01	fch 1.5	fch 2
No. genes detected	(462↑, 200↓)	(3↑, 3↓)	-	164↑, 81↓)	(-↑, 1↓)	-

The **PCA scatter** plot revealed **high inter-sample variation** for epidermal cyst samples (red points) and healthy epidermis samples (blue points) in overall gene expression (Figure 41A). One sample (30-2008 epidermal cyst) differed from all other samples, as it was the single sample located at the left side of the grid (sample of highest intensity in QA/QC histogram, Supplementary Figure 1). For one patient (21-2009) epidermal cyst and healthy epidermis revealed very similar distribution (Figure 41B). The corresponding hierachical clustering heat map did not reveal any clustering for the 6 genes with -fch 1.5 (Supplementary Figure 5). Expression analysis for epidermal cyst vs. healthy skin of FAP patients was not further proceeded, as obviously no major expression changes were revealed.

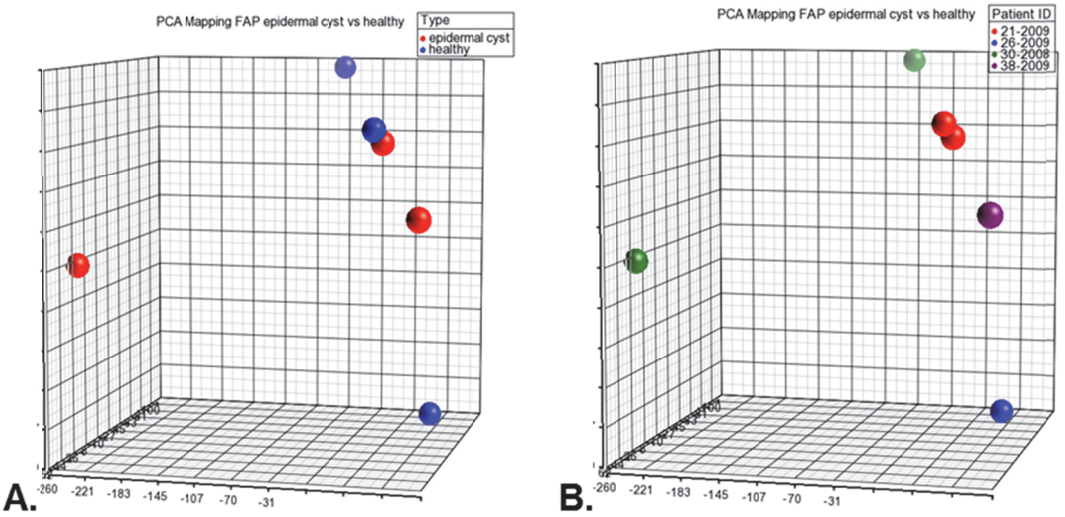

Figure 41. PCA scatter plot illustrating microarray chips of epidermal cyst and healthy epidermis samples from FAP patients. The grid shows the whole human genome and points represent single arrays. **A.** illustrates the distribution of epidermal cysts (red points) and healthy samples (blue points). **B.** indicates the same distribution but assigns *patient IDs* to the chip samples. Axes represent the three components of the gene expression intensities.

6 DISCUSSION

6.1 *APC* second hit mutation analysis

In this study, we systematically investigated three different types of benign skin lesions of FAP patients with known *APC* germline mutation for somatic mutations, i.e. second hits, therein. For this purpose we used a variety of methods to analyze the DNA and RNA isolated from the lesional biopsies and identified three different alterations in one out of 3 lipoma and one out of 3 epidermal cysts.

By direct sequencing of the MCR we identified a second hit mutation (c.4778delA; p.K1593Sfs*57) in the epidermal cyst sample of patient 30-2008. Such second hit mutations affecting 1-2bp have been reported to account for approximately 33% of all second hit mutations in colorectal cancer. These lead to protein truncation by either nonsense or frameshift mutations in most of the cases[67,204]. A similar observation was made in the sole study of FAP-associated skin lesions, where a frameshift mutation in an epidermal cyst is reported[205]. Other somatic mutations in *APC* have not yet been described in human FAP-associated fibromas and lipomas. Furthermore, the presence of second hits in epidermal cysts associated with FAP in an 1638N*Apc* mouse model was shown to amount to about 50%[99]. Comparable to the common occurrence of somatic *APC* mutations in colorectal cancer or other gastrointestinal tumors as well as desmoids (Table 19), the frequency of 33% (1 out of 3) appears to be relatively low. Clearly, our study, as well as the one from Blaker *et al.* 2004, is limited by the small number of samples analyzed, as well as the fact, that somatic mutations outside the MCR or the presence of large genomic rearrangements could, due to the paucity of material, not be excluded.

In accordance with previously published data the analysis of *APC* cDNA resulted in different *APC* isoforms. These alternative transcripts of *APC* have already been described for different tissues but not for skin[27,128-133]. Here, we have identified 8 alternative splice products, which were present in addition to the expected *APC* product. Other groups could also confirm the transcripts and showed that the resulting proteins are co-expressed with the full-length APC protein[131,133]. Since we could not extract proteins from the small lesions we do not know which transcripts and exons are finally translated into protein.

Additionally, the epidermal cyst of 30-2008 as well as the lipoma of 29-2008 revealed an altered microsatellite pattern for *APC* marker locus D5S346 at 5q22.2 with loss of heterozygosity (LOH) as well as microsatellite instability (MSI) indicated by novel alleles. LOH has been shown to represent an important mechanism in the development of different skin pathologies, e.g. in BCC, SCC, and malignant melanomas. Furthermore, it is involved in the development of several benign cutaneous tumors and non-neoplastic skin disorders,

such as neurofibromas in neurofibromatosis type 1[206-208]. For these benign cutaneous neurofibromas in neurofibromatosis type 1, somatic deletions of the *NF1* (17q11.2) gene, but also for *TP53* and *RB1* were described. Furthermore, in patients with multiple endocrine neoplasia type 1 loss of function of the *MEN1* gene (11q13) was shown for angiofibromas, collagenomas, and one lipoma[209]. To the best of our knowledge, LOH at D5S346 in primary or FAP-associated human cutaneous epidermal cysts or lipomas has thus far not been reported. As the marker D5S346 is located near to *APC* on chromosome 5, we suppose that changes (especially LOH) encountered in D5S346 might also reveal any indication for changes in *APC*.

Novel alleles at the D5S346 locus are indicative for microsatellite instability. To diagnose MSI, the Bethesda panel (including D5S346, BAT25, and BAT26) is used in colorectal cancer, especially in Lynch syndrome[210]. In contrast to this autosomal dominantly inherited disease, that is caused by mutations in DNA mismatch repair genes[5], MSI does not typically occur in FAP-associated colorectal cancer but individuals suffering from the Lynch syndrome variant Muir Torre syndrome may also develop benign skin tumors[211]. MSI has been described in several of their skin lesions such as sebaceous adenomas, -warts, -tumors, and -epithelioma, as well as stucco keratosis[212] and cystic sebaceous tumors[213]. Furthermore, MSI was found in primary melanomas and dysplastic nevi[214], Spitz nevi[215], neurofibromas[208], actinic keratoses, and SCC[216]. Instability at D5S346 in primary or FAP-associated epidermal cysts or lipomas, however, has thus far not been reported. General MMR deficiency leading to the development of lipomas and epidermal cysts in our patients could be largely excluded by the additional analysis of the mononucleotide markers BAT25 and BAT26[217], which are known to be highly sensitive to detect MSI-high cancers. Since a general impairment of the MMR system has been excluded for the two skin lesion samples, we hypothesize an unequal chromosomal rearrangement as possible mechanism for the aberrant microsatellite pattern[206,218].

Table 19. Frequency of *APC*-associated somatic mutations in cutaneous and gastrointestinal tissues. Listed are results of the present study completed with results from the literature, by considering truncating mutations (especially in MCR) and allelic loss. Several samples could arise from the same patient. Numbers of patients are indicated in brackets if available.

tissue	**number of samples** [number of examined patients]	**overall frequency of second hits** [number of patients]	**frequency of somatic *APC* mutations** [number of patients]	**frequency of LOH** [number of patients]	***APC* gene coverage/ LOH analysis**	**references**
fibroma	**9** [9]	-	-	-	MCR (cd. 1139-1640) LOH: D5S346	**this study**
lipoma	**3** [3]	**1/3 (33%)** [1]		LOH + allelic instability 1/3 (33%) [1]	MCR (cd. 1139-1640) LOH: D5S346	**this study**
angiofibrolipoma	1	-	-	-	MCR (cd. 1289-1680)	Bläker *et al*, 2004[205]
epidermal cyst	**3** [3]	**2/3 (66%)** [1]	**1/3 (33%)** [1]	LOH + allelic instability: 1/3 (33%) [1]	MCR (cd. 1139-1640) LOH: D5S346	**this study**
	2 [2]	1/2 (50%) [1]	1/2 (50%) [1]	-	MCR (cd. 1289-1680)	Bläker *et al*, 2004[205]
seborrhoic wart	1	-	-	-	MCR (cd. 1289-1680)	Bläker *et al*, 2004[205]
desmoid	23	19/23 (83%)	12/19 (63%) 1/19 (5%) exonic del	6/19 (32%)	coding exons 1-15/ LOH: D5S346, D5S82, D5S1965, D5S421	Latchford *et al*, 2007[72]
	8 [7]	8/8 (100%)	7/8 (88%) [6]	1/8 (12%) [1]	coding exons 1-15	Miyaki *et al*, 1993[219]
gastric fundic gland polyps (GFP)	41 [16]	21/41 (51%) [12]	15/21 (37%) [10]	6/21 (15%) [2]	MCR (cd.1417-1596) LOH: D5S299, D5S346, and D5S82	Abraham *et al*, 2000[17]
gastroduodenal tumors	75 [21]	47/75 (62%)	47/75 (62%)	-	*APC* ex 5-9; 13-15i	Toyooka *et al*, 1995[220]
duodenal polyps	49 [39]	9/49 (18%) [7]	6/9 (12%) [6]	3/9 (6%) [1]	MCR (1147-1693) LOH: D5S346 and D5S656	Groves *et al*, 2002[221]
colorectal adenomas	233 [39]	n/a	52/156 (33%)	52/233 (22%)	*APC* ex ex 4-14 ; 15A-I LOH: D5S346, D5S656, D5S421	Crabtree *et al*, 2003[68]
	133 [6]	105/133 (79%)	85/105 (63%) [6]	23/105 (17%) [3]	PTT ex 15 (cd. 654-2844) LOH: D5S346 and D5S404	Albuquerque *et al*, 2002[69]
	210 [35]	n/a	n/a	42/210 (20%) [11]	LOH: D5S656, D5S489 and D5S82	Lamlum *et al*, 1999[67]
colorectal tumors	359 [70]	n/a	180/359 (50%)	136/254 (54%)	*APC* ex 1-15K LOH: *APC* locus	Miyaki *et al*, 1994[222]

6.2 Gene expression analyses

The gene expression profiles of benign neoplasia associated with the FAP disease are rarely investigated and whole genome expression of FAP-associated fibromas, lipomas, or epidermal cysts has not yet been analyzed, to the best of our knowledge. In the presented study, we revealed changed expression patterns for fibroma and lipoma skin neoplasia from FAP patients compared to healthy skin samples, as well as for FAP lipomas compared to lipomas of non-FAP individuals. Several potentially interesting targets were found for each skin lesion group that are in the following discussed in more detail.

FAP fibroma vs. FAP healthy dermis

Expression analyses on FAP fibroma compared to healthy dermis revealed a clearly different mRNA expression pattern. Results of additional analyses as gene ontology and IPA® included only few genes, wherefore we decided to mainly concentrate on highest changed DEGs.

Unexpected result-high amount of epidermal components

An unexpected observation noticed by results from gene ontology as well as by detailed annotation analyses, especially among genes down-regulated in FAP fibroma, was the predominance of epidermal components. By gene ontology analysis several changed processes were found to relate to the development and differentiation of epithelia, epidermis, and keratinocytes. Furthermore, total expression profile indicated epidermal components such as several cytokeratins, and components of epidermis-dermis junctions including desmogleins and desmoplakins. Comparable results also referred to the functions of the selected 12 mRNAs. Such major presence of epidermis-related genes would not be suspected as the fibroma lesion applies to the dermal rather than to the epidermal part of the skin and mainly consists of connective tissue and fibroblasts rather than of keratinocytes[85]. A possible explanation could be the inclusion of adnexal structures such as hairs during isolations especially of healthy dermis samples (as epidermis-related genes were down-regulated in fibroma compared to healthy skin). In addition, according Spemann[223] organization fields which include all germ layers are important in embryogenesis.

Highest changed DEGs in FAP fibroma vs. FAP healthy skin

In total, 12 targets were selected based on a 3-fold expression change and gene annotations relating to functions in skin and proliferation. Almost all of them (11/12) were successfully confirmed by qPCR, whereas six of them significantly. Those six DEGs indicated functions in skin as well as relevance in cell proliferation or suppression of

metastasis. Among those genes several associated skin diseases were identified, such as melanoma[134,154], squamous cell carcinoma (SCC)[141,224], chondromyxoid fibroma[135], and sclerodermal fibroblasts[143]**.** All those skin diseases affect different cell types in contrast to the benign mesenchymal neoplasm of a FAP fibroma which consists mainly of collagen bundles and interspersed fibroblasts[85]. However, our results indicate a relevance of such DEGs in skin. Functions in cell proliferation were hypothesized to be of major importance for the development of the fibroma neoplasm. Relating to annotations for high DEGs we revealed genes possibly operating as proto-oncogenes (responsible for proliferation and development of fibroma) or as tumor suppressor genes (that prevent a potential malignant progression).

Up-regulated *S100B, CHL1*, and *SERPINE2* might influence FAP fibroma development by their proto-oncogenic functions

The highest up-fold regulated target ***S100B*** in FAP fibroma encodes a calcium binding protein that was found to be usually expressed in tissue of neuroectodermal and mesodermal origin[134] such as in melanocytes and Langerhans' cells (epidermis), Schwann cells and sensory corpuscles (dermis) and in sweat glands[225]. In melanoma cells, overexpressed S100B serum levels have been reported to correlate with melanoma progression. This effect has been explained by an increased protein-protein interaction of overexpressed S100B with the transactivation domain and the C-terminus of tumor suppressor p53, therefore inhibiting its apoptotic function on potential melanoma cells[136]. Relating to these results, a similar proto-oncogenic mechanism could probably also influence the development of FAP fibromas.

Another high significantly confirmed target indicates ***CHL1***, a transmembrane cell adhesion molecule that mediates cell-cell and cell-matrix interactions. As a member of the L1 gene family of neural cell adhesion molecules it is involved in neural recognition and signal transduction pathways but has also been described to play a role in cancer growth and metastasis[141,226]. They suggested a dual role for *CHL1* as a putative tumor suppressor during primary tumor growth on the one hand (e.g. in colorectal cancer, tumors of the small intestine, breast cancer, melanoma and SCC) and as an oncogene to promote local invasive growth and metastatic spread on the other hand (e.g. metastatic growth of melanoma, colon, ovary, and breast cancer[141,142,227]). In these metastatic colorectal cancer cells, *CHL1* has furthermore been identified as a β-catenin target gene that increases cell motility, invasion and tumorigenesis, if overexpressed[142]. This function might also explain its up-fold regulation in FAP fibroma revealed in the presented study. As *APC* germline mutations in FAP patients lead to an aberrant activation of β-catenin[36] target genes such as

also *CHL1* are dys-regulated. This might in the present case trigger the formation of the fibroma neoplasm but without leading to metastasis such as reported for other tumor types. However, for healthy skin samples of FAP patients, β-catenin is supposed to be equally regulated. Therefore an additional regulation of *CHL1* by other genes is supposed to lead to an overexpression in FAP fibroma compared to FAP healthy skin.

SERPINE2, also known as protease nexin 1, is an inhibitor of several growth-modulating serine proteases (thrombin, urokinase, plasmin and trypsin)[228]. Due to their anti-proteolytic function, SERPINEs impair extracellular matrix degradation and therefore increase the invasion and metastasis of cancer cells[146]. Similar to our results in FAP fibroma, up-regulated *SERPINE2* has also been reported for a number of different cancers (pancreas carcinoma[144], breast carcinoma[145], and colorectal carcinoma[147,148]). Relating to oral and cutaneous tissues, up-regulated *SERPINE2* expression was reported for oral SCC[224] and in fibroblasts of scleroderma patients (a disease characterized by extracellular matrix accumulation[143]). In colorectal tumorigenesis, *SERPINE2* was identified as a target of ERK signaling. Up-regulated *SERPINE2* mRNA expression in colorectal and intestinal cancer was shown to be activated by mutations of MAPK pathway molecules, such as *Ras*, *BRAF* and *MEK*[148]. The oncogenic functions of *SERPINE2* may possibly also influence cell growth in FAP fibromas, possibly also due to an impairment of extracellular matrix degradation or activation of ERK signaling.

Up-regulated *CDH19* and down-regulated *CARD18* might inhibit continuing tumor growth and invasion in FAP fibroma by their tumor suppressive functions

CDH19 represents a member of the huge cadherin family of cell adhesion molecules[229]. Loss of cadherins is frequently reported in cancer, especially E-cadherin (CDH1). Cancer formation is supported by cell adhesion defects due to altered cadherin-catenin complexes, β-catenin amongst others[138]. *CDH19* mRNA down-regulation has previously been reported in cholesteatoma tissue, a gradually expanding destructive epithelial lesion within the middle ear[137]. In the presented study an up-regulation of *CDH19* might indicate an increase of tumor suppressive function that possibly prevents invasive growth in benign FAP fibroma.

CARD18 (caspase associated recruitment domain 18) is member of a protein family known to mediate protein-protein interactions between key apoptotic signaling molecules[157]. According to the presented study, no other study was found to report a down-regulation in any human neoplasm or other cutaneous disease, to the best of our knowledge. In contrast, over-expression of *CARD18* mRNA and CARD18 protein has been reported in internal cancers (gastric adenoma and its lymph node metastasis[159]) and lung SCC[230].

Relating to this function, in the presented study, *CARD18* down-regulation in FAP fibroma might suppress invasive growth in FAP fibroma.

Down-regulated *CST6* might influence normal skin function in FAP fibroma

***CST6*,** an endogenous inhibitor of cysteine proteinases (cathepsins and asparaginyl endopeptidase legumain) was described to prevent invasion and metastasis of melanoma cells[154]. In accordance to the presented study, decreased expression was related to metastasis of mammary epithelial tumor cells and malignant melanomas[231,232]. In skin, CST6 was found to be expressed in differentiating and cornifying layers of the epidermis, and in appendages such as hair follicles, sebaceous glands, and sweat glands. Furthermore, CST6 has been found to be an important regulator of epidermal terminal differentiation[152]. Loss of expression has been correlated with phenotypes resulting in faulty cornification, desquamation and follicle morphogenesis[153]. Such results indicate a major importance of CST6 for the normal epidermal function and development. Here, this study discloses its function in dermis, revealed in a down-regulation in FAP fibroma.

Comparison to prior gene expression analyses for FAP fibroma neoplasms

Prior investigations on FAP-associated fibromas merely dealt with the selective expression analysis of Wnt pathway molecules applying immunohistochemistry (IHC). Such studies revealed positive reactivity for β-catenin, β-catenin target genes cyclin D1 and c-myc, as well as CD34, CD99, and vimentin[46,86,90,92,93,96,97]. Apart from Wnt pathway-associated molecules, the importance of TGFβ1 as a regulator of fibroblast proliferation was reported, and has also been described to be overexpressed in fibroma cell cultures of patients with Gardner syndrome[233]. In the presented study, such genes revealed unremarkable expression changes not included within the defined minimum 1.5-fold expression change and FDR-unadjusted p-value <0.05 (Table 20). As Wnt pathway genes revealed no significant expression difference, we would rather suggest other than Wnt-correlated mechanisms as a main cause for fibroma development in FAP patients. This suggestion is supported by a previously published study of our group[22] that did not found a significantly higher prevalence of single skin lesions (fibromas, lipomas, and epidermal cysts) in FAP patients compared to such in the normal population.

In concordance with our data, several molecules in Gardner-associated fibroma have been reported to reveal negative reactivity in IHC[46,86,90,92,93,96,97]. Only *S100B* revealed a remarkable and significant up-regulation in fibroma tissues (Table 20).

In summary, according to presented expression results, the development of FAP fibroma tend to be influenced by target genes mainly involved in proliferation processes. FAP

fibroma might develop by the activation of proto-oncogenes such as *S100B, SERPINE2*, and *CHL1.* A further invasive growth might be prevented by an increased activation of tumor suppressors such as *CDH19* and *CHL1* (dual function) and deactivation of proto-oncogenes such as *CARD18*. Another possible role might also play the deregulation of genes important for normal skin development such as *CST6*. Wnt pathway genes in contrast tend to have less impact on the development of FAP fibromas what differs from several prior studies on FAP-associated fibromas (Table 20).

Table 20. Comparison of prior studies on FAP fibromas to presented gene expression profile. Molecules already examined in prior gene expression analyses on FAP-associated fibromas are illustrated in comparison to our expression profile. Almost all molecules were reported to reveal positivity or negativity in IHC studies, and several of the positive molecules relate to Wnt signaling. Furthermore, transforming growth factor β1 (TGFβ1) mRNA and protein was reported to be overexpressed in FAP fibroma cells[233]. Indicated -fch and p-values relate to results of the present whole genome expression analysis on FAP fibroma vs. FAP healthy dermis samples. Molecules with reported IHC positivity as well as for TGFβ1 revealed unremarkable expression changes not reaching minimum expression difference of at least 1.5-fold with unadjusted p-value <0.05. In contrast, most of the molecules negative for FAP fibroma could have been confirmed with our expression data. In contrast to other IHC investigations, a high *S100B* up-fold regulation was revealed in the presented analysis.

Molecules with reported IHC positivity or mRNA/protein overexpression in FAP fibroma

gene ID	gene name	localization	fch	p-value	reference
CTNNB1	β-catenin 1		1.22	0.14	Coffin 2007[46]
CCND1	cyclin D1	11q13	1.04	0.05	Coffin 2007[46]
MYC	v-myc myelocytomatosis viral oncogene homolog (avian);	8q24.21	1.04	0.86	Coffin 2007[46]
CD34	CD34 molecule	1q32	-1.63	0.03	Wehrli 2001[86]; Lanckohr 2011[90]; Michal 2004[97]
CD99	CD99 molecule	Xp22.32; Yp11.3	-1.08	0.67	Linos 2011[96]
VIM	vimentin	10p13	1.37	0.06	Wehrli 2001[86]; Lanckohr 2011[90]; Michal 2004[97]
TGFB1	transforming growth factor, β 1	19q13.2|19q13.1	1.06	0.47	Lilli 2002[233]

Molecules with reported IHC negativity in FAP fibroma

gene ID	gene name	localization	fch	p-value	reference
ACTC1	muscle specific actin actin, α, cardiac muscle 1	15q11-q14	-1.12	0.29	Wehrli 2001[86]; Lanckohr 2011[90]; Michal 1999[93], 2000[92], 2004[97]; Linos 2011[96]
ACTA2	smooth muscle actin contractile apparatus; skeletal muscle	10q23.3	-1.97	0.02	Wehrli 2001[86]; Lanckohr 2011[90]; Michal 1999[93], 2000[92], 2004[97]; Linos 2011[96]
DES	desmin muscle specific intermediate filament	2q35	-1.26	0.1	Wehrli 2001[86]; Lanckohr 2011[90]; Michal 2000[92], 2004[97]; Linos 2011[96]
S100	S100 calcium binding protein		5.26	0.03	Lanckohr 2011[90]; Michal 2000[92], 2004[97]; Linos 2011[96]
EMA	epithelial membrane antigen mucin 1, cell surface associated	1q21	-1.16	0.23	Linos 2011[96]; Michal 1999[93]
GFAP	glial fibrillary acidic protein	17q21	-1.12	0.12	Michal 1999[93]
Cytokeratins			almost all down		Michal 2000[92], 2004[97]
Ki-67 (MKI67)	marker of proliferation /antigen identified by monoclonal antibody Ki-67	10q26.2	-1.23	0.06	Linos 2011[96]

FAP lipoma vs. FAP healthy dermis

Lipomas compared to healthy skin of FAP patients revealed a clearly differential expression profile. Same as in the fibroma analysis, we decided to mainly focus on highest changed DEGs. All such genes were found to reveal increased mRNA expression in FAP lipoma and to function in lipid metabolism or in modulation of cell proliferation.

Influence of mRNA targets *FABP4* and *RBP7* involved in lipid binding and lipid metabolism on the development of FAP and non-FAP lipomas

Two genes (*FABP4, RBP7*) were found to encode for members of intracellular lipid-binding proteins[234]. ***FABP4*** was reported to be especially expressed in adipocytes and to function in fatty acid uptake, transport and metabolism[235]. In a recent study, several soft tissue tumors of mature and immature fat cells have been shown to positively stain for FABP4 in contrast to non-adipose mesenchymal and non-mesenchymal tumors[175]. ***RBP7***, a retinol binding protein, is known to function in the stabilization, intracellular transfer and metabolism of otherwise rather unstable vitamin A[234]. The up-regulation of such genes in FAP lipoma compared to FAP healthy dermis may therefore be explained by their predominant expression in lipid tissue. Interestingly, both genes were also found to be overexpressed in non-FAP lipoma tissue compared to FAP lipoma. This might be explained by a possible difference in lipoma type derived from FAP patients or healthy individuals. Another explanation could be provided by an influence of Wnt signaling in FAP adipose tumors. Wnt molecules have been described to block the development of white and brown adipose tissue[107] and to inhibit adipocyte differentiation[236]. Furthermore, *FABP4* and other major genes of the adipogenesis pathway were reported to be down-regulated by Wnt signaling-induced β-catenin up-regulation[108]. Therefore, decreased mRNA expression of such lipid binding molecules in FAP lipoma might be influenced by the *APC* germline mutation. This mutation is suggested to lead to a deregulated β-catenin increase and therefore to a decrease of lipid binding proteins. The up-regulation of lipid binding proteins in FAP lipoma compared to FAP healthy dermal skin might in contrast be explained by the interaction of other regulatory proteins that favor the proliferation of adipocytes and therefore an increase in fatty acid binding proteins despite *APC* germline mutation.

Up-regulated proto-oncogenes *DDX5* and *MXRA5* possibly induce FAP lipoma development

DDX5 (DEAD box ATP-dependent RNA helicase) was described to be involved in several cellular processes of RNA secondary structure alteration, in cellular growth and division, and in cancer cell proliferation[237]. Similar to our results in FAP lipoma, overexpression of *DDX5* mRNA or protein has been reported in several tumor tissues (prostate carcinoma[238],

colorectal adenomas and colorectal carcinomas[171], and breast cancer[237,239]) and has therefore been suggested as a potential tumor promoter[240]. In prostate and colorectal carcinoma, DDX5 was described to facilitate tumor progression by interaction with β-catenin[240]. In breast cancer, *DDX5* was found to regulate DNA replication (G1-S-phase progression), transcription and expression of DNA replication genes[237]. Relating to its function in skin, *DDX5* was reported to positively contribute to wound repair. Increased *DDX5* levels have been found in keratinocyte nuclei of wound margins that lead to serum induced keratinocyte proliferation and expression of vascular endothelial growth factor (VEGF)[170]. ***MXRA5*** encodes for a matrix-remodeling associated protein that was described to function in extracellular matrix remodeling and cell-cell adhesion[172]. For this target, increased expression has also been reported in other tumors (colorectal adenoma and cancer[173], esophageal squamous cell carcinoma[241], and ovarian cancer[242]). The exact role in tumorigenesis of *MXRA5* is not known but possible mechanisms in cell adhesion defects and modulation of signal transduction have been suggested[172]. Such mechanisms reported for *DDX5* and *MXRA5* for other tumors could also lead to the proliferation of adipose tissue and the development of lipoma in FAP patients. Possible invasive growth is, same as for FAP fibroma, supposed to be inhibited by other regulatory mechanisms and the counteraction of tumor suppressors.

A possible proto-oncogenic role in FAP lipoma might also play ***SHOC2*** (soc-2 suppressor of clear homolog). It encodes for a scaffold protein linking RAS to downstream signal transducers in the MAP kinase signaling cascade and therefore acts as a positive modulator of ERK1/2 signaling[179]. As dys-regulated MAPK signaling is known to cause a variety of human cancers[243], *SHOC2* dys-regulation could possibly also influence overgrowth of adipose tissue in FAP and non-FAP lipoma tumors. In contrast, *SHOC2* has been reported to be down-regulated in colorectal cancer[244]. Relating to skin, mutations in *SHOC2* are known to cause Noonan-like syndrome, an autosomal dominantly inherited RASopathy with loose anagen hair, dark pigmentation, eczema or ichthyosis besides other growth, mental or cardiac defects[178]. These results implement that an intact SHOC2 protein is important for normal development of skin and hairs. In the presented study, a highly increased *SHOC2* expression level was also revealed in control lipomas compared to FAP lipomas. This could possibly be explained by additional regulatory mechanisms in FAP-associated lipomas, possibly influenced by the pathogenic *APC* mutation.

Up-regulated tumor suppressors *TMEM47*, *SMARCA1*, and *SFRP2* possibly inhibit invasive growth of FAP lipomas

TMEM47 encodes for a transmembrane protein of the PMP22/EMP/claudin protein family[169]. Claudins in general are important constituents of tight junctions[245]. A tumor suppressive function of *TMEM47* has been reported for malignant melanoma[169]. They revealed a decreased mRNA expression in such tumors caused by promoter methylation and allelic deletion. Another putative tumor suppressor indicated the matrix associated chromatin regulator ***SMARCA1.*** This target was found to regulate the transcription of certain genes by altering their chromatin structure. In melanoma tumors, down-regulated mRNA and protein levels were shown to increase melanoma cell proliferation and migration due to activation of otherwise modulated Wnt signaling[182]. For both genes, *TMEM47* and *SMARCA1*, an up-regulation of tumor suppressive function is suggested to prevent metastatic growth in benign lipomas. This tumor suppressive function seemed to be even stronger in control lipoma, as mRNA expression of both targets was decreased in FAP lipoma compared to control lipoma. This could be caused by other regulatory mechanisms, possibly influenced by the underlying *APC* germline mutation in FAP lipomas. The Wnt modulator ***SFRP2*** might indicate another putative tumor suppressor in FAP lipomas. Down-regulation by epigenetic inactivation has been reported in several cancers (esophageal squamous cell carcinoma[246], colorectal cancer[177], gastric cancer[247]). Secreted frizzled related proteins contain a domain similar to the Wnt receptor frizzled proteins that enables the binding of such proteins to Wnt receptors, with resulting down-regulation of pathway signaling during development[177,248]. In contrast to *TMEM47* and *SMARCA1*, *SFRP2* revealed up-fold mRNA regulation in FAP lipoma compared to control lipoma. This could possibly be explained by other regulatory mechanisms that support the tumor suppressive and Wnt modulatory effect of *SFRP2* especially in FAP-associated lipoma tissue. Relating to cutaneous tissues, similar to our results, *SFRP2* expression has been reported to be increased in hypertrophic scar fibroblasts. There an anti-apoptotic role of SFRP2 was suggested to explain the development of such fibroproliferative skin disorders[176,249,250]. A similar process could possibly also explain the development of lipomas in FAP and healthy individuals.

Increased *UBE2R2* and *HIST1H1C* expression possibly influences FAP lipoma development by increasing β-catenin degradation or transcriptional repression

The ubiquitin conjugating enzyme **UBE2R2** is known to be involved in ubiquitin-mediated proteasomal degradation of β-catenin[181,251]. An increased regulation could therefore result in increased β-catenin degradation, possibly preventing metastatic progression in lipomas. Other regulatory mechanisms in FAP lipomas are thought to further repress *UBE2R2* (possibly similar as for *TMEM47* and *SMARCA1*) in FAP lipomas relative to non-FAP lipomas.

Linker histone **HIST1H1C** is in contrast known to compact nucleosomes into higher order structures and is therefore associated with transcriptional repression of several genes. Recently, it has been reported to suppress p53-mediated transcription and therefore to influence p53-dependent DNA damage response pathways[180,252]. Furthermore, it was reported to participate in epigenetic regulation of gene expression[253]. Of particular interest might possibly be also the localization of *HIST1H1C* at 6p21.3, as in lipomas several chromosomal rearrangements are known to affect chromosomal positions 6p21-23[254].

In summary FAP lipomas, same as FAP fibromas tend to be influenced by proto-oncogenes (*DDX5, MXRA5*) as well as tumor suppressor genes (*TMEM47, SMARCA1, SFRP2*). Especially tumor suppressors *TMEM47* and *SMARCA1* were found to also play a role in control lipoma development. Other genes (*UBE2R2, HIST1H1C*) might also suppress malignant growth by other mechanisms. In addition two lipid binding proteins (FABP4, RBP7) could be involved in FAP and especially in control lipoma development. The higher expression in control lipoma is explained by the particular lipoma type and by an influence of Wnt signaling. Wnt signaling is known to suppress adipose tissue formation and to suppress targets of the lipid signaling pathway[107,236]. An interesting target especially for the development of FAP lipomas presented the Wnt modulator *SFRP2*. This target gene might suppress tumor promotion by its tumor suppressive activity. But it could also induce the development of FAP lipomas due to an anti-apoptotic mechanism. In addition the development of FAP lipomas compared to FAP healthy skin could be influenced by several upstream regulators that connect some of the DEGs

FAP lipoma vs. control lipoma

Among studies on differential gene expression, FAP lipomas compared to control lipomas revealed highest expression changes. Selected targets indicate a tendency by which up-regulated genes could influence FAP lipoma development by functions in cell proliferation, whereas control lipoma rather related to lipid metabolism targets as well as to proto-oncogenes.

Up-regulated *SLPI* and *CD24* with proto-oncogenic functions and possible association with the *APC* germline mutation

The secretory leukocyte peptidase inhibitor (***SLPI***) is known to protect epithelial tissues from serine proteases. Furthermore, *SLPI* has been reported to promote cancer growth and survival and to induce metastasis. Similar to our results, an up-regulated *SLPI* mRNA and protein expression has been reported among others in gastric cancer[189,255] and epithelial ovarian cancer[256]. In gastric cancer cells, *SLPI* was shown to promote invasive growth and cell migration by increasing the expression of matrix metalloproteinases *MMP2* and *MMP9* through phosphorylation of transcription factor *Elk1*[189]. Related to skin, it was found to function as an important endogenous factor for normal cutaneous and intra-oral wound healing[187,188]. Similarly, an overexpression of the cell adhesion molecule **CD24** has been reported in colorectal cancer, cervical cancer and several other tumors[257,191,258]. *CD24* has furthermore been identified as a putative β-catenin target gene[192]. Relating to skin, CD24 was observed to be overexpressed in blood leukocytes of patients with non-melanoma skin cancers such as SCC and BCC[190]. Such mechanisms of cancer growth already reported for cutaneous and other tumors could also influence the development of lipomas in FAP patients. Interestingly, mRNA expression of *SLPI* was also increased in FAP lipomas vs. FAP healthy skin, but to a much higher extent in FAP lipomas compared to non-FAP lipoma. This difference might possibly be explained by other regulatory mechanisms possibly induced by aberrant Wnt signaling.

SFRP2 presents another target that possibly relates to the underlying FAP disease. Same as for *SLPI,* mRNA expression was increased in FAP lipoma vs. FAP healthy skin and to a higher extent in FAP lipoma compared to non-FAP lipoma. As already discussed, this gene might suppress cell proliferation by modulation of Wnt signaling[248] but it might also promote the formation of hypertrophic scars by affecting apoptosis of hypertrophic scar fibroblasts[176,249,250]. This anti-apoptotic function has previously been shown by interation of SFRP2 with the transcription factor Slug in a caspase 3-dependent pathway[176]. Furthermore, similar to our results, an increased *SFRP2* mRNA expression was revealed in

keloid skin[249]. Finally, both functions of *SFRP2* are thought to be plausible to influence FAP lipoma development

Increased expression of *CAPNS2* might inhibit invasive growth in FAP lipoma by inducing apoptosis

Calpain small subunit 2 (**CAPNS2***)* is a calcium-activated widely expressed cysteine protease[259]. Such proteases act as key regulators of several cellular mechanisms (cellular signaling, remodeling, degradation, cell death) by cleaving a variety of important proteins after activation. In traumatic brain injury cells, it has been found to increase apoptosis due to sustained activation[184]. Relating to this mechanism, the increased expression of *CAPN2* in FAP lipoma could prevent invasive growth by inducing apoptosis of potentially malignant cells.

LEP, *EGFL6*, and *GPAM* with decreased expression in FAP lipoma are related to lipid tissue and could indicate possible proto-oncogenes for non-FAP lipoma development

*Leptin (**LEP**)* is an adipocyte-derived cytokine-like peptide that binds to leptin receptors in hypothalamus and many other tissues (also in skin). Leptin is known to modulate energy balance and maintenance of body weight[195] and high *LEP* serum levels are positively associated with obesity[260]. *Leptin* and its receptors were found to be expressed in several neoplasms of adipose tissue[195,261] and increased *LEP* mRNA was found in lipoma compared to normal adipose tissue[262]. Similarly, in the presented study, *LEP* mRNA was increased in non-FAP lipoma compared to FAP lipoma. This result is suggested to be caused by a difference in lipoma type or due to other regulatory mechanisms, as also discussed for genes encoding the lipid binding molecules FABP4 and RBP7. As *LEP* overexpression is known to correlate with obesity[260] we cannot exclude obesity as a potential confounder among the non-FAP lipoma cohort. A proto-oncogenic potential has been described in breast cancer and obesity-induced colorectal cancer[198,263]. In breast cancer, *LEP* was shown to induce tumor progression and invasion by induction of epithelial-mesenchymal transition caused by *β-catenin* activation in the Wnt pathway. In *Apc* Min mice that carry *Apc* Min mutation, leptin was found to induce pre-neoplastic colon epithelial cells to orchestrate VEGF-driven angiogenesis and vascular development[263]. Such functions of *LEP* could indicate a growth promoting effect in non-FAP lipoma. Another target with proto-oncogenic and lipid tissue-specific properties indicated the cell adhesion molecule ***EGFL6*.** It is a member of the epidermal growth factor repeat superfamily and known to be involved in the regulation of cell cycle proliferation and developmental processes[201]. EGFL6 is secreted from adipose tissue and increased expression related to human obesity where it promotes the proliferation of adipose tissue-derived stromal

vascular cells[199]. Furthermore, it was reported to function as a signaling molecule in hair follicle development to promote angiogenesis and attraction of vascular endothelial cells[200]. Relating to cell proliferation, *EGFL6* overexpression has been reported for fibroblastic meningioma (a benign intracranial mesenchymal tumor arising from arachnoid cells) and ovarian cancer[242,264]. Based on these informations, *EGFL6* might, same as *LEP*, also be involved in the development of non-FAP lipomas, possibly by enhancing vascularization and angiogenesis in adipocytes. The particular association of this gene to non-FAP lipoma is supposed to relate to the particular lipoma type. Obesity as a possible confounder in the present study can not be excluded certainly. An additional target involved in lipid metabolism and with possible proto-oncogenic function represented ***GPAM***. The *Glycerol-3-phosphate acyltransferase* is known to catalyze the first step in the biosynthesis of glycerolipids[265]. *GPAM* overexpression has further been reported for breast cancer[266]. These authors suggested a possible role of *GPAM* in tumor progression and a general relevance of metabolic changes in cancer. A similar mechanism could possibly also influence the development of control lipomas.

CIDEC with decreased expression in FAP lipoma possibly represses invasive growth in FAP as well as in non-FAP lipoma

CIDEC is predominantly expressed in white adipose tissue. For its protein, several important functions related to lipid tissue have been described. A depletion of this protein in mice resulted in lean mice with reduced lipid droplet size in white adipose tissue and increased metabolic rate[202]. Relating to the enhanced expression in non-FAP lipoma, overexpression of CIDEC in hepatocellular carcinoma was shown to induce apoptosis and to inhibit oncogenesis and tumor development by interaction with lipopolysaccharide-induced tumor necrosis factor[185]. A similar function could be expected in non-FAP lipoma, preventing an invasive growth of the lipoma tissue.

In summary, FAP lipomas compared to control lipomas tend to develop by the influence of up-regulated proto-oncogenes (*SLPI, CD24*). Invasive growth of the FAP lipoma could possibly be inhibited by up-regulation of tumor suppressor genes (*SFRP2*, *CAPNS2)*. All such genes are thought to directly relate to the FAP disease and must be influenced by the underlying *APC* germline mutation. In contrast down-regulated genes are thought to mainly influence the development of investigated non-FAP lipomas. A major influence of lipid tissue specific genes is suggested for the development of non-FAP lipomas. Furthermore, proto-oncogenes (*LEP, EGFL6, GPAM*) could influence lipoma development in healthy individuals. Same as in FAP lipomas, other genes are supposed to suppress invasive growth in control lipoma (*CIDEC*).

FAP epidermal cyst vs. FAP healthy epidermis

Microarray analyses on FAP epidermal cyst vs. FAP healthy skin did not reach major differences in gene expression. Based on the determined minimal significance level of unadjusted p-value <0.05 and -fold change 1.5, only three up-and three down-regulated genes were received. Furthermore, relating to their annotations (regulators of antivirus response, chromosome open reading frames, eyes shut homologs of drosophila, or hemoglobin-β) they were not found to be important for this study. For this, the development of such FAP-specific cysts is rather thought to be influenced by other mechanisms than by a dysregulation of certain genes. However, this investigation is supposed to be highly impacted by the very small sample number of merely three epidermal cyst and three healthy skin samples.

6.2.1 Limitations of the gene expression studies on FAP neoplasms

The **small sample number** included in presented analyses of gene expression as well as in second hit analyses indicated an important limitation of the study. Especially, qPCR confirmation analyses would ideally have needed a higher sample number to confirm results revealed from microarray calculations. The high inter-sample variation mostly seen in PCA, explained by the inter-individual patterns of human material, is most probably also amplified by some extend by the small number of included samples. The impossibility to calculate differential gene expression based on FDR-corrected false positive rates was also interpreted as a consequence of the small sample number. Based on prior investigations, around 45 arrays per group would ideally be needed to reach a sufficiently low FDR rate of 10%[124]. In the presented analysis, only 6-11 arrays per group were applied, and DEGs would only be reached on a much higher FDR rate than 10%. Besides the sample number, a major limitation presented the **small size of the skin lesion biopsies**. In order to reduce scar formation to a minimum after skin lesion biopsy, small 4mm punch biopsies have been taken. Such small skin lesion biopsies did not enable histological examination. Instead, diagnosis was based on clinical diagnosis of one clinically experienced dermatologist. Furthermore, the small sample sizes disabled additional, potentially interesting investigations, as analyses on protein level, based on same FAP skin lesion samples . Another limitation presented the **quality of the skin sample isolates**, which appeared to be impacted. This was most obvious in qPCR runs for FAP lipoma vs. FAP healthy skin samples, where most of the samples did not perform well. The cause for the affected quality is unknown but affection during isolation could be a probable explanation.

However, as FAP represents a rare disease and skin lesions occur in approximately 50%[22] of all FAP patients, a higher number of biopsies is difficult to include and is thought to might only be reached my means of international collaboration. In addition, for each skin lesion biopsy, the individual risk for a possible development of desmoid tumors following skin lesion biopsy must be considered.

6.2.2 Novelty and importance of expression results

To the best of our knowledge, up to now, no extensive whole genome expression analyses have been published for FAP-associated skin lesions such as fibromas, lipomas or epidermal cysts. Therefore, this study aimed for the first time to find potentially important gene candidates that could influence the development of such skin lesions in FAP. Furthermore, this study achieved to reveal primary insights into possible influencing factors in the development of FAP lipomas in relation to similar lipomas of the general population. Final results could be taken as primary implementation for further studies probably including higher sample numbers and other techniques.

7 CONCLUSION

In conclusion this is the first study to extensively analyze several FAP-associated skin lesions, especially fibromas and lipomas, for second hit mutations in *APC* as well as for changes in whole genome expression.

By applying several techniques for *APC* second hit analysis, we identified for one out of three lipomas as well as one out of three epidermal cysts both an LOH and microsatellite instability in D5S346. The same epidermal cyst sample also revealed a second hit mutation in *APC* MCR. Although several alternative *APC* transcripts were detected in the skin lesions, none of them were indicative for a particular somatic splice site mutation. Therefore, we assume that somatic *APC* alterations such as mutations in MCR or LOH in FAP-associated benign cutaneous neoplasms, at least in fibromas, are not the major cause for the development of skin lesions in FAP patients. Clearly, as the somatic mutation frequencies of 33% for lipomas and epidermal cysts were based on only 3 samples, further comprehensive *APC* mutation analysis on larger numbers of such FAP-associated skin lesions is recommended. Based on our microsatellite analyses, we alternatively suggest that chromosomal rearrangements could influence the development of skin lesions in FAP patients rather than aberrant splicing.

Gene expression results support the theory of a Wnt-independent mechanism responsible for skin lesion development in FAP. Genes involved in Wnt signaling were not among the highest DEGs in FAP fibroma or FAP lipoma studies. Highest DEGs for both groups revealed functions in cell proliferation (either as proto-oncogenes or as tumor suppressor genes). Therefore the development of such skin lesions was thought to be on the one hand induced by targets promoting cell proliferation. On the other hand, tumor suppressive mechanisms are thought to inhibit further tumor progression and invasion. In addition, a dysregulation of genes important for normal skin development might influence the skin lesion development. In contrast to those results, no differential gene expression was revealed for FAP epidermal cysts.

Comparative expression analyses for FAP lipoma and control lipoma revealed also increased expression of lipid tissue specific genes. Such genes are therefore expected to specifically influence the development of control lipoma in addition to proto-oncogenes. Such differences could account for the particular lipoma type in FAP and non-FAP individuals. Worth mentioning is that expression change was more clear in FAP lipomas compared to control lipomas.

In general, all such results could be confounded by the low number of examined samples and a larger number of samples is recommended for future studies.

8 OUTLOOK

Overall, a larger number of FAP-associated skin lesions should confirm presented results. Larger skin biopsies would enable a separate isolation of DNA, RNA, and protein samples as well as histological investigation. The separate isolation of DNA and RNA samples could enable better quality of samples and therefore more reliable results in subsequent analyses. Since FAP-associated skin lesions are known to occur early in life a possible inclusion of children or adolescents might be considered in future studies.

Relating to second hit analyses, especially a larger number of lipomas and epidermal cysts of FAP patients should be investigated to confirm or confute presented results in such lesions. Possibly, other techniques such as MLPA or the protein truncation test could complete the diagnostic repertoire of *APC* mutation analysis. Subsequent analysis of the resulting protein (by Western blot analysis) could reveal further information about the size of translated APC. Similarly, a larger number of samples should confirm highly changed targets that were received in whole genome expression analyses on mRNA as well as on protein level.

Based on results for both lipoma groups (FAP lipomas vs. FAP healthy skin as well as FAP lipoma compared to control lipoma), a possible connection of molecules regulated by same upstream regulators as well as detected pathways should be investigated.

Analysis of differential gene expression between FAP fibromas/epidermal cysts and control fibromas/epidermal cysts possibly reveal information about a potentially different development of such lesions in FAP and non-FAP individuals, as it has been done for lipomas.

A possible interdependence of changed gene targets could be investigated by transfection studies to reveal information of parallel expression in cell cultures.

9 REFERENCES

1. Galiatsatos P, Foulkes WD: Familial adenomatous polyposis. *Am J Gastroenterol* 2006; **101:** 385-398.

2. Menzel D: De excrescentiis verrucoso cristosis copiose in intestinis crassis dysenteriam passi observatis.: Acta Med Berol, 1721, pp 68–71 (citation from Bülow 2006; original publication was not available).

3. Bussey HJR: Familial polyposis coli. Familiy studies, histopathology, differential diagnosis and results of treatment. Baltimore: Johns Hopkins University Press, 1975 (citation from Bülow 2006; original publication was not available).

4. Bulow S: Results of national registration of familial adenomatous polyposis. *Gut* 2003; **52:** 742-746.

5. Lynch HT, Smyrk TC, Watson P *et al*: Genetics, natural history, tumor spectrum, and pathology of hereditary nonpolyposis colorectal cancer: an updated review. *Gastroenterology* 1993; **104:** 1535-1549.

6. Schreibman IR, Baker M, Amos C, McGarrity TJ: The hamartomatous polyposis syndromes: a clinical and molecular review. *Am J Gastroenterol* 2005; **100:** 476-490.

7. Jasperson KW, Tuohy TM, Neklason DW, Burt RW: Hereditary and familial colon cancer. *Gastroenterology* 2010; **138:** 2044-2058.

8. Knudsen AL, Bisgaard ML, Bulow S: Attenuated familial adenomatous polyposis (AFAP). A review of the literature. *Fam Cancer* 2003; **2:** 43-55.

9. Nagase H, Miyoshi Y, Horii A *et al*: Correlation between the location of germ-line mutations in the APC gene and the number of colorectal polyps in familial adenomatous polyposis patients. *Cancer Res* 1992; **52:** 4055-4057.

10. Miyaki M, Yamaguchi T, Iijima T *et al*: Difference in characteristics of APC mutations between colonic and extracolonic tumors of FAP patients: variations with phenotype. *Int J Cancer* 2008; **122:** 2491-2497.

11. Nielsen M, Hes FJ, Nagengast FM *et al*: Germline mutations in APC and MUTYH are responsible for the majority of families with attenuated familial adenomatous polyposis. *Clin Genet* 2007; **71:** 427-433.

12. Al-Tassan N, Chmiel NH, Maynard J *et al*: Inherited variants of MYH associated with somatic G:C-->T:A mutations in colorectal tumors. *Nat Genet* 2002; **30:** 227-232.

13. Sieber OM, Lipton L, Crabtree M *et al*: Multiple colorectal adenomas, classic adenomatous polyposis, and germ-line mutations in MYH. *N Engl J Med* 2003; **348:** 791-799.

14. Poulsen ML, Bisgaard ML: MUTYH Associated Polyposis (MAP). *Curr Genomics* 2008; **9:** 420-435.

15. Bertario L, Russo A, Sala P *et al*: Multiple approach to the exploration of genotype-phenotype correlations in familial adenomatous polyposis: *J Clin Oncol*. United States, 2003, Vol 21, pp 1698-1707.

16. Bulow S, Bjork J, Christensen IJ *et al*: Duodenal adenomatosis in familial adenomatous polyposis. *Gut* 2004; **53:** 381-386.

17. Abraham SC, Nobukawa B, Giardiello FM, Hamilton SR, Wu TT: Fundic gland polyps in familial adenomatous polyposis: neoplasms with frequent somatic adenomatous polyposis coli gene alterations. *Am J Pathol* 2000; **157:** 747-754.

18. Tiret A, Parc C: Fundus lesions of adenomatous polyposis. *Curr Opin Ophthalmol* 1999; **10:** 168-172.

19. Gardner EJ, Richards RC: Multiple cutaneous and subcutaneous lesions occurring simultaneously with hereditary polyposis and osteomatosis. *Am J Hum Genet* 1953; **5:** 139-147.

20. Truta B, Allen BA, Conrad PG *et al*: Genotype and phenotype of patients with both familial adenomatous polyposis and thyroid carcinoma. *Fam Cancer* 2003; **2:** 95-99.

21. Giardiello FM, Petersen GM, Brensinger JD *et al*: Hepatoblastoma and APC gene mutation in familial adenomatous polyposis. *Gut* 1996; **39:** 867-869.

22. Burger B, Cattani N, Trueb S *et al*: Prevalence of skin lesions in familial adenomatous polyposis: a marker for presymptomatic diagnosis?: *Oncologist*. United States, 2011, Vol 16, pp 1698-1705.

23. Turcot J, Despres JP, St Pierre F: Malignant tumors of the central nervous system associated with familial polyposis of the colon: report of two cases. *Dis Colon Rectum* 1959; **2:** 465-468.

24. Eccles DM, van der Luijt R, Breukel C *et al*: Hereditary desmoid disease due to a frameshift mutation at codon 1924 of the APC gene. *Am J Hum Genet* 1996; **59:** 1193-1201.

25. Bodmer WF, Bailey CJ, Bodmer J *et al*: Localization of the gene for familial adenomatous polyposis on chromosome 5. *Nature* 1987; **328:** 614-616.

26. Leppert M, Dobbs M, Scambler P *et al*: The gene for familial polyposis coli maps to the long arm of chromosome 5. *Science* 1987; **238:** 1411-1413.

27. Groden J, Thliveris A, Samowitz W *et al*: Identification and characterization of the familial adenomatous polyposis coli gene. *Cell* 1991; **66:** 589-600.

28. Joslyn G, Carlson M, Thliveris A *et al*: Identification of deletion mutations and three new genes at the familial polyposis locus. *Cell* 1991; **66:** 601-613.

29. Kinzler KW, Nilbert MC, Su LK *et al*: Identification of FAP locus genes from chromosome 5q21. *Science* 1991; **253:** 661-665.

30. Nishisho I, Nakamura Y, Miyoshi Y *et al*: Mutations of chromosome 5q21 genes in FAP and colorectal cancer patients. *Science* 1991; **253:** 665-669.

31. van Es JH, Giles RH, Clevers HC: The many faces of the tumor suppressor gene APC: *Exp Cell Res*. United States: 2001 Academic Press., 2001, Vol 264, pp 126-134.

32. Midgley CA, White S, Howitt R *et al*: APC expression in normal human tissues: *J Pathol*. England, 1997, Vol 181, pp 426-433.

33. Kuraguchi M, Wang XP, Bronson RT *et al*: Adenomatous polyposis coli (APC) is required for normal development of skin and thymus. *PLoS Genet* 2006; **2:** e146.

34. Chaw SY, Majeed AA, Dalley AJ, Chan A, Stein S, Farah CS: Epithelial to mesenchymal transition (EMT) biomarkers--E-cadherin, beta-catenin, APC and Vimentin--in oral squamous cell carcinogenesis and transformation. *Oral Oncol* 2012; **48:** 997-1006.

35. Aretz S, Uhlhaas S, Sun Y *et al*: Familial adenomatous polyposis: aberrant splicing due to missense or silent mutations in the APC gene. *Hum Mutat* 2004; **24:** 370-380.

36. Fearnhead NS, Britton MP, Bodmer WF: The ABC of APC. *Hum Mol Genet* 2001; **10:** 721-733.

37. Brocardo M, Henderson BR: APC shuttling to the membrane, nucleus and beyond. *Trends Cell Biol* 2008; **18:** 587-596.

38. Miller JR: The Wnts. *Genome Biol* 2002; **3:** Reviews3001.

39. Giles RH, van Es JH, Clevers H: Caught up in a Wnt storm: Wnt signaling in cancer. *Biochim Biophys Acta* 2003; **1653:** 1-24.

40. Widelitz R: Wnt signaling in skin organogenesis. *Organogenesis* 2008; **4:** 123-133.

41. Fodde R, Smits R, Clevers H: APC, signal transduction and genetic instability in colorectal cancer. *Nat Rev Cancer* 2001; **1:** 55-67.

42. Phelps RA, Broadbent TJ, Stafforini DM, Jones DA: New perspectives on APC control of cell fate and proliferation in colorectal cancer. *Cell Cycle* 2009; **8:** 2549-2556.

43. Sieber O, Tomlinson I, Lamlum H: The adenomatous polyposis coli (APC) tumour suppressor--genetics, function and disease. *Mol Med Today* 2000; **6:** 462-469.

44. Fu J, Hsu W: Epidermal Wnt controls hair follicle induction by orchestrating dynamic signaling crosstalk between the epidermis and dermis. *J Invest Dermatol* 2013; **133:** 890-898.

45. Weeraratna AT: A Wnt-er wonderland--the complexity of Wnt signaling in melanoma. *Cancer Metastasis Rev* 2005; **24:** 237-250.

46. Coffin CM, Hornick JL, Zhou H, Fletcher CD: Gardner fibroma: a clinicopathologic and immunohistochemical analysis of 45 patients with 57 fibromas. *Am J Surg Pathol* 2007; **31:** 410-416.

47. Colombo C, Foo WC, Whiting D *et al*: FAP-related desmoid tumors: a series of 44 patients evaluated in a cancer referral center. *Histol Histopathol* 2012; **27:** 641-649.

48. Tejpar S, Michils G, Denys H *et al*: Analysis of Wnt/Beta catenin signalling in desmoid tumors. *Acta Gastroenterol Belg* 2005; **68:** 5-9.

49. Kajino Y, Yamaguchi A, Hashimoto N, Matsuura A, Sato N, Kikuchi K: beta-Catenin gene mutation in human hair follicle-related tumors. *Pathol Int* 2001; **51:** 543-548.

50. Gat U, DasGupta R, Degenstein L, Fuchs E: De Novo hair follicle morphogenesis and hair tumors in mice expressing a truncated beta-catenin in skin. *Cell* 1998; **95:** 605-614.

51. Nieuwenhuis M, Vasen H: Correlations between mutation site in APC and phenotype of familial adenomatous polyposis (FAP): a review of the literature. *Crit Rev Oncol Hematol* 2007; **61:** 153-161.

52. Spirio L, Olschwang S, Groden J *et al*: Alleles of the APC gene: an attenuated form of familial polyposis: *Cell*. United States, 1993, Vol 75, pp 951-957.

53. van der Luijt RB, Vasen HF, Tops CM, Breukel C, Fodde R, Meera Khan P: APC mutation in the alternatively spliced region of exon 9 associated with late onset familial adenomatous polyposis. *Hum Genet* 1995; **96:** 705-710.

54. Heinimann K, Mullhaupt B, Weber W *et al*: Phenotypic differences in familial adenomatous polyposis based on APC gene mutation status. *Gut* 1998; **43:** 675-679.

55. Gebert JF, Dupon C, Kadmon M *et al*: Combined molecular and clinical approaches for the identification of families with familial adenomatous polyposis coli. *Ann Surg* 1999; **229:** 350-361.

56. Friedl W, Caspari R, Sengteller M *et al*: Can APC mutation analysis contribute to therapeutic decisions in familial adenomatous polyposis? Experience from 680 FAP families. *Gut* 2001; **48:** 515-521.

57. Bisgaard ML, Bulow S: Familial adenomatous polyposis (FAP): genotype correlation to FAP phenotype with osteomas and sebaceous cysts. *Am J Med Genet A* 2006; **140:** 200-204.

58. Spier I, Horpaopan S, Vogt S *et al*: Deep intronic APC mutations explain a substantial proportion of patients with familial or early-onset adenomatous polyposis. *Hum Mutat* 2012; **33:** 1045-1050.

59. Bisgaard ML, Fenger K, Bulow S, Niebuhr E, Mohr J: Familial adenomatous polyposis (FAP): frequency, penetrance, and mutation rate. *Hum Mutat* 1994; **3:** 121-125.

60. Ripa R, Bisgaard ML, Bulow S, Nielsen FC: De novo mutations in familial adenomatous polyposis (FAP). *Eur J Hum Genet* 2002; **10:** 631-637.

61. Aretz S, Uhlhaas S, Caspari R *et al*: Frequency and parental origin of de novo APC mutations in familial adenomatous polyposis. *Eur J Hum Genet* 2004; **12:** 52-58.

62. Necker J, Kovac M, Attenhofer M, Reichlin B, Heinimann K: Detection of APC germ line mosaicism in patients with de novo familial adenomatous polyposis: a plea for the protein truncation test. *J Med Genet* 2011; **48:** 526-529.

63. Beroud C, Soussi T: APC gene: database of germline and somatic mutations in human tumors and cell lines: *Nucleic Acids Res*. England, 1996, Vol 24, pp 121-124.

64. Knudson AG, Jr.: Mutation and cancer: statistical study of retinoblastoma. *Proc Natl Acad Sci U S A* 1971; **68:** 820-823.

65. Knudson AG: Two genetic hits (more or less) to cancer. *Nat Rev Cancer* 2001; **1:** 157-162.

66. Miyoshi Y, Nagase H, Ando H *et al*: Somatic mutations of the APC gene in colorectal tumors: mutation cluster region in the APC gene. *Hum Mol Genet* 1992; **1:** 229-233.

67. Lamlum H, Ilyas M, Rowan A *et al*: The type of somatic mutation at APC in familial adenomatous polyposis is determined by the site of the germline mutation: a new facet to Knudson's 'two-hit' hypothesis. *Nat Med* 1999; **5:** 1071-1075.

68. Crabtree M, Sieber OM, Lipton L *et al*: Refining the relation between 'first hits' and 'second hits' at the APC locus: the 'loose fit' model and evidence for differences in somatic mutation spectra among patients: *Oncogene*. England, 2003, Vol 22, pp 4257-4265.

69. Albuquerque C, Breukel C, van der Luijt R *et al*: The 'just-right' signaling model: APC somatic mutations are selected based on a specific level of activation of the beta-catenin signaling cascade. *Hum Mol Genet* 2002; **11:** 1549-1560.

70. Segditsas S, Rowan A, Howarth K *et al*: APC and the three-hit hypothesis. *Oncogene* 2009; **28:** 146-155.

71. Kim K, Pang KM, Evans M, Hay ED: Overexpression of beta-catenin induces apoptosis independent of its transactivation function with LEF-1 or the involvement of major G1 cell cycle regulators. *Mol Biol Cell* 2000; **11:** 3509-3523.

72. Latchford A, Volikos E, Johnson V *et al*: APC mutations in FAP-associated desmoid tumours are non-random but not 'just right'. *Hum Mol Genet* 2007; **16:** 78-82.

73. Fader M, Kline SN, Spatz SS, Zubrow HJ: Gardner's syndrome (intestinal polyposis, osteomas, sebaceous cysts) and a new dental discovery. *Oral Surg Oral Med Oral Pathol* 1962; **15:** 153-172.

74. Gardner EJ: Follow-up study of a family group exhibiting dominant inheritance for a syndrome including intestinal polyps, osteomas, fibromas and epidermal cysts. *Am J Hum Genet* 1962; **14:** 376-390.

75. Wolf J, Jarvinen HJ, Hietanen J: Gardner's dento-maxillary stigmas in patients with familial adenomatosis coli. *Br J Oral Maxillofac Surg* 1986; **24:** 410-416.

76. Fotiadis C, Tsekouras DK, Antonakis P, Sfiniadakis J, Genetzakis M, Zografos GC: Gardner's syndrome: a case report and review of the literature. *World J Gastroenterol* 2005; **11:** 5408-5411.

77. Shah KR, Boland CR, Patel M, Thrash B, Menter A: Cutaneous manifestations of gastrointestinal disease: part I. *J Am Acad Dermatol* 2013; **68:** 189.e181-121; quiz 210.

78. Kanitakis J: Adnexal tumours of the skin as markers of cancer-prone syndromes. *J Eur Acad Dermatol Venereol* 2010; **24:** 379-387.

79. Pujol RM, Casanova JM, Egido R, Pujol J, de Moragas JM: Multiple familial pilomatricomas: a cutaneous marker for Gardner syndrome? *Pediatr Dermatol* 1995; **12:** 331-335.

80. Trufant J, Kurz W, Frankel A *et al*: Familial multiple pilomatrixomas as a presentation of attenuated adenomatosis polyposis coli. *J Cutan Pathol* 2012; **39:** 440-443.

81. Itin PH, Heinimann K, Attenhofer M *et al*: Precalcaneal congenital fibrolipomatous hamartomas: is there a pathogenetic relationship with Gardner Syndrome?: *Eur J Dermatol*. France, 2010, Vol 20, pp 246-247.

82. Cazorla A, Viennet G, Uro-Coste E, Valmary-Degano S: Mucoepidermoid carcinoma: A yet unreported cancer associated with familial adenomatous polyposis. *J Craniomaxillofac Surg* 2014; **42:** 262-264.

83. Ali SY, Prabhat S, Ramanamurty Ch V, Salma M, Hussain S, Murtaza AS: Coexistence of porokeratosis of Mibelli with Gardner's syndrome: A rare case report. *Indian Dermatol Online J* 2011; **2:** 94-96.

84. Hartig M, Hicks MJ, Levy ML: Dermal Hypertrophies; in: Wolff K GL, Katz SI et al., eds. Fitzpatrick's Dermatology in General Medicine (ed). New York: McGraw-Hill Professional, 2007, Seventh Edition edn, pp 550-557.

85. Coffin CM: Gardner fibroma; in: Fletcher CDM UK, Mertens F, eds. Pathology and Genetics: Tumours of Soft Tissue, Tumours. aBWHOCo (eds). Lyon: IARC Press, 2002, p 76.

86. Wehrli BM, Weiss SW, Yandow S, Coffin CM: Gardner-associated fibromas (GAF) in young patients: a distinct fibrous lesion. *Am J Surg Pathol* 2001; **25:** 645-651.

87. Coffin CM, Davis JL, Borinstein SC: Syndrome-associated soft tissue tumours. *Histopathology* 2013.

88. Levesque S, Ahmed N, Nguyen VH *et al*: Neonatal Gardner Fibroma: A Sentinel Presentation of Severe Familial Adenomatous Polyposis. *Pediatrics* 2010.

89. Clark SK, Phillips RK: Desmoids in familial adenomatous polyposis. *Br J Surg* 1996; **83:** 1494-1504.

90. Lanckohr C, Debiec-Rychter M, Muller O *et al*: [Gardner fibroma: case report and discussion of a new soft tissue tumor entity]. *Pathologe* 2010; **31:** 97-105.

91. Dawes LC, La Hei ER, Tobias V, Kern I, Stening W: Nuchal fibroma should be recognized as a new extracolonic manifestation of Gardner-variant familial adenomatous polyposis. *Aust N Z J Surg* 2000; **70:** 824-826.

92. Michal M: Non-nuchal-type fibroma associated with Gardner's syndrome. A hitherto-unreported mesenchymal tumor different from fibromatosis and nuchal-type fibroma. *Pathol Res Pract* 2000; **196:** 857-860.

93. Michal M, Fetsch JF, Hes O, Miettinen M: Nuchal-type fibroma: a clinicopathologic study of 52 cases. *Cancer* 1999; **85:** 156-163.

94. Diwan AH, Graves ED, King JA, Horenstein MG: Nuchal-type fibroma in two related patients with Gardner's syndrome. *Am J Surg Pathol* 2000; **24:** 1563-1567.

95. Michal M: Nuchal-type fibroma; in: Fletcher C.D.M. UKK MF, eds. Pathology and Genetics of Tumours of Soft Tissue and Bone. World Health Organization Classification of Tumours. (ed). Lyon: IARC Press, 2002, p 75.

96. Linos K, Sedivcova M, Cerna K *et al*: Extra nuchal-type fibroma associated with elastosis, traumatic neuroma, a rare APC gene missense mutation, and a very rare MUTYH gene polymorphism: a case report and review of the literature*. *J Cutan Pathol* 2011; **38:** 911-918.

97. Michal M, Boudova L, Mukensnabl P: Gardner's syndrome associated fibromas. *Pathol Int* 2004; **54:** 523-526.

98. Lynch HT, Fitzgibbons R, Jr.: Surgery, desmoid tumors, and familial adenomatous polyposis: case report and literature review. *Am J Gastroenterol* 1996; **91:** 2598-2601.

99. Smits R, van der Houven van Oordt W, Luz A *et al*: Apc1638N: a mouse model for familial adenomatous polyposis-associated desmoid tumors and cutaneous cysts: *Gastroenterology*. United States, 1998, Vol 114, pp 275-283.

100. Robanus-Maandag E, Bosch C, Amini-Nik S *et al*: Familial adenomatous polyposis-associated desmoids display significantly more genetic changes than sporadic desmoids. *PLoS One* 2011; **6:** e24354.

101. Goldblum JR, Fletcher JA: Desmoid-type fibromatoses; in: Fletcher CDM UK, Mertens F, eds. Pathology and Genetics: Tumours of Soft Tissue and Bone. World Health Organization Classification of Tumours. (ed). Lyon: IARC Press, 2002, p 83.

102. Tejpar S, Nollet F, Li C *et al*: Predominance of beta-catenin mutations and beta-catenin dysregulation in sporadic aggressive fibromatosis (desmoid tumor). *Oncogene* 1999; **18:** 6615-6620.

103. Nielsen GP, Mandahl N: Lipoma; in: Fletcher CDM, Unni KK, Mertens F, eds. Pathology and Genetics: Tumours of Soft Tissue and Bone. World Health Organization Classification of Tumours. (eds). Lyon: IARC Press, 2002, pp 20-22.

104. Brenn T: Neoplasms of Subcutaneous Fat; in: Wolff K, Goldsmith, L.A., Katz, S.I. *et al*., eds. Fitzpatrick's Dermatology in General Medicine (ed). New York: McGraw-Hill Professional, 2007, Seventh Edition edn, p 1190.

105. Bianchini L, Birtwisle L, Saada E *et al*: Identification of PPAP2B as a novel recurrent translocation partner gene of HMGA2 in lipomas. *Genes Chromosomes Cancer* 2013; **52:** 580-590.

106. Dreijerink KM, Varier RA, van Beekum O *et al*: The multiple endocrine neoplasia type 1 (MEN1) tumor suppressor regulates peroxisome proliferator-activated receptor gamma-dependent adipocyte differentiation. *Mol Cell Biol* 2009; **29:** 5060-5069.

107. Longo KA, Wright WS, Kang S *et al*: Wnt10b inhibits development of white and brown adipose tissues. *J Biol Chem* 2004; **279:** 35503-35509.

108. Lee H, Bae S, Yoon Y: The anti-adipogenic effects of (-)epigallocatechin gallate are dependent on the WNT/beta-catenin pathway. *J Nutr Biochem* 2013; **24:** 1232-1240.

109. Leppard B, Bussey HJ: Epidermoid cysts, polyposis coli and Gardner's syndrome. *Br J Surg* 1975; **62:** 387-393.

110. Thomas VD, Swanson NA, Lee KK: Benign Epithelial Tumors, Hamartomas, and Hyperplasias; in: Wolff K, Goldsmith LA, Katz SI*ea,* eds. Fitzpatrick's Dermatology in General Medicine (eds). New York: McGraw-Hill Professional, 2007, Seventh Edition edn, pp 1054-1067.

111. Narisawa Y, Kohda H: Cutaneous cysts of Gardner's syndrome are similar to follicular stem cells. *J Cutan Pathol* 1995; **22:** 115-121.

112. Plasilova M, Russell AM, Wanner A *et al*: Exclusion of an extracolonic disease modifier locus on chromosome 1p33-36 in a large Swiss familial adenomatous polyposis kindred: *Eur J Hum Genet*. England, 2004, Vol 12, pp 365-371.

113. Miller SA, Dykes DD, Polesky HF: A simple salting out procedure for extracting DNA from human nucleated cells. *Nucleic Acids Res* 1988; **16:** 1215.

114. Untergasser A, Cutcutache I, Koressaar T *et al*: Primer3--new capabilities and interfaces. *Nucleic Acids Res* 2012; **40:** e115.

115. Koressaar T, Remm M: Enhancements and modifications of primer design program Primer3: *Bioinformatics*. England, 2007, Vol 23, pp 1289-1291.

116. Canzian F, Salovaara R, Hemminki A *et al*: Semiautomated assessment of loss of heterozygosity and replication error in tumors. *Cancer Res* 1996; **56:** 3331-3337.

117. Affymetrix.com: GeneChip® Human Gene ST Arrays.

118. Irizarry RA, Hobbs B, Collin F *et al*: Exploration, normalization, and summaries of high density oligonucleotide array probe level data. *Biostatistics* 2003; **4:** 249-264.

119. Bolstad BM, Irizarry RA, Astrand M, Speed TP: A comparison of normalization methods for high density oligonucleotide array data based on variance and bias. *Bioinformatics* 2003; **19:** 185-193.

120. Raychaudhuri S, Stuart JM, Altman RB: Principal components analysis to summarize microarray experiments: application to sporulation time series. *Pac Symp Biocomput* 2000**:** 455-466.

121. Affymetrix.com: GeneChip® Expression Analysis, Data Analysis Fundamentals, 2002-2004, pp 57-72.

122. O'Neill M: ANOVA & REML, a guide to linear mixed models in an experimental design context; Statistical Advisory & Training Service Pty Ltd, 2010.

123. Benjamini Y, Drai D, Elmer G, Kafkafi N, Golani I: Controlling the false discovery rate in behavior genetics research. *Behav Brain Res* 2001; **125:** 279-284.

124. Pawitan Y, Michiels S, Koscielny S, Gusnanto A, Ploner A: False discovery rate, sensitivity and sample size for microarray studies. *Bioinformatics* 2005; **21:** 3017-3024.

125. Huang da W, Sherman BT, Lempicki RA: Systematic and integrative analysis of large gene lists using DAVID bioinformatics resources. *Nat Protoc* 2009; **4:** 44-57.

126. Hellemans J, Mortier G, De Paepe A, Speleman F, Vandesompele J: qBase relative quantification framework and software for management and automated analysis of real-time quantitative PCR data. *Genome Biol* 2007; **8:** R19.

127. Huang SP, Ting WC, Chen LM *et al*: Association analysis of Wnt pathway genes on prostate-specific antigen recurrence after radical prostatectomy. *Ann Surg Oncol* 2010; **17:** 312-322.

128. Thliveris A, Samowitz W, Matsunami N, Groden J, White R: Demonstration of promoter activity and alternative splicing in the region 5' to exon 1 of the APC gene. *Cancer Res* 1994; **54:** 2991-2995.

129. De Rosa M, Morelli G, Cesaro E *et al*: Alternative splicing and nonsense-mediated mRNA decay in the regulation of a new adenomatous polyposis coli transcript: *Gene*. Netherlands, 2007, Vol 395, pp 8-14.

130. Neklason DW, Solomon CH, Dalton AL, Kuwada SK, Burt RW: Intron 4 mutation in APC gene results in splice defect and attenuated FAP phenotype: *Fam Cancer*. Netherlands, 2004, Vol 3, pp 35-40.

131. Sulekova Z, Ballhausen WG: A novel coding exon of the human adenomatous polyposis coli gene. *Hum Genet* 1995; **96:** 469-471.

132. Xia L, St Denis KA, Bapat B: Evidence for a novel exon in the coding region of the adenomatous polyposis coli (APC) gene: *Genomics*. United States, 1995, Vol 28, pp 589-591.

133. Sulekova Z, Reina-Sanchez J, Ballhausen WG: Multiple APC messenger RNA isoforms encoding exon 15 short open reading frames are expressed in the context of a novel exon 10A-derived sequence. *Int J Cancer* 1995; **63:** 435-441.

134. Kruijff S, Bastiaannet E, Brouwers AH *et al*: Use of S-100B to evaluate therapy effects during bevacizumab induction treatment in AJCC stage III melanoma. *Ann Surg Oncol* 2012; **19:** 620-626.

135. Park HR, Park YK, Jang KT, Unni KK: Expression of collagen type II, S100B, S100A2 and osteocalcin in chondroblastoma and chondromyxoid fibroma. *Oncol Rep* 2002; **9:** 1087-1091.

136. Lin J, Yang Q, Wilder PT, Carrier F, Weber DJ: The calcium-binding protein S100B down-regulates p53 and apoptosis in malignant melanoma. *J Biol Chem* 2010; **285:** 27487-27498.

137. Klenke C, Janowski S, Borck D *et al*: Identification of novel cholesteatoma-related gene expression signatures using full-genome microarrays. *PLoS One* 2012; **7:** e52718.

138. Hajra KM, Fearon ER: Cadherin and catenin alterations in human cancer. *Genes Chromosomes Cancer* 2002; **34:** 255-268.

139. Vogel BE, Hedgecock EM: Hemicentin, a conserved extracellular member of the immunoglobulin superfamily, organizes epithelial and other cell attachments into oriented line-shaped junctions. *Development* 2001; **128:** 883-894.

140. Argraves WS, Greene LM, Cooley MA, Gallagher WM: Fibulins: physiological and disease perspectives. *EMBO Rep* 2003; **4:** 1127-1131.

141. Senchenko VN, Krasnov GS, Dmitriev AA *et al*: Differential expression of CHL1 gene during development of major human cancers. *PLoS One* 2011; **6:** e15612.

142. Gavert N, Conacci-Sorrell M, Gast D *et al*: L1, a novel target of beta-catenin signaling, transforms cells and is expressed at the invasive front of colon cancers. *J Cell Biol* 2005; **168:** 633-642.

143. Strehlow D, Jelaska A, Strehlow K, Korn JH: A potential role for protease nexin 1 overexpression in the pathogenesis of scleroderma. *J Clin Invest* 1999; **103:** 1179-1190.

144. Buchholz M, Biebl A, Neesse A *et al*: SERPINE2 (protease nexin I) promotes extracellular matrix production and local invasion of pancreatic tumors in vivo. *Cancer Res* 2003; **63:** 4945-4951.

145. Candia BJ, Hines WC, Heaphy CM, Griffith JK, Orlando RA: Protease nexin-1 expression is altered in human breast cancer. *Cancer Cell Int* 2006; **6:** 16.

146. Fayard B, Bianchi F, Dey J *et al*: The serine protease inhibitor protease nexin-1 controls mammary cancer metastasis through LRP-1-mediated MMP-9 expression. *Cancer Res* 2009; **69:** 5690-5698.

147. Selzer-Plon J, Bornholdt J, Friis S *et al*: Expression of prostasin and its inhibitors during colorectal cancer carcinogenesis. *BMC Cancer* 2009; **9:** 201.

148. Bergeron S, Lemieux E, Durand V *et al*: The serine protease inhibitor serpinE2 is a novel target of ERK signaling involved in human colorectal tumorigenesis. *Mol Cancer* 2010; **9:** 271.

149. Ostrowski ML, Spjut HJ, Bridge JA: Chondromyxoid fibroma; in: Fletcher CDM, Unni KK, Mertens F (eds): *World Health Organization Classification of Tumours; Pathology and Genetics of Tumours of Soft Tissue and Bone*. Lyon: IARC Press, 2002, pp 243-245.

150. Cabral A, Voskamp P, Cleton-Jansen AM, South A, Nizetic D, Backendorf C: Structural organization and regulation of the small proline-rich family of cornified envelope precursors suggest a role in adaptive barrier function. *J Biol Chem* 2001; **276:** 19231-19237.

151. Kainu K, Kivinen K, Zucchelli M *et al*: Association of psoriasis to PGLYRP and SPRR genes at PSORS4 locus on 1q shows heterogeneity between Finnish, Swedish and Irish families. *Exp Dermatol* 2009; **18:** 109-115.

152. Cheng T, van Vlijmen-Willems IM, Hitomi K *et al*: Colocalization of cystatin M/E and its target proteases suggests a role in terminal differentiation of human hair follicle and nail. *J Invest Dermatol* 2009; **129:** 1232-1242.

153. Zeeuwen PL, Cheng T, Schalkwijk J: The biology of cystatin M/E and its cognate target proteases. *J Invest Dermatol* 2009; **129:** 1327-1338.

154. Briggs JJ, Haugen MH, Johansen HT *et al*: Cystatin E/M suppresses legumain activity and invasion of human melanoma. *BMC Cancer* 2010; **10:** 17.

155. Chavanas S, Bodemer C, Rochat A *et al*: Mutations in SPINK5, encoding a serine protease inhibitor, cause Netherton syndrome. *Nat Genet* 2000; **25:** 141-142.

156. Fortugno P, Furio L, Teson M *et al*: The 420K LEKTI variant alters LEKTI proteolytic activation and results in protease deregulation: implications for atopic dermatitis. *Hum Mol Genet* 2012; **21:** 4187-4200.

157. Razmara M, Srinivasula SM, Wang L *et al*: CARD-8 protein, a new CARD family member that regulates caspase-1 activation and apoptosis. *J Biol Chem* 2002; **277:** 13952-13958.

158. Humke EW, Shriver SK, Starovasnik MA, Fairbrother WJ, Dixit VM: ICEBERG: a novel inhibitor of interleukin-1beta generation. *Cell* 2000; **103:** 99-111.

159. Tan C, Liu S, Xiang Z: The expression of CARD18 in apoptin-transfected gastric cancer cells and gastric adenocarcinoma tissues. *Xi Bao Yu Fen Zi Mian Yi Xue Za Zhi* 2013; **29:** 858-861.

160. Yamaguchi T, Osumi T: Chanarin-Dorfman syndrome: deficiency in CGI-58, a lipid droplet-bound coactivator of lipase. *Biochim Biophys Acta* 2009; **1791:** 519-523.

161. Grosse B, Cassio D, Yousef N, Bernardo C, Jacquemin E, Gonzales E: Claudin-1 involved in neonatal ichthyosis sclerosing cholangitis syndrome regulates hepatic paracellular permeability. *Hepatology* 2012; **55:** 1249-1259.

162. Bhat AA, Sharma A, Pope J *et al*: Caudal homeobox protein Cdx-2 cooperates with Wnt pathway to regulate claudin-1 expression in colon cancer cells. *PLoS One* 2012; **7:** e37174.

163. Miwa N, Furuse M, Tsukita S, Niikawa N, Nakamura Y, Furukawa Y: Involvement of claudin-1 in the beta-catenin/Tcf signaling pathway and its frequent upregulation in human colorectal cancers. *Oncol Res* 2001; **12:** 469-476.

164. Al-Owain M, Wakil S, Shareef F *et al*: Novel homozygous mutation in DSP causing skin fragility-woolly hair syndrome: report of a large family and review of the desmoplakin-related phenotypes. *Clin Genet* 2011; **80:** 50-58.

165. Yang L, Chen Y, Cui T *et al*: Desmoplakin acts as a tumor suppressor by inhibition of the Wnt/beta-catenin signaling pathway in human lung cancer. *Carcinogenesis* 2012; **33:** 1863-1870.

166. Bär M, Bär D, Lehmann B: Selection and validation of candidate housekeeping genes for studies of human keratinocytes--review and recommendations. *J Invest Dermatol* 2009; **129:** 535-537.

167. Minner F, Poumay Y: Candidate housekeeping genes require evaluation before their selection for studies of human epidermal keratinocytes. *J Invest Dermatol* 2009; **129:** 770-773.

168. de Kok J, Roelofs R, Giesendorf B *et al*: Normalization of gene expression measurements in tumor tissues: comparison of 13 endogenous control genes. *Lab Invest* 2005; **85:** 154-159.

169. Mithani SK, Smith IM, Califano JA: Use of integrative epigenetic and cytogenetic analyses to identify novel tumor-suppressor genes in malignant melanoma. *Melanoma Res* 2011; **21:** 298-307.

170. Kahlina K, Goren I, Pfeilschifter J, Frank S: p68 DEAD box RNA helicase expression in keratinocytes. Regulation, nucleolar localization, and functional connection to proliferation and vascular endothelial growth factor gene expression. *J Biol Chem* 2004; **279:** 44872-44882.

171. Causevic M, Hislop RG, Kernohan NM *et al*: Overexpression and poly-ubiquitylation of the DEAD-box RNA helicase p68 in colorectal tumours. *Oncogene* 2001; **20:** 7734-7743.

172. Xiong D, Li G, Li K *et al*: Exome sequencing identifies MXRA5 as a novel cancer gene frequently mutated in non-small cell lung carcinoma from Chinese patients. *Carcinogenesis* 2012; **33:** 1797-1805.

173. Wang GH, Yao L, Xu HW *et al*: Identification of MXRA5 as a novel biomarker in colorectal cancer. *Oncol Lett* 2013; **5:** 544-548.

174. Wojciechowicz K, Gledhill K, Ambler CA, Manning CB, Jahoda CA: Development of the mouse dermal adipose layer occurs independently of subcutaneous adipose tissue and is marked by restricted early expression of FABP4. *PLoS One* 2013; **8:** e59811.

175. Kashima TG, Turley H, Dongre A, Pezzella F, Athanasou NA: Diagnostic utility of aP2/FABP4 expression in soft tissue tumours. *Virchows Arch* 2013; **462:** 465-472.

176. Chen L, Wang Z, Li S, Zhao G, Tian M, Sun Z: SFRP2 and slug contribute to cellular resistance to apoptosis in hypertrophic scars. *PLoS One* 2012; **7:** e50229.

177. Takeda M, Nagasaka T, Dong-Sheng S *et al*: Expansion of CpG methylation in the SFRP2 promoter region during colorectal tumorigenesis. *Acta Med Okayama* 2011; **65:** 169-177.

178. Cordeddu V, Di Schiavi E, Pennacchio LA *et al*: Mutation of SHOC2 promotes aberrant protein N-myristoylation and causes Noonan-like syndrome with loose anagen hair. *Nat Genet* 2009; **41:** 1022-1026.

179. Jeoung M, Abdelmoti L, Jang ER, Vander Kooi CW, Galperin E: Functional Integration of the Conserved Domains of Shoc2 Scaffold. *PLoS One* 2013; **8:** e66067.

180. Kim K, Jeong KW, Kim H *et al*: Functional interplay between p53 acetylation and H1.2 phosphorylation in p53-regulated transcription. *Oncogene* 2012; **31:** 4290-4301.

181. Semplici F, Meggio F, Pinna LA, Oliviero S: CK2-dependent phosphorylation of the E2 ubiquitin conjugating enzyme UBC3B induces its interaction with beta-TrCP and enhances beta-catenin degradation. *Oncogene* 2002; **21:** 3978-3987.

182. Eckey M, Kuphal S, Straub T *et al*: Nucleosome remodeler SNF2L suppresses cell proliferation and migration and attenuates Wnt signaling. *Mol Cell Biol* 2012; **32:** 2359-2371.

183. Gabrielsson BG, Olofsson LE, Sjogren A *et al*: Evaluation of reference genes for studies of gene expression in human adipose tissue. *Obes Res* 2005; **13:** 649-652.

184. Bralic M, Stemberga V: Calpain expression in the brain cortex after traumatic brain injury. *Coll Antropol* 2012; **36:** 1319-1323.

185. Min J, Zhang W, Gu Y *et al*: CIDE-3 interacts with lipopolysaccharide-induced tumor necrosis factor, and overexpression increases apoptosis in hepatocellular carcinoma. *Med Oncol* 2011; **28** Suppl 1: S219-227.

186. Skrzeczynska-Moncznik J, Wlodarczyk A, Zabieglo K *et al*: Secretory leukocyte proteinase inhibitor-competent DNA deposits are potent stimulators of plasmacytoid dendritic cells: implication for psoriasis. *J Immunol* 2012; **189:** 1611-1617.

187. Ashcroft GS, Lei K, Jin W *et al*: Secretory leukocyte protease inhibitor mediates non-redundant functions necessary for normal wound healing. *Nat Med* 2000; **6:** 1147-1153.

188. Angelov N, Moutsopoulos N, Jeong MJ, Nares S, Ashcroft G, Wahl SM: Aberrant mucosal wound repair in the absence of secretory leukocyte protease inhibitor. *Thromb Haemost* 2004; **92:** 288-297.

189. Choi BD, Jeong SJ, Wang G *et al*: Secretory leukocyte protease inhibitor is associated with MMP-2 and MMP-9 to promote migration and invasion in SNU638 gastric cancer cells. *Int J Mol Med* 2011; **28:** 527-534.

190. Miller E, Shapira S, Gur E *et al*: Increased expression of CD24 in nonmelanoma skin cancer. *Int J Biol Markers* 2012; **27:** e331-336.

191. Lee JH, Kim SH, Lee ES, Kim YS: CD24 overexpression in cancer development and progression: a meta-analysis. *Oncol Rep* 2009; **22:** 1149-1156.

192. Shulewitz M, Soloviev I, Wu T, Koeppen H, Polakis P, Sakanaka C: Repressor roles for TCF-4 and Sfrp1 in Wnt signaling in breast cancer. *Oncogene* 2006; **25:** 4361-4369.

193. Vickaryous N, Polanco-Echeverry G, Morrow S *et al*: Smooth-muscle myosin mutations in hereditary non-polyposis colorectal cancer syndrome. *Br J Cancer* 2008; **99:** 1726-1728.

194. Alhopuro P, Phichith D, Tuupanen S *et al*: Unregulated smooth-muscle myosin in human intestinal neoplasia. *Proc Natl Acad Sci U S A* 2008; **105:** 5513-5518.

195. Oliveira AM, Nascimento AG, Lloyd RV: Leptin and leptin receptor mRNA are widely expressed in tumors of adipocytic differentiation. *Mod Pathol* 2001; **14:** 549-555.

196. Cerman AA, Bozkurt S, Sav A, Tulunay A, Elbasi MO, Ergun T: Serum leptin levels, skin leptin and leptin receptor expression in psoriasis. *Br J Dermatol* 2008; **159:** 820-826.

197. Aly DG, Abdallah IY, Hanafy NS, Elsaie ML, Hafiz NA: Elevated serum leptin levels in nonobese patients with psoriasis. *J Drugs Dermatol* 2013; **12:** e25-29.

198. Yan D, Avtanski D, Saxena NK, Sharma D: Leptin-induced epithelial-mesenchymal transition in breast cancer cells requires beta-catenin activation via Akt/GSK3- and MTA1/Wnt1 protein-dependent pathways. *J Biol Chem* 2012; **287:** 8598-8612.

199. Oberauer R, Rist W, Lenter MC, Hamilton BS, Neubauer H: EGFL6 is increasingly expressed in human obesity and promotes proliferation of adipose tissue-derived stromal vascular cells. *Mol Cell Biochem* 2010; **343:** 257-269.

200. Xiao Y, Woo WM, Nagao K *et al*: Perivascular hair follicle stem cells associate with a venule annulus. *J Invest Dermatol* 2013; **133:** 2324-2331.

201. Yeung G, Mulero JJ, Berntsen RP, Loeb DB, Drmanac R, Ford JE: Cloning of a novel epidermal growth factor repeat containing gene EGFL6: expressed in tumor and fetal tissues. *Genomics* 1999; **62:** 304-307.

202. Magnusson B, Gummesson A, Glad CA *et al*: Cell death-inducing DFF45-like effector C is reduced by caloric restriction and regulates adipocyte lipid metabolism. *Metabolism* 2008; **57:** 1307-1313.

203. Yonezawa T, Kurata R, Kimura M, Inoko H: Which CIDE are you on? Apoptosis and energy metabolism. *Mol Biosyst* 2011; **7:** 91-100.

204. Laurent-Puig P, Beroud C, Soussi T: APC gene: database of germline and somatic mutations in human tumors and cell lines: *Nucleic Acids Res*. England, 1998, Vol 26, pp 269-270.

205. Blaker H, Sutter C, Kadmon M *et al*: Analysis of somatic APC mutations in rare extracolonic tumors of patients with familial adenomatous polyposis coli. *Genes Chromosomes Cancer* 2004; **41:** 93-98.

206. Happle R: Loss of heterozygosity in human skin. *Journal of the American Academy of Dermatology* 1999; **41:** 143-164.

207. Colman SD, Williams CA, Wallace MR: Benign neurofibromas in type 1 neurofibromatosis (NF1) show somatic deletions of the NF1 gene. *Nat Genet* 1995; **11:** 90-92.

208. Thomas L, Kluwe L, Chuzhanova N, Mautner V, Upadhyaya M: Analysis of NF1 somatic mutations in cutaneous neurofibromas from patients with high tumor burden. *Neurogenetics* 2010; **11:** 391-400.

209. Pack S, Turner ML, Zhuang Z *et al*: Cutaneous tumors in patients with multiple endocrine neoplasia type 1 show allelic deletion of the MEN1 gene. *J Invest Dermatol* 1998; **110:** 438-440.

210. Boland CR, Thibodeau SN, Hamilton SR *et al*: A National Cancer Institute Workshop on Microsatellite Instability for cancer detection and familial predisposition: development of international criteria for the determination of microsatellite instability in colorectal cancer. *Cancer Res* 1998; **58:** 5248-5257.

211. Lynch HT, Fusaro RM, Roberts L, Voorhees GJ, Lynch JF: Muir-Torre syndrome in several members of a family with a variant of the Cancer Family Syndrome. *Br J Dermatol* 1985; **113:** 295-301.

212. Swale VJ, Quinn AG, Wheeler JM *et al*: Microsatellite instability in benign skin lesions in hereditary non-polyposis colorectal cancer syndrome. *J Invest Dermatol* 1999; **113:** 901-905.

213. Rutten A, Burgdorf W, Hugel H *et al*: Cystic sebaceous tumors as marker lesions for the Muir-Torre syndrome: a histopathologic and molecular genetic study. *Am J Dermatopathol* 1999; **21:** 405-413.

214. Palmieri G, Ascierto PA, Cossu A *et al*: Assessment of genetic instability in melanocytic skin lesions through microsatellite analysis of benign naevi, dysplastic naevi, and primary melanomas and their metastases. *Melanoma Res* 2003; **13:** 167-170.

215. Bogdan I, Burg G, Boni R: Spitz nevi display allelic deletions. *Arch Dermatol* 2001; **137:** 1417-1420.

216. Cabral LS, Festa Neto C, Sanches JA, Jr., Ruiz IR: Genomic instability in human actinic keratosis and squamous cell carcinoma. *Clinics (Sao Paulo)* 2011; **66:** 523-528.

217. Loukola A, Eklin K, Laiho P *et al*: Microsatellite marker analysis in screening for hereditary nonpolyposis colorectal cancer (HNPCC). *Cancer Res* 2001; **61:** 4545-4549.

218. Cavenee WK, Dryja TP, Phillips RA *et al*: Expression of recessive alleles by chromosomal mechanisms in retinoblastoma. *Nature* 1983; **305:** 779-784.

219. Miyaki M, Konishi M, Kikuchi-Yanoshita R *et al*: Coexistence of somatic and germ-line mutations of APC gene in desmoid tumors from patients with familial adenomatous polyposis. *Cancer Res* 1993; **53:** 5079-5082.

220. Toyooka M, Konishi M, Kikuchi-Yanoshita R, Iwama T, Miyaki M: Somatic mutations of the adenomatous polyposis coli gene in gastroduodenal tumors from patients with familial adenomatous polyposis. *Cancer Res* 1995; **55:** 3165-3170.

221. Groves C, Lamlum H, Crabtree M *et al*: Mutation cluster region, association between germline and somatic mutations and genotype-phenotype correlation in upper gastrointestinal familial adenomatous polyposis. *Am J Pathol* 2002; **160:** 2055-2061.

222. Miyaki M, Konishi M, Kikuchi-Yanoshita R *et al*: Characteristics of somatic mutation of the adenomatous polyposis coli gene in colorectal tumors. *Cancer Res* 1994; **54:** 3011-3020.

223. Spemann H: Embryonic development and induction. University of Wisconsin - Madison: Yale University Press, 1938.

224. Gao S, Krogdahl A, Sorensen JA, Kousted TM, Dabelsteen E, Andreasen PA: Overexpression of protease nexin-1 mRNA and protein in oral squamous cell carcinomas. *Oral Oncol* 2008; **44:** 309-313.

225. Boni R, Burg G, Doguoglu A *et al*: Immunohistochemical localization of the Ca2+ binding S100 proteins in normal human skin and melanocytic lesions. *Br J Dermatol* 1997; **137:** 39-43.

226. He LH, Ma Q, Shi YH *et al*: CHL1 is involved in human breast tumorigenesis and progression. *Biochem Biophys Res Commun* 2013; **438:** 433-438.

227. Thies A, Schachner M, Moll I *et al*: Overexpression of the cell adhesion molecule L1 is associated with metastasis in cutaneous malignant melanoma. *Eur J Cancer* 2002; **38:** 1708-1716.

228. Gloor S, Odink K, Guenther J, Nick H, Monard D: A glia-derived neurite promoting factor with protease inhibitory activity belongs to the protease nexins. *Cell* 1986; **47:** 687-693.

229. Kools P, Van Imschoot G, van Roy F: Characterization of three novel human cadherin genes (CDH7, CDH19, and CDH20) clustered on chromosome 18q22-q23 and with high homology to chicken cadherin-7. *Genomics* 2000; **68:** 283-295.

230. Wright CM, Savarimuthu Francis SM, Tan ME *et al*: MS4A1 dysregulation in asbestos-related lung squamous cell carcinoma is due to CD20 stromal lymphocyte expression. *PLoS One* 2012; **7:** e34943.

231. Sotiropoulou G, Anisowicz A, Sager R: Identification, cloning, and characterization of cystatin M, a novel cysteine proteinase inhibitor, down-regulated in breast cancer. *J Biol Chem* 1997; **272:** 903-910.

232. Riker AI, Enkemann SA, Fodstad O *et al*: The gene expression profiles of primary and metastatic melanoma yields a transition point of tumor progression and metastasis. *BMC Med Genomics* 2008; **1:** 13.

233. Lilli C, Marinucci L, Bellocchio S *et al*: Effects of transforming growth factor-beta1 and tumour necrosis factor-alpha on cultured fibroblasts from skin fibroma as modulated by toremifene. *Int J Cancer* 2002; **98:** 824-832.

234. Folli C, Calderone V, Ramazzina I, Zanotti G, Berni R: Ligand binding and structural analysis of a human putative cellular retinol-binding protein. *J Biol Chem* 2002; **277:** 41970-41977.

235. Furuhashi M, Hotamisligil GS: Fatty acid-binding proteins: role in metabolic diseases and potential as drug targets. *Nat Rev Drug Discov* 2008; **7:** 489-503.

236. Prestwich TC, Macdougald OA: Wnt/beta-catenin signaling in adipogenesis and metabolism. *Curr Opin Cell Biol* 2007; **19:** 612-617.

237. Mazurek A, Luo W, Krasnitz A, Hicks J, Powers RS, Stillman B: DDX5 regulates DNA replication and is required for cell proliferation in a subset of breast cancer cells. *Cancer Discov* 2012; **2:** 812-825.

238. Clark EL, Coulson A, Dalgliesh C *et al*: The RNA helicase p68 is a novel androgen receptor coactivator involved in splicing and is overexpressed in prostate cancer. *Cancer Res* 2008; **68:** 7938-7946.

239. Wang D, Huang J, Hu Z: RNA helicase DDX5 regulates microRNA expression and contributes to cytoskeletal reorganization in basal breast cancer cells. *Mol Cell Proteomics* 2012; **11:** M111.011932.

240. Clark EL, Hadjimichael C, Temperley R, Barnard A, Fuller-Pace FV, Robson CN: p68/DdX5 supports beta-catenin & RNAP II during androgen receptor mediated transcription in prostate cancer. *PLoS One* 2013; **8:** e54150.

241. Zhang C, Fu L, Fu J *et al*: Fibroblast growth factor receptor 2-positive fibroblasts provide a suitable microenvironment for tumor development and progression in esophageal carcinoma. *Clin Cancer Res* 2009; **15:** 4017-4027.

242. Buckanovich RJ, Sasaroli D, O'Brien-Jenkins A *et al*: Tumor vascular proteins as biomarkers in ovarian cancer. *J Clin Oncol* 2007; **25:** 852-861.

243. Roberts PJ, Der CJ: Targeting the Raf-MEK-ERK mitogen-activated protein kinase cascade for the treatment of cancer. *Oncogene* 2007; **26:** 3291-3310.

244. Piepoli A, Palmieri O, Maglietta R *et al*: The expression of leucine-rich repeat gene family members in colorectal cancer. *Exp Biol Med (Maywood)* 2012; **237:** 1123-1128.

245. Ding L, Lu Z, Lu Q, Chen YH: The claudin family of proteins in human malignancy: a clinical perspective: *Cancer Manag Res*, 2013, Vol 5, pp 367-375.

246. Hao XW, Zhu ST, He YL, Li P, Wang YJ, Zhang ST: Epigenetic inactivation of secreted frizzled-related protein 2 in esophageal squamous cell carcinoma. *World J Gastroenterol* 2012; **18:** 532-540.

247. Cheng YY, Yu J, Wong YP *et al*: Frequent epigenetic inactivation of secreted frizzled-related protein 2 (SFRP2) by promoter methylation in human gastric cancer. *Br J Cancer* 2007; **97:** 895-901.

248. Jones SE, Jomary C: Secreted Frizzled-related proteins: searching for relationships and patterns. *Bioessays* 2002; **24:** 811-820.

249. Chen W, Fu X, Sun X, Sun T, Zhao Z, Sheng Z: Analysis of differentially expressed genes in keloids and normal skin with cDNA microarray. *J Surg Res* 2003; **113:** 208-216.

250. Sun Z, Li S, Cao C, Wu J, Ma B, Tran V: shRNA targeting SFRP2 promotes the apoptosis of hypertrophic scar fibroblast. *Mol Cell Biochem* 2011; **352:** 25-33.

251. Markson G, Kiel C, Hyde R *et al*: Analysis of the human E2 ubiquitin conjugating enzyme protein interaction network. *Genome Res* 2009; **19:** 1905-1911.

252. Kim K, Choi J, Heo K *et al*: Isolation and characterization of a novel H1.2 complex that acts as a repressor of p53-mediated transcription. *J Biol Chem* 2008; **283:** 9113-9126.

253. Fan Y, Nikitina T, Zhao J *et al*: Histone H1 depletion in mammals alters global chromatin structure but causes specific changes in gene regulation. *Cell* 2005; **123:** 1199-1212.

254. Sandberg AA: Updates on the cytogenetics and molecular genetics of bone and soft tissue tumors: lipoma: *Cancer Genet Cytogenet*. United States, 2004, Vol 150, pp 93-115.

255. Cheng WL, Wang CS, Huang YH *et al*: Overexpression of a secretory leukocyte protease inhibitor in human gastric cancer. *Int J Cancer* 2008; **123:** 1787-1796.

256. Devoogdt N, Rasool N, Hoskins E, Simpkins F, Tchabo N, Kohn EC: Overexpression of protease inhibitor-dead secretory leukocyte protease inhibitor causes more aggressive ovarian cancer in vitro and in vivo. *Cancer Sci* 2009; **100:** 434-440.

257. Ahmed MA, Al-Attar A, Kim J *et al*: CD24 shows early upregulation and nuclear expression but is not a prognostic marker in colorectal cancer. *J Clin Pathol* 2009; **62:** 1117-1122.

258. Huang LW, Lee CC: Cluster of differentiation 24 expression is an independent prognostic factor of adverse outcome in cervical carcinoma. *Int J Gynecol Cancer* 2013; **23:** 325-330.

259. Ma H, Nakajima E, Shih M, Azuma M, Shearer TR: Expression of calpain small subunit 2 in mammalian tissues. *Curr Eye Res* 2004; **29:** 337-347.

260. Considine RV, Sinha MK, Heiman ML *et al*: Serum immunoreactive-leptin concentrations in normal-weight and obese humans. *N Engl J Med* 1996; **334:** 292-295.

261. Deutscher J, Meyer K, Blutters-Sawatzki R, Franke FE, Kiess W: Leptin and leptin receptor expression in a lipoblastoma in an 8-year-old girl. *Horm Res* 1999; **51:** 253-255.

262. Suga H, Eto H, Inoue K *et al*: Cellular and molecular features of lipoma tissue: comparison with normal adipose tissue. *Br J Dermatol* 2009; **161:** 819-825.

263. Birmingham JM, Busik JV, Hansen-Smith FM, Fenton JI: Novel mechanism for obesity-induced colon cancer progression. *Carcinogenesis* 2009; **30:** 690-697.

264. Wang X, Gong Y, Wang D *et al*: Analysis of gene expression profiling in meningioma: deregulated signaling pathways associated with meningioma and EGFL6 overexpression in benign meningioma tissue and serum. *PLoS One* 2012; **7:** e52707.

265. Igal RA, Wang S, Gonzalez-Baro M, Coleman RA: Mitochondrial glycerol phosphate acyltransferase directs the incorporation of exogenous fatty acids into triacylglycerol. *J Biol Chem* 2001; **276:** 42205-42212.

266. Brockmoller SF, Bucher E, Muller BM *et al*: Integration of metabolomics and expression of glycerol-3-phosphate acyltransferase (GPAM) in breast cancer-link to patient survival, hormone receptor status, and metabolic profiling. *J Proteome Res* 2012; **11:** 850-860.

267. Swierczynski J, Zabrocka L, Goyke E, Raczynska S, Adamonis W, Sledzinski Z: Enhanced glycerol 3-phosphate dehydrogenase activity in adipose tissue of obese humans. *Mol Cell Biochem* 2003; **254:** 55-59.

268. Schweiger M, Paar M, Eder C *et al*: G0/G1 switch gene-2 regulates human adipocyte lipolysis by affecting activity and localization of adipose triglyceride lipase. *J Lipid Res* 2012; **53:** 2307-2317.

10 SUPPLEMENTS

Supplementary Table 1. Primer sequences for verification of the patient specific germline mutation in skin lesion samples (exons 1-14).

primer ID	sequence	primer localization
APC ex 1 fwd	5'-TTCTTTAAAAACAAGCAGCCACT	5' site of 5'UTR
APC ex 1 rev	5'-AAATGCTAACTTTTGCAAGAAAGA	in intron 1
APC ex 2 fwd	5'-GTGCGTGCTTTGAGAGTGAT	in intron 1
APC ex 2 rev	5'-CCCAAATCGAGAGAAGCTGT	in intron 2
APC ex 3 fwd	5'-TAACTTAGATAGCAGTAATTTCCC	in exon 3
APC ex 3 rev	5'-ACAATAAACTGGAGTACACAAGG	in intron 3
APC ex 4 fwd*	5'-GCTCTTCTGCAGTCTTTATTAGCA	in intron 3
APC ex 4 fwd*	5'-ATAGGTCATTGCTTCTTGCTGAT	in intron 3
APC ex 4 rev	5'-GAATTTTAATGGATTACCTAGGT	in intron 4
APC ex 5 fwd	5'-CATGCACCATGACTGACGTA	in intron 4
APC ex 5 rev	5'-GTTGCTCAGCAGCCATGATA	in intron 5
APC ex 6 fwd	5'-CCTGAGCTTTTAAGTGGTAGCC	in intron 5
APC ex 6 rev	5'-TGCCTAAAAGTTAGATAAAATCAAAA	in intron 6
APC ex 7 fwd	5'-CACAGTTCCATGCCTTTATCA	in intron 6
APC ex 7 rev	5'-TGGTACTGAATGCTTCTGGAAA	in intron 7
APC ex 8 fwd	5'-ACCTATAGTCTAAATTATACCATC	in intron 7
APC ex 8 rev	5'-GTCATGGCATTAGTGACCAG	in intron 8
APC ex 9 fwd	5'-ATTGGTTTTTGGCTTTTGGA	in intron 8
APC ex 9 rev	5'-CATTTGCTTTGAAACATGCAC	in intron 9
APC ex 10 fwd	5'-AAACATCATTGCTCTTCAAATAAC	in intron 9
APC ex 10 rev	5'-TACCATGATTTAAAAATCCACCAG	in intron 10
APC ex 11 fwd	5'-GATGATTGTCTTTTTCCTCTTGC	intron 10-exon 11
APC ex 11 rev	5'-CTGAGCTATCTTAAGAAATACATG	in intron 11
APC ex 12 fwd	5'-TTTTAATGATCCTCTATTCTGTAT	in in 11/ex 12
APC ex 12 rev	5'-ACAGAGTGAGACCCTGCCTCAAAG	in intron 12
APC ex 13 fwd	5'-TTTCTATTCTTACTGCT	in intron 12
APC ex 13 rev	5'-ATACACAGGTAAGAAATTAGG	in intron 13
APC ex 14 fwd	5'-TAGATGACCCATATTCT	intron 13-exon 14
APC ex 14 rev	5'-CAATTAGGTCTTTTTGAGAGT	in intron 14

primer ID and exon localization was following classical *APC* exon numbering with exons 1-15 = exons 4-18 ; *For exon 4 two different fwd primers were used for PCR reactions and sequencing.

Supplementary Table 2. Primer sequences for verification of the patient specific germline mutation in skin lesion samples (exon 15).

primer ID	sequence	primer localization
APC Ex 15 a fwd	5'-TTTGTTGTTACTGCAT	in intron 14
APC Ex 15 a rev	5'-GATGAGATGCCTTGGGACTT	in exon 15
APC Ex 15 b/c fwd	5'-CCCAAGGCATCTCATC	in exon 15
APC Ex 15 b/c rev	5'-TTCAGTGGTAGACCCAGAACTT	in exon 15
APC Ex 15 c fwd	5'-ATTTGAATACTACAGTGTTACCC	in exon 15
APC Ex 15 c rev	5'-CTTGTATTCTAATTTGGCATAAGG	in exon 15
APC Ex 15 d fwd	5'-CTGCCCATACACATTCAAACAC	in exon 15
APC Ex 15 d rev	5'-TGTTTGGGTCTTGCCCATCT	in exon 15
APC Ex 15 d/e fwd	5'-AGTGTCAGTAGTAGTG	in exon 15
APC Ex 15 d/e rev	5'-TTCCTTGATTGTCTTTGCTC	in exon 15
APC Ex 15 e fwd	5'-AGTCTTAAATATTCAGATGAGCAG	in exon 15
APC Ex 15 e rev	5'-GTTTCTCTTCATTATATTTTATGCTA	in exon 15
APC Ex 15 e/g fwd	5'-GCATGAAGAAGAAGAGAGACCAA	in exon 15
APC Ex 15 e/g rev	5'-TCTGCTTCCTGTGTCGTCTG	in exon 15
APC Ex 15 f fwd	5'-AAGCCTACCAATTATAGTGAACG	in exon 15
APC Ex 15 f rev	5'-AGCTGATGACAAAGATGATAATG	in exon 15
APC Ex 15 g fwd	5'-AAGAAACAATACAGACTTATTGTG	in exon 15
APC Ex 15 g rev	5'-GAGTGGGGTCTCCTGAAC	in exon 15
APC Ex 15 g/h fwd	5'-AGAATCAGCCAGGCACAAAG	in exon 15
APC Ex 15 g/h rev	5'-TGGAAGATCACTGGGGCTTA	in exon 15
APC Ex 15 h fwd	5'-ATCTCCCTCCAAAAGTGGTGC	in exon 15
APC Ex 15 h rev	5'-TCCATCTGGAGTACTTTCCGTG	in exon 15
APC Ex 15 i fwd	5'-AGTAAATGCTGCAGTTC	in exon 15
APC Ex 15 i rev	5'-CCGTGGCATATCATCCCCC	in exon 15
APC Ex 15 j fwd	5'-CCCAGACTGCTTCAAAATTACC	in exon 15
APC Ex 15 j rev	5'-GAGCCTCATCTGTACTTCTGC	in exon 15
APC Ex 15 k fwd	5'-CCCTCCAAATGAGTTAGCTGC	in exon 15
APC Ex 15 k rev	5'-TTGTGGTATAGGTTTTACTGGTG	in exon 15
APC Ex 15 l fwd	5'-ACCCAACAAAAATCAGTTAGATG	in exon 15
APC Ex 15 l rev	5'-GTGGCTGGTAACTTTAGCCTC	in exon 15
APC Ex 15 m fwd	5'-ATGATGTTGACCTTTCCAGGG	in exon 15
APC Ex 15 m rev	5'-ATTCTGTAACTTTTCATCAGTTGC	in exon 15
APC Ex 15 n fwd	5'-AAAGACATACCAGACAGAGGG	in exon 15
APC Ex 15 n rev	5'-CTTTTTTGGCATTGCGGAGCT	in exon 15
APC Ex 15 o fwd	5'-AAGATGACCTGTTGCAGGAATG	in exon 15
APC Ex 15 o rev	5'-AATCTGAATCAGACGAAGCTTGTCTAGAT	in exon 15
APC Ex 15 p fwd	5'-CCATAGTAAGTAGTTTACATCAAG	in exon 15
APC Ex 15 p rev	5'-AAACAGGACTTGTACTTGAGGA	in exon 15
APC Ex 15 q fwd	5'-AGCCCCTTCAAGCAAACAT	in exon 15
APC Ex 15 q rev	5'-GGTTCTGTTGGCTCATCTGTC	in exon 15
APC Ex 15 r fwd	5'-CTCCTGGCCGAAACTCAAT	in exon 15
APC Ex 15 r rev	5'-TTGACTGGCGTACTAATACAGGTC	in exon 15
APC Ex 15 s fwd	5'-GGTAATGGAGCCAATAAAAAGG	in exon 15
APC Ex 15 s rev	5'-TTCAGAATGAGACCGTGCAA	in exon 15
APC Ex 15 t fwd	5'-TCTCTATCCACACATTCGTCT	in exon 15

APC Ex 15 t rev	5'-TTCCTTTTGCGGATACTTGG	in exon 15
APC Ex 15 u fwd	5'-GCACTTGGAGAAGAACTGGAA	in exon 15
APC Ex 15 u rev	5'-TTGTTTTGCCTGATTATCTTTTGA	in exon 15
APC Ex 15 v fwd	5'-TTGGGTGAGAATTGAGGACTG	in exon 15
APC Ex 15 v rev	5'-CTGTGTTTGCTTGAGCTGCTA	in exon 15
APC Ex 15 w fwd	5'-CAGGACAAAATAATCCTGTCCC	in exon 15
APC Ex 15 w rev	5'-ATTTTCTTAGTTTCATTCTTCCTC	3' site of 3'UTR

primer ID and exon localization was following classical *APC* exon numbering with exons 1-15 = exons 4-18

Supplementary Table 3. Primer sequences used for direct sequencing of the MCR.

primer ID	sequence	exon	Codon position (CDS)
255_APC ex 15f fwd	5'-AAGCCTACCAATTATAGTGAACG	18f	p.1139-1283
256_APC ex 15f rev	5'-AGCTGATGACAAAGATGATAATG		
257_APC ex 15g fwd	5'-AAGAAACAATACAGACTTATTGTG	18g	p.1256-1382
258_APC ex 15g rev	5'-GAGTGGGGTCTCCTGAAC		
259_APC ex 15g/h fwd	5'-AGAATCAGCCAGGCACAAAG	18g/h	p.1344-1424
260_APC ex 15g/h rev	5'-TGGAAGATCACTGGGGCTTA		
261_APC ex 15h fwd	5'-ATCTCCCTCCAAAAGTGGTGC	18h	p.1359-1499
262_APC ex 15h rev	5'-TCCATCTGGAGTACTTTCCGTG		
263_APC ex 15i fwd	5'-AGTAAATGCTGCAGTTC	18i	p.1471-1640
264_APC ex 15i rev	5'-CCGTGGCATATCATCCCCC		
503_APC ex 15i fwd	5'-GTCCAGGTTCTTCCAGATGC	18i	p.1478-1666
504_APC ex 15i rev	5'-TGGAGGGGATTCGATTGTTA		

primer ID and exon localization was following classical *APC* exon numbering with exons 1-15 = exons 4-18. For exons 15i two different primer sets were alternatively applied.

Supplementary Table 4. Primer sequences applied for *APC* transcript analysis.

fragment	primer ID	sequence	length	exons	nucleotide position
F1	407 APC ex 1-4 fwd*	5'-CTTCCCACCTCCCACAAGAT	626	1 - 4	c.-568 – 58
	408 APC ex 1-4 rev	5'-TCTCCATCTTCAGTGCCTCA			
F2	409 APC ex 4-8 fwd	5'-AGGATGGCTGCAGCTTCATA	610	4 - 8	c.-3 – 606
	410 APC ex 4-8 rev	5'-TTCTTCCATCGCAACTCTGA			
F3	381 APC ex 6-11 fwd	5'-AAGCCGGGAAGGATCTGTAT	629	6 - 11	c.290 – 919
	382A APC ex 6-11 rev	5'-GACTTGTCAGCCTTCGAGGT			
F4	367 APC ex 10-14 fwd	5'-GTGGGAGAAATCAACATGGCA	666	10 - 14	c.795 – 1461
	368a APC ex 10-14 rev	5'-CCCATACATTTCACAGTCCAC			
F5	369 APC ex 13-17 fwd	5'-CAGATCTGTCCTGCTGTGTGT	506	13 - 17	c.1332 – 1838
	370a APC ex 13-17 rev	5'-AGTGCACCATCTACAGCACAT			
F6	371 APC ex 16-18 fwd	5'-GACGTTGCGAGAAGTTGGAAG	563	16 - 18	c.1682 – 2247
	372a APC ex 16-18 rev	5'-CAAGCTTGAGCCAGGAGACAT			

*located in non-coding exon 1

Supplementary Table 5. Primer sequences for microsatellite markers D5S346, BAT25, and BAT26.

primer ID	sequence
415 APC D5S346 fwd	5'-FAM-ACTCACTCTAGTGATAAATCGGG
416 APC D5S346 rev	5'-AGCAGATAAGACAGTATTACTAGTT
BAT25-fwd	5'- FAM-TCGCCTCCAAGAATGTAAGT
BAT25-rev	5'-TCTGCATTTTAACTATGGCTC
BAT26-fwd	5'- FAM-ACTCACTCTAGTGATAAATCGGG
BAT26-rev	5'-AACCATTCAACATTTTTAACC

fwd primers were 5' modified with FAM label

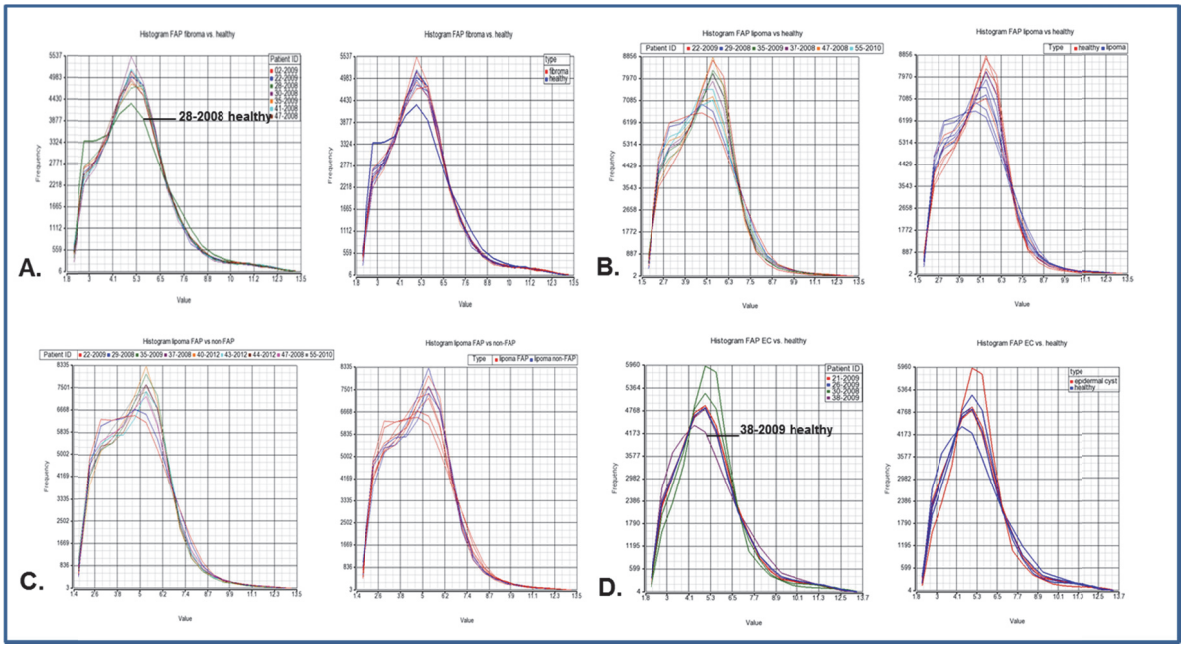

Supplementary Figure 1. QA/QC histograms of array samples. Partek histogram plots for all 4 groups analyzed in this study. In a histogram, the intensities of the gene probes (x-axis) are graphed versus the frequency with which the intensity of the gene probes occur (y-axis). Based on the distribution pattern of the intensities, possible outliers might be easily observed. Samples of the different groups were separately analyzed: **A.** FAP fibroma vs. healthy dermis, **B.** FAP lipoma vs. healthy dermis, **C.** FAP lipoma vs. control lipoma, and **D.** FAP epidermal cyst vs. healthy epidermis. Histograms were illustrated for patient ID and tissue type. Two samples (28-2008 healthy dermis, 38-2009 healthy epidermis) were excluded from microarray analysis based on their histogram profiles that were supposed to differ from such of other samples of the same group. The epidermal cyst sample of 30-2008, described by the curve that reaches highest intensities, was included because the curve was supposed to describe same overall shape as the other samples (**D.**). Samples of the lipoma groups (**B./C.**) indicated an overall higher inter-sample variation, and were therefore all decided to be included - also with regard to a higher sample number for analysis.

Supplementary Table 6. **DEGs in FAP fibroma vs. healthy dermis.** The table illustrates the 96 genes (26 up- and 70 down-regulated) that reach 2-fold expression change and FDR-unadjusted p-values of <0.05. Up-regulated genes are sorted from top to bottom by decreasing -fold change. Down-regulated genes are sorted from top to bottom by decreasing negative -fold change. DEGs chosen for qPCR validation are indicated in bold (gene ID).

Up-regulated genes

gene ID	gene assignment	localization	fch	p-value
S100B	S100 calcium binding protein B	chr21	5.26	0.030
CDH19	cadherin 19, type 2	chr18	4.78	0.048
HMCN1	hemicentin 1	chr1	3.98	0.028
GPM6B	glycoprotein M6B	chrX	3.81	0.026
CHL1	cell adhesion molecule with homology to L1CAM (close homolog of L1)	chr3	3.73	0.036
SERPINE2	serpin peptidase inhibitor, clade E (nexin, plasminogen activator inhibitor type 1), member 2	chr2	3.39	0.037
SDCBP	syndecan binding protein (syntenin)	chr8	3.14	0.029
ETV5	ets variant 5	chr3	2.97	0.049
ST3GAL6	ST3 beta-galactoside alpha-2,3-sialyltransferase 6	chr3	2.88	0.049
SGCE	sarcoglycan, epsilon	chr7	2.72	0.009
ADAM23	ADAM metallopeptidase domain 23	chr2	2.70	0.020
RFTN2	raftlin family member 2	chr2	2.69	0.015
GAS2L3	growth arrest-specific 2 like 3	chr12	2.65	0.019
ETV1	ets variant 1	chr7	2.58	0.018
AP1S2	adaptor-related protein complex 1, sigma 2 subunit	chr17	2.49	0.001
LDHB	lactate dehydrogenase B	chr12	2.49	0.028
SLC16A4	solute carrier family 16, member 4	chr1	2.49	0.013
PTPRJ	protein tyrosine phosphatase, receptor type, J	chr11	2.48	0.034
SOX5	SRY (sex determining region Y)-box 5	chr12	2.40	0.011
PRSS23	protease, serine, 23	chr11	2.34	0.004
SNCA	synuclein, alpha (non A4 component of amyloid precursor)	chr4	2.29	0.030
NLGN1	neuroligin 1	chr3	2.23	0.018
SLC6A15	solute carrier family 6 (neutral amino acid transporter)	chr12	2.14	0.046
CHML	choroideremia-like (Rab escort protein 2)	chr1	2.09	0.029
AP1S2	adaptor-related protein complex 1, sigma 2 subunit	chrX	2.06	0.022
PEG10	paternally expressed 10	chr7	2.03	0.024

Down-regulated genes

gene ID	gene assignment	localization	fch	p-value
SPRR2E	small proline-rich protein 2E	chr1	-4.43	0.014
MSMB	microseminoprotein, beta-	chr10	-4.10	0.020
CST6	cystatin E/M	chr11	-4.09	0.044
SPINK5	serine peptidase inhibitor, Kazal type 5	chr5	-3.81	0.023
KRT6B	keratin 6B	chr12	-3.69	0.030
CARD18	caspase recruitment domain family, member 18	chr11	-3.55	0.015
TMEM45A	transmembrane protein 45A	chr3	-3.46	0.019
SBSN	suprabasin	chr19	-3.16	0.028
ABHD5	abhydrolase domain containing 5	chr3	-3.14	0.019
CLDN1	claudin 1	chr3	-3.13	0.015
HBB	hemoglobin, beta	chr11	-3.10	0.029
DSP	desmoplakin	chr6	-3.08	0.018
CLCA2	chloride channel accessory 2	chr1	-3.07	0.011
DSG1	desmoglein 1	chr18	-2.99	0.026
TSPAN8	tetraspanin 8	chr12	-2.95	0.036
DSC3	desmocollin	chr18	-2.91	0.012
PCP4	Purkinje cell protein 4	chr21	-2.91	0.018
PNLIPRP3	pancreatic lipase-related protein 3	chr10	-2.90	0.003
MYH11	myosin, heavy chain 11, smooth muscle	chr16	-2.78	0.031
HMGCS1	3-hydroxy-3-methylglutaryl-CoA synthase 1 (soluble)	chr5	-2.72	0.018
KRT6C	keratin 6C	chr12	-2.69	0.025
SC4MOL	sterol-C4-methyl oxidase-like	chr4	-2.67	0.015
GPR87	G protein-coupled receptor 87	chr3	-2.58	0.003
LPHN3	latrophilin 3	chr4	-2.58	0.002
DSC2	desmocollin 2	chr18	-2.56	0.044
MUC15	mucin 15, cell surface associated	chr11	-2.50	0.013
CA6	carbonic anhydrase VI	chr1	-2.49	0.018
TMPRSS11E	transmembrane protease, serine 11E	chr4	-2.49	0.035
CORIN	corin, serine peptidase	chr4	-2.44	0.038
ESRP1	epithelial splicing regulatory protein 1	chr8	-2.42	0.005
SCEL	sciellin	chr13	-2.42	0.020
TMPRSS11E	transmembrane protease, serine 11E	chr4	-2.41	0.044
KRT5	keratin 5	chr12	-2.41	0.047
MAL2	mal, T-cell differentiation protein 2	chr8	-2.37	0.014
CYB5A	cytochrome b5 type A (microsomal)	chr18	-2.35	0.023
ACSL1	acyl-CoA synthetase long-chain family member 1	chr4	-2.35	0.003
DEFB1	defensin, beta 1	chr8	-2.34	0.020
KRT17	keratin 1	chr17	-2.33	0.018
KRT6A	keratin 6A	chr12	-2.33	0.032
ME1	malic enzyme 1, NADP(+)-dependent, cytosolic	chr6	-2.29	0.020
HBA1	hemoglobin, alpha 1	chr16	-2.28	0.031
HBA2	hemoglobin, alpha 2	chr16	-2.28	0.031
DAPL1	death associated protein-like	chr2	-2.28	0.039
S100A2	S100 calcium binding protein A	chr1	-2.27	0.023
ABCA12	ATP-binding cassette, sub-family A (ABC1), member 12	chr2	-2.26	0.016
CASP14	caspase 14, apoptosis-related cysteine peptidase	chr19	-2.26	0.010

SLPI	secretory leukocyte peptidase inhibitor	chr20	-2.26	0.020
VSNL1	visinin-like 1	chr2	-2.25	0.024
ATP6V0A4	ATPase, H+ transporting, lysosomal V0 subunit a4	chr7	-2.24	0.030
PM20D1	peptidase M20 domain containing 1	chr1	-2.24	0.007
SOAT1	sterol O-acyltransferase 1	chr1	-2.19	0.004
EHF	ets homologous factor	chr11	-2.15	0.007
LGALS7	lectin, galactoside-binding, soluble, 7	chr19	-2.15	0.008
SPRR1B	small proline-rich protein 1B	chr1	-2.14	0.025
RBP1	retinol binding protein 1, cellular	chr3	-2.14	0.015
SLC15A1	solute carrier family 15 (oligopeptide transporter)	chr13	-2.13	0.005
ZNF750	zinc finger protein 750	chr17	-2.10	0.039
TP63	tumor protein p63	chr3	-2.09	0.031
AIM1	absent in melanoma 1	chr6	-2.09	0.013
LGALS7	lectin, galactoside-binding, soluble, 7	chr19	-2.08	0.007
EMP2	epithelial membrane protein 2	chr16	-2.07	0.036
ACTG2	actin, gamma 2, smooth muscle, enteric	chr2	-2.07	0.011
DSG3	desmoglein 3	chr18	-2.07	0.032
HSPA4L	heat shock 70kDa protein 4-like	chr4	-2.05	0.006
EFNB2	ephrin-B2	chr13	-2.05	0.006
TMEM154	transmembrane protein 154	chr4	-2.04	0.036
KRT14	keratin 14	chr17	-2.04	0.021
TTC39B	tetratricopeptide repeat domain 39B	chr9	-2.02	0.020
C6orf105	chromosome 6 open reading frame 105	chr6	-2.01	0.028
AADACL3	arylacetamide deacetylase-like 3	chr1	-2.00	0.020

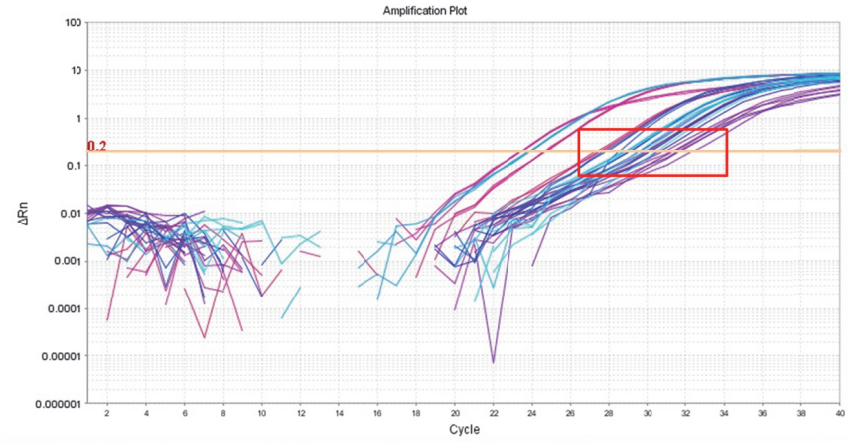

Supplementary Figure 2. Illustration of qPCR raw data for 30-2008 FAP healthy skin. For almost all targets, curves for 30-2008 healthy dermis did not not reach ideal exponential curve shape (red frame). Furthermore, runs for several targets were unstable and revealed high intra-sample variation and variation in run repeats. Better results were reached only for three targets with C_T values at lower cycle numbers. Raw data were analyzed using ABI 7500 software v.2.0.6.

Supplementary Table 7. DEGs in FAP lipoma vs. FAP healthy dermis. The table illustrates the 62 genes (59 up- and 3 down-regulated) that reach 2.5-fold expression change and FDR-unadjusted p-values of <0.05. Up-regulated genes are sorted from top to bottom by decreasing -fold change. Down-regulated genes are sorted from top to bottom by decreasing negative -fold change. DEGs chosen for qPCR validation are indicated in bold (gene ID).

Up-regulated genes

gene ID	gene assignment	localization	fch	p-value
TMEM47	transmembrane protein 47	Xp11.4	4.20	0.03
RBP7	retinol binding protein 7, cellular	1p36.22	3.82	0.03
DDX5	DEAD (Asp-Glu-Ala-Asp) box polypeptide 5	17q21	3.79	0.03
MXRA5	matrix-remodelling associated 5	Xp22.33	3.60	0.02
FABP4	fatty acid binding protein 4, adipocyte	8q21	3.53	0.02
SFRP2	secreted frizzled-related protein 2	4q31.3	3.32	0.04
ABCA8	ATP-binding cassette, sub-family A (ABC1), member 8	17q24	3.21	0.05
KDELR1	KDEL (Lys-Asp-Glu-Leu) endoplasmic reticulum protein retention receptor 1	19q13.3	3.17	0.04
SHOC2	soc-2 suppressor of clear homolog (C. elegans)	10q25	3.14	0.04
HIST1H1C	histone cluster 1, H1c	6p21.3	3.12	0.05
UBE2R2	ubiquitin-conjugating enzyme E2R2	9p13.3	3.12	0.04
MFAP4	microfibrillar-associated protein 4	17p11.2	3.12	0.05
COX7A1	cytochrome c oxidase subunit VIIa polypeptide 1 (muscle)	19q13.1	3.10	0.03
NKTR	natural killer-tumor recognition sequence	3p23-p21	3.09	0.05
CHIC2	cysteine-rich hydrophobic domain 2	4q11	3.08	0.04
SMARCA1	SWI/SNF related, matrix associated, actin dependent regulator of chromatin, subfamily a, member 1	Xq25	3.05	0.04

FMOD	fibromodulin	1q32	2.96	0.03
GXYLT2	glucoside xylosyltransferase 2	3p13	2.96	0.03
GFPT1	glutamine--fructose-6-phosphate transaminase 1	2p13	2.94	0.04
MBNL2	muscleblind-like 2 (Drosophila)	13q32.1	2.94	0.04
SESN3	sestrin 3	11q21	2.91	0.03
HTRA1	HtrA serine peptidase 1	10q26.3	2.90	0.04
COL3A1	collagen, type III, alpha 1	2q31	2.86	0.05
YTHDC2	YTH domain containing 2	5q22.2	2.86	0.05
TNKS	tankyrase, TRF1-interacting ankyrin-related ADP-ribose polymerase	8p23.1	2.85	0.03
FGF7	fibroblast growth factor 7	15q21.2	2.82	0.05
OGN	osteoglycin	9q22	2.77	0.05
BMPR2	bone morphogenetic protein receptor, type II (serine/threonine kinase)	2q33-q34	2.77	0.05
FAR1	fatty acyl CoA reductase 1	11p15.2	2.76	0.04
RAPH1	Ras association (RalGDS/AF-6) and pleckstrin homology domains 1	2q33	2.74	0.04
ARPP19	cAMP-regulated phosphoprotein, 19kD	15q21.2	2.72	0.04
C3orf10	chromosome 3 open reading frame 10	3p25.3	2.72	0.04
ZDHHC21	zinc finger, DHHC-type containing 21	9p22.3	2.71	0.03
ANXA7	annexin A7	10q22.2	2.71	0.05
CAMSAP1L1	calmodulin regulated spectrin-associated protein 1-like 1	1q32.1	2.71	0.04
AGPS	alkylglycerone phosphate synthase	2q31.2	2.71	0.05
UBA3	ubiquitin-like modifier activating enzyme 3	3p24.3-p1	2.68	0.03
LTBP1	latent transforming growth factor beta binding protein 1	2p22-p21	2.67	0.04
RAB23	RAB23, member RAS oncogene family	6p11	2.67	0.04
GOLGA5	golgin A5	14q	2.65	0.05
NFIC	nuclear factor I/C (CCAAT-binding transcription factor)	19p13.3	2.65	0.04
SLPI	secretory leukocyte peptidase inhibitor	20q12	2.64	0.05
SOS2	son of sevenless homolog 2 (Drosophila)0	14q21	2.63	0.02
ARHGEF6	Rac/Cdc42 guanine nucleotide exchange factor (GEF) 6	Xq26.3	2.63	0.03
VPS39	vacuolar protein sorting 39 homolog (S. Cerevisiae	15q15.1	2.62	0.05
ARHGAP12	Rho GTPase activating protein 12	10p11.22	2.61	0.04
C10orf118	chromosome 10 open reading frame 118	10q25.3	2.60	0.05
LOC550643	hypothetical LOC550643	Xp11.1	2.60	0.03
SPIN1	spindlin 1	9q22.1	2.59	0.03
HNRNPR	heterogeneous nuclear ribonucleoprotein R	1p36.12	2.56	0.04
YEATS4	YEATS domain containing 4	12q13-q15	2.55	0.05
DUSP1	dual specificity phosphatase 1	5q34	2.54	0.03
MGP	matrix Gla protein	12p12.3	2.54	0.03
KIAA0196	KIAA0196	8q24.13	2.53	0.04
MAP3K2	mitogen-activated protein kinase kinase kinase 2	2q14.3	2.52	0.05

PTBP2	polypyrimidine tract binding protein 2	1p21.3	2.51	0.03
MEX3C	mex-3 homolog C (C. elegans)	18q21.2	2.50	0.05
FAT1	FAT tumor suppressor homolog 1 (Drosophila)	4q35	2.50	0.04

Down-regulated genes

gene ID	gene assignment	localization	fch	p-value
PRAMEF1	PRAME family member 1	1p36.21	-3.02	0.04
SNORD115-25	small nucleolar RNA, C/D box	15q11.2	-2.56	0.04
DEFB4A	defensin, beta 4A	8p23.1	-2.51	0.01

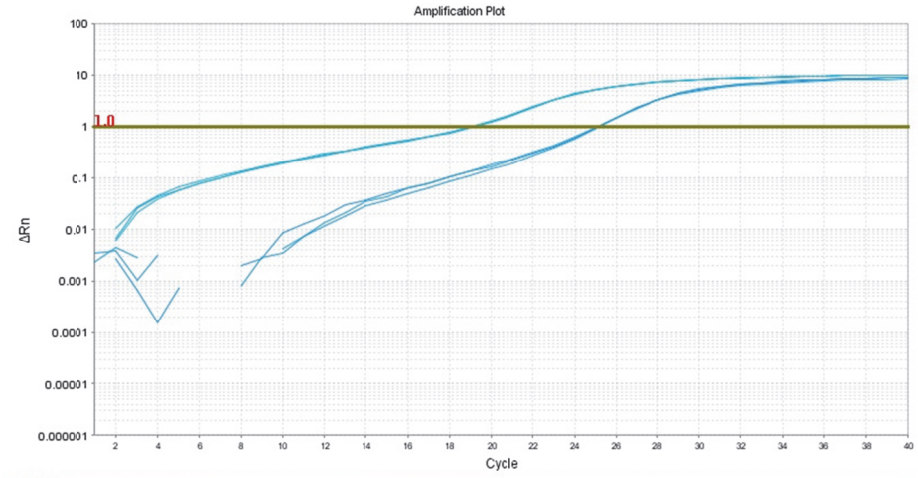

Supplementary Figure 3. qPCR raw data for lipoma and healthy skin of FAP patient 47-2008 revealed sigmoid curve shape. Sigmoid curves are illustrated for *GAPDH* with 47-2008 lipoma (left) and healthy dermis sample (right curves) with C_T at lower cycle numbers. Raw data were analyzed using ABI 7500 software v.2.0.6.

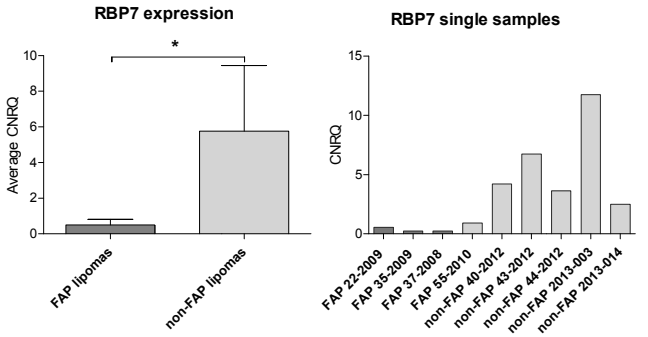
RBP7 expression
Average CNRQ
FAP lipomas
non-FAP lipomas
*

RBP7 single samples
CNRQ
FAP 22-2009
FAP 35-2009
FAP 37-2008
FAP 55-2010
non-FAP 40-2012
non-FAP 43-2012
non-FAP 44-2012
non-FAP 2013-003
non-FAP 2013-014

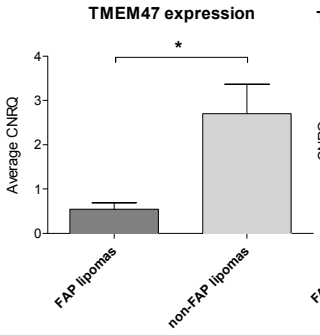
TMEM47 expression
Average CNRQ
FAP lipomas
non-FAP lipomas
*

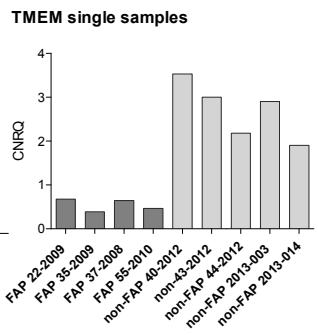
TMEM single samples
CNRQ
FAP 22-2009
FAP 35-2009
FAP 37-2008
FAP 55-2010
non-FAP 40-2012
non-43-2012
non-FAP 44-2012
non-FAP 2013-003
non-FAP 2013-014

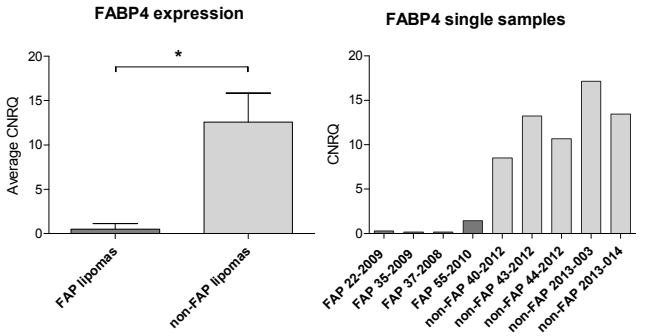
FABP4 expression
Average CNRQ
FAP lipomas
non-FAP lipomas
*

FABP4 single samples
CNRQ
FAP 22-2009
FAP 35-2009
FAP 37-2008
FAP 55-2010
non-FAP 40-2012
non-FAP 43-2012
non-FAP 44-2012
non-FAP 2013-003
non-FAP 2013-014

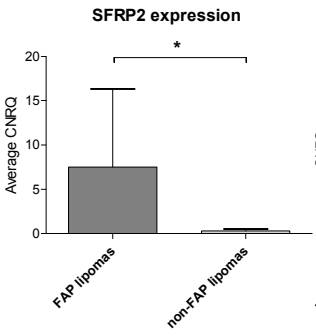
SFRP2 expression
Average CNRQ
FAP lipomas
non-FAP lipomas
*

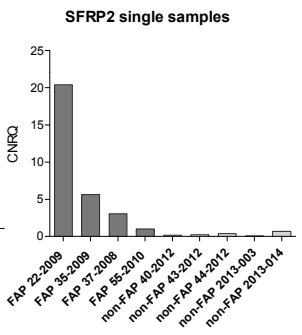
SFRP2 single samples
CNRQ
FAP 22-2009
FAP 35-2009
FAP 37-2008
FAP 55-2010
non-FAP 40-2012
non-FAP 43-2012
non-FAP 44-2012
non-FAP 2013-003
non-FAP 2013-014

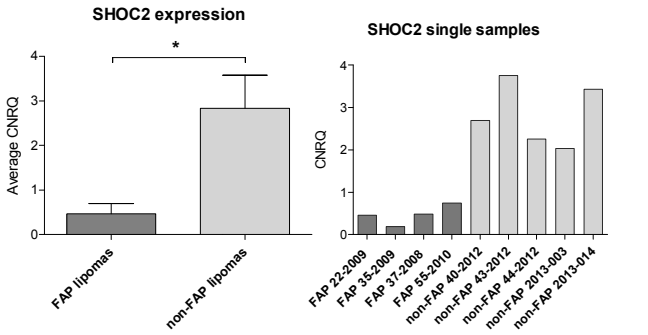
SHOC2 expression
Average CNRQ
FAP lipomas
non-FAP lipomas
*

SHOC2 single samples
CNRQ
FAP 22-2009
FAP 35-2009
FAP 37-2008
FAP 55-2010
non-FAP 40-2012
non-FAP 43-2012
non-FAP 44-2012
non-FAP 2013-003
non-FAP 2013-014

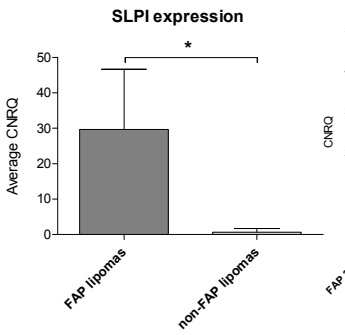
SLPI expression
Average CNRQ
FAP lipomas
non-FAP lipomas
*

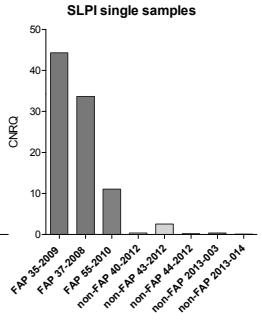
SLPI single samples
CNRQ
FAP 35-2009
FAP 37-2008
FAP 55-2010
non-FAP 40-2012
non-FAP 43-2012
non-FAP 44-2012
non-FAP 2013-003
non-FAP 2013-014

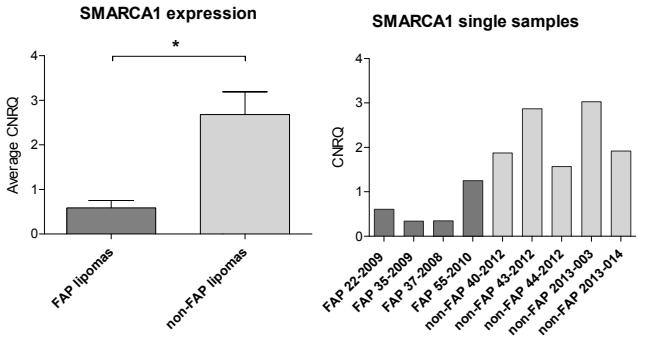
SMARCA1 expression
Average CNRQ
FAP lipomas
non-FAP lipomas
*

SMARCA1 single samples
CNRQ
FAP 22-2009
FAP 35-2009
FAP 37-2008
FAP 55-2010
non-FAP 40-2012
non-FAP 43-2012
non-FAP 44-2012
non-FAP 2013-003
non-FAP 2013-014

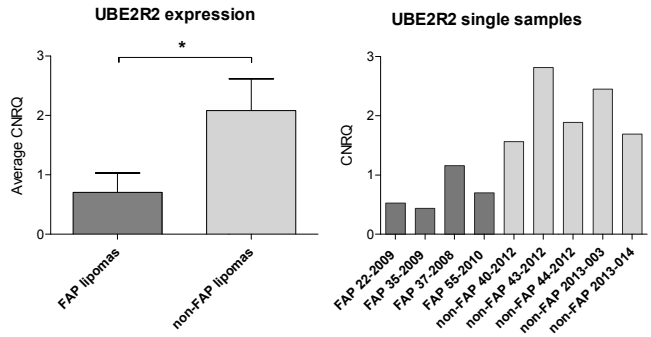
UBE2R2 expression
Average CNRQ
FAP lipomas
non-FAP lipomas
*

UBE2R2 single samples
CNRQ
FAP 22-2009
FAP 35-2009
FAP 37-2008
FAP 55-2010
non-FAP 40-2012
non-FAP 43-2012
non-FAP 44-2012
non-FAP 2013-003
non-FAP 2013-014

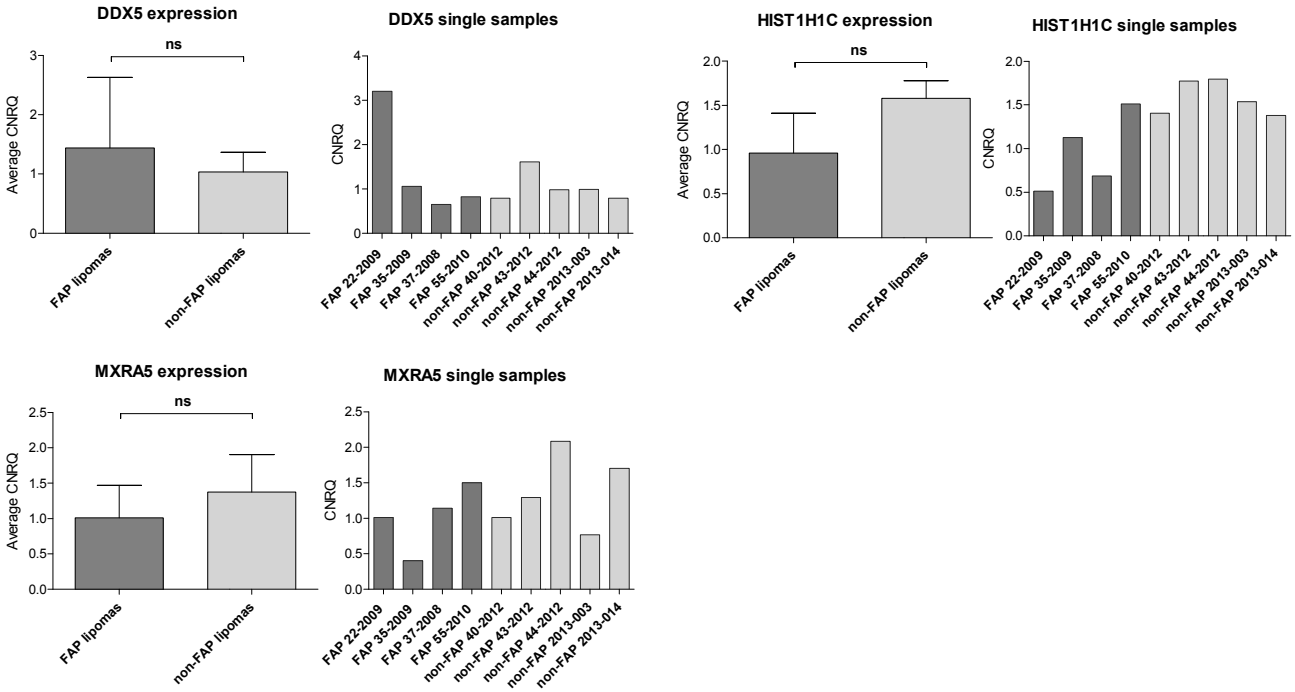

Supplementary Figure 4. Illustration of mRNA expression levels between FAP lipoma and control lipoma samples after qPCR. For each target, selected after microarray expression analysis of FAP lipoma vs. FAP healthy skin, averaged normalized mRNA expression for FAP lipoma (dark bars) and control lipoma (bright bars) as well as normalized mRNA expression for each patient sample are illustrated. Values are presented as mean of the qbasePLUS calibrated normalized relative quantities (CNRQ) + SD or as calibrated normalized relative quantities (CNRQ) for each patient sample. CNRQ values were reached after normalization to *HPRT1* and *LRP10*. Targets are sorted referring to Figure 35 and according to significance values of the results. Statistical analysis was done using a Wilcoxon rank sum test based on sample medians. Calculation was performed on four FAP lipoma and five control lipoma samples, except *SLPI* (FAP lipoma n=3, lacking 22-2009).*p< 0.05; ns not significant.

Supplementary Table 8. DEGs in FAP lipoma vs. control lipoma. The table illustrates the 41 genes (14 up- and 27 down-regulated) that reached 4-fold expression change and FDR-unadjusted p-values <0.01. Up-regulated genes are sorted from top to bottom by decreasing -fold change. Down-regulated genes are sorted from top to bottom by decreasing negative -fold change. DEGs investigated in detail are indicated in bold (gene ID).

Up-regulated genes

gene ID	gene assignment	localization	fch	p-value
SLPI	secretory leukocyte peptidase inhibitor	20q12	22.98	0.000
CD24	CD24 molecule	6q21	17.22	0.005
CAPNS2	calpain, small subunit 2	16q12.2	11.51	0.010
SPINK5	serine peptidase inhibitor, Kazal type 5	5q32	11.49	0.010
MYH11	myosin, heavy chain 11, smooth muscle	16p13.11	8.27	0.004
ESRP1	epithelial splicing regulatory protein 1	8q22.1	7.82	0.004
SFRP2	secreted frizzled-related protein 2	4q31.3	7.39	0.005
DSC2	desmocollin 2	18q12.1	5.81	0.001
CTSK	cathepsin K	1q21	5.04	0.000
CD55	CD55 molecule, decay accelerating factor for complement	1q32	4.96	0.000
SLC38A1	solute carrier family 38, member 1	12q13.11	4.95	0.003
CCL21	chemokine (C-C motif) ligand 21	9p13	4.62	0.003
HSPA4L	heat shock 70kDa protein 4-like	4q28	4.61	0.004
ANGPTL1	angiopoietin-like 1	1q25.2	4.15	0.005

Down-regulated genes

gene ID	gene assignment	localization	fch	p-value
LEP	leptin	7q31.3	-19.17	0.001
EGFL6	EGF-like-domain, multiple 6	Xp22	-16.27	0.000
GPAM	glycerol-3-phosphate acyltransferase, mitochondrial	10q25.2	-12.87	0.006
CIDEC	cell death-inducing DFFA-like effector c	3p25.3	-11.76	0.005
PLIN1	perilipin 1	15q26	-9.63	0.004
PDE3B	phosphodiesterase 3B, cGMP-inhibited	11p15.1	-9.25	0.003
LPL	lipoprotein lipase	8p22	-9.15	0.007
H19	H19, imprinted maternally expressed transcript (non-protein coding)	11p15.5	-7.76	0.000
LIPE	lipase, hormone-sensitive	19q13.2	-7.68	0.004
PRKAR2B	protein kinase, cAMP-dependent, regulatory, type II, beta	7q22	-7.15	0.001
CD36	CD36 molecule (thrombospondin receptor)	7q11.2	-6.63	0.008
AQP7P1	aquaporin 7 pseudogene 1	9q13	-6.13	0.000
PPP1R1A	protein phosphatase 1, regulatory (inhibitor) subunit 1A	12q13.2	-5.68	0.006
PLIN4	perilipin 4	19p13.3	-5.44	0.005
TUSC5	tumor suppressor candidate 5	17p13.3	-5.39	0.002
SERPINI1	serpin peptidase inhibitor, clade I (neuroserpin), member 1	3q26.1	-5.35	0.005

GLYAT	glycine-N-acyltransferase	11q12.1	-5.31	0.003
AQP7	aquaporin 7	9p13	-5.25	0.000
PLA2G16	phospholipase A2, group XVI	11q12.3	-5.14	0.001
GPD1	glycerol-3-phosphate dehydrogenase 1 (soluble)	12q12-q13	-4.94	0.002
ESM1	endothelial cell-specific molecule 1	5q11.2	-4.82	0.001
HEPN1	HEPACAM opposite strand 1	11q24	-4.80	0.005
THBS4	thrombospondin 4	5q13	-4.67	0.000
G0S2	G0/G1switch 2	1q32.2	-4.62	0.008
NQO1	NAD(P)H dehydrogenase, quinone 1	16q22.1	-4.50	0.000
HRASLS5	HRAS-like suppressor family, member 5	11q13.2	-4.41	0.006
ACVR1C	activin A receptor, type IC	2q24.1	-4.19	0.001

Supplementary Table 9. Selected down-regulated mRNAs regulated by same upstream regulators. In total nine additional mRNAs are listed which were found to be regulated by same upstream regulators including PPAR, TNF and LEP. All of these genes (with fold differences of at least 4) hold functions in lipid binding and lipid storage, as well as transport and metabolism of fatty acids. Genes are sorted by increasing fold change. Results were revealed by IPA® analysis.

gene ID	gene name and known gene function	regulator	localization	fold change	p-value
PLIN1	**perilipin 1** - coats lipid storage droplets in adipocytes - role in lipolysis inhibition	PPAR, TNF, LEP	15q26	**-9.63**	0.004
PDE3B	**phosphodiesterase 3B, cGMP-inhibited** - regulates energy metabolism and energy intake	PPAR, LEP	11p15.1	**-9.25**	0.003
LPL	**lipoprotein lipase** - LPL deficiency results in type I hyperlipoproteinemia	PPAR, TNF, LEP	8p22	**-9.15**	0.007
LIPE	**lipase, hormone, sensitive** - hydrolyzes stored triglycerides to free fatty acids - in adipose and steroidogenic tissues	PPAR, LEP	19q13.2	**-7.68**	0.004
CD36	**CD36 molecule (thrombospondin receptor)** - cell adhesion molecule - binds long chain fatty acids - regulator of fatty acid transport	PPAR, TNF, LEP	7q11.2	**-6.63**	0.008
PLIN4	**perilipin 4** - coating of intracellular lipid storage droplets	PPAR, TNF	19p13.3	**-5.44**	0.005
AQP7	**aquaporin 7** - glycerol channel in adipose tissue - controls the accumulation of triglycerides and development of obesity/diabetes	PPAR, TNF, LEP	9p13	**-5.25**	<0.001
GPD1	**glycerol-3-phosphate dehydrogenase 1 (soluble)** - critical role in carbohydrate and lipid metabolism, enhanced activity in adipose tissue[267] - mutations in transient infantile hypertriglyceridemia	PPAR, TNF	12q12-q13	**-4.94**	0.002
G0S2	**G0/G1switch 2** - role in adipocyte differentiation and lipolysis[268]	PPAR, TNF	1q32.2	**-4.62**	0.008

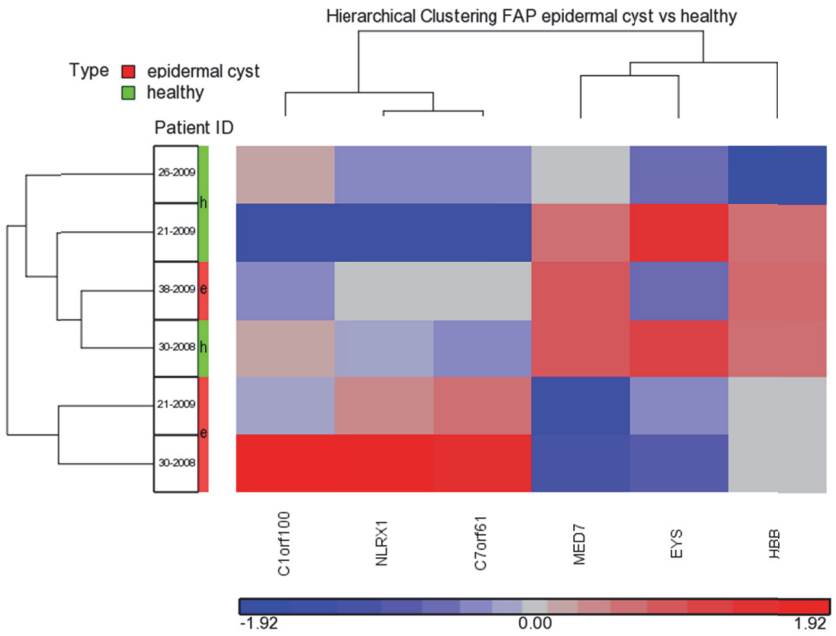

Supplementary Figure 5. Hierarchical clustering of differentially expressed mRNAs in FAP epidermal cyst vs. FAP healthy epidermis. The heat map displays gene expression levels of the six DEGs for each patient sample. It is generated for significantly regulated genes with 1.5-fold expression difference and unadjusted p-values <0.05. Each row indicates a single patient sample whereas genes are depicted by independent columns. Up-regulated genes are represented by red and down-regulated genes by blue areas. Grey areas assign genes of unchanged expression between epidermal cysts vs. healthy epidermis. The dendrograms represent similarities in mRNA expression intensitites between different patients or between different genes. No clustering of epidermal cyst and healthy epidermis samples was reached for this gene set

Supplementary Table 10. DEGs in FAP epidermal cyst vs. healthy epidermal skin. The table illustrates the six genes (three up- and three down-regulated) that reach minimum 1.5-fold expression change and FDR-unadjusted p-values of <0.05. Up-regulated genes are sorted from top to bottom by decreasing -fold change. Down-regulated genes are sorted from top to bottom by decreasing negative -fold change. Annotations were determined not to be of major interest for epidermal cyst development.

gene ID	gene assignment	localization	fch	p-value
NLRX1	**NLR family member X1** regulator of mitochondrial antivirus responses	11q23.3	**1.60**	0.021
C1orf100	**chromosome 1 open reading frame 100**	1q44	**1.52**	0.029
C7orf61	**chromosome 7 open reading frame 61**	7q22.1	**1.51**	0.017
HBB	**hemoglobin, beta** component of hemoglobine	11p15.5	**-1.91**	0.019
MED7	**mediator complex subunit 7** gene transcription activators	5q33.3	**-1.70**	0.004
EYS	**eyes shut homolog (Drosophila)** epidermal growth factor (EGF)-like and LamG domains; expressed in the photoreceptor layer of the retina	6q12	**-1.56**	0.047

The study was performed after obtaining informed consent according to guidelines of the Ethical Committee of Basel (EKBB), Switzerland (EK258/05 and EK15/08).
The study was funded by the national cancer league “Krebsliga beider Basel”.

11 ACKNOWLEDGEMENT

There are several people who have accompanied and supported me during my PhD to which I want to offer my cordial acknowledgement at this point.

First of all, I want to offer a great thank you to Dr. Bettina Burger for her supervision and support according to the whole project. I appreciated her patient teaching in molecular biologic techniques, her scientific help and support, and her encouragement. Furthermore, I am very thankful for her critical revision of manuscripts and constructive discussions.

I want to offer my special thanks to Prof. Peter Itin for giving me the possibility to work in his research group. I always appreciated the close collaboration with the clinic and I am very pleased for the deepened insight into dermatology I got over the past years. Furthermore, I want to thank him for critical revision of manuscripts and valuable inputs in all dermatological questions. Furthermore, I want to thank him and Dr. Bettina Burger for giving me the opportunity to visit very interesting national and international congresses as well as for letting me participate in the “FAP-tour” right at the beginning of my PhD.

Many thanks I want to spend also to Sandra Hasler for her help in all administrative questions concerning the Dermatology Unit.

A great thank you goes also to Prof. Karl Heinimann for the great collaboration, without which this study would not have been possible. I also want to thank him for his valuable inputs in all genetic questions concerning FAP and my whole project. Furthermore, I want to thank him for the critical revision of the manuscript and constructive feedback.
I want to thank the whole team of the Research Group of Human Genetics for their heartily acquaintance and support. Especially, I want to thank Michèle Attenhofer for her very educative technical support concerning microsatellite analyses and MLPA. I also want to thank Marianne Häusler for providing us with all patient information and for helping me in illustrating FAP family trees.

Many thanks go to Dr. med. Andreas Volz from the dermatologic surgery for providing me fresh skin tissues for my experiments.

I want to thank Philippe Demougin, from the Microarray core facility at the Biocenter, for his technical support with microarray experiments and Partek® analysis.

I would like to offer a great thank you to Prof. Stephan Krähenbühl for his availability as faculty representative and to Prof. Raija Lindberg Gasser for her contribution as co-referee.

Furthermore, I want to thank Dr. Iris Spörri Werner for technical training and valuable discussions. In addition I want to thank her, Hedwig Wariwoda and all former members of Lab 317 for their contribution to a pleasant lab atmosphere.

And last in a more personal sense, I want to thank all my friends from neighboring labs, especially Daniela Schmid, for her heartily support and encouragement. A great thank you goes to my friends Sarah and Luky outside of research for all their support and reconstructive talks during the last past years. And finally, I would like to offer a huge thank you to my parents for their never ending patience, their encouragement and support at all times.